UiT The Arctic University of Norway

Faculty of Biosciences, Fisheries and Economics. Department of Arctic and Marine Biology

Shifts in bacterial biodiversity along an environmental gradient in high-Arctic tundra

Aslak von Düring

Master thesis in Molecular Environmental Biology …. BIO-3950 …. november 2019

Shifts in bacterial biodiversity along an environmental gradient in high-Arctic tundra

Aslak von Düring. Faculty of Biosciences, Fisheries and Economics
Department of Arctic and Marine Biology

15th of November 2019

Supervisors: Prof. Mette Marianne Svenning & Postdoc. Christophe Victor Seppey

List of content

List of Tables

List of Figures

Figure 8: The pie charts show the microbial communities in the top and deep layer of the dry and wet sites for OS. The circles from inner to outer represents the taxonomic levels in the following order: Domain, Phylum, Class and Order, while the text outside diagram represents the Family level. Colours indicating respective taxa are given in the legend. Figure show taxa that make up >1% of the community. Taxa representing <1% of the community is grouped into higher level taxa.

Figure 9: Plot of a distance based redundancy analysis (dbRDA) performed on the bacterial communities. A Hellinger transformed OTU-matrix was used to calculate a Bray-Curtis dissimilarity matrix which was used as a response variable, with site, depth, moisture, pH and C-N as explanatory variables. In A; the sites KH and OS, B; moisture gradient, C; shows the depth. Arrows display the variables implemented in the model. The red arrow shows the moisture content (MC). C_N shows the carbon nitrogen ratio.

Figure 10: Comparison of two PCR protocols performed on the mcrA gene. A; Primers from Luton et al. (2002) and the PCR program described in Frey et al. (2011), B; PCR performed with primers and program from Steinberg and Regan (2008). Lanes are labelled with sample number. Lad = Ladder, PC= Positive control

Figure 11: A Maximum Likelihood (ML) tree of the gammaproteobacterial MOB based on the Le and Gascuel Le and Gascuel (2008) model of amino acid substitution. A discrete Gamma distribution was applied to model evolutionary rate differences among sites The Neighbor-Join and BioNJ algorithms was applied to a matrix of pairwise distances estimated using a Jones-Taylor-Thornton (JTT) (Jones et al., 1992) model and selecting the topology with greater log likelihood. Involved in the analysis were 39 amino acid sequences with a total of 157 positions included in the final dataset. The three was rooted with an alphaproteobacterial outgroup. Environmental sequences are marked with an asterix, while others are type strain MOB. Highlighted in bold are environmental sequences acquired in this study. Scale bar indicate

number of substitutions per site. In parentheses are the NCBI accession numbers. The program MEGAX was used for analysis

Figure 12: A Maximum Likelihood (ML) tree of the alphaproteobacterial MOB based on the Le and Gascuel (2008) model of amino acid substitution. A discrete Gamma distribution was applied to model evolutionary rate differences among sites. The Neighbor-Join and BioNJ algorithms was applied to a matrix of pairwise distances estimated using a Jones-Taylor-Thornton (JTT) (Jones et al., 1992) model and selecting the topology with greater log likelihood. Involved in the analysis were 33 amino acid sequences with a total of 155 positions included in the final dataset. The program MEGAX was used for analysis (Kumar et al., 2018). Environmental sequences are marked with an asterix, while others are type strain MOB. Highlighted in bold are environmental sequences acquired in this study. Scale bar indicate number of substitutions per site. In parentheses are the NCBI accession numbers.

Figure 13: Plot of a distance based redundancy analysis (dbRDA) performed on the MOB communities. A Hellinger transformed OTU-matrix was used to calculate a Bray-Curtis dissimilarity matrix which was used as response variable, with site, depth, moisture, pH and C-N ratio as explanatory variables. In A; the sites KH and OS, B; moisture gradient, C; the depth. Arrows display the variables implemented in the model. The red arrow shows the moisture content (MC). C_N shows the carbon nitrogen ratio. The 6 most abundant MOB OTU's are plotted and shown in

Figure 14: Plot of a distance based redundancy analysis (dbRDA) performed on the MOB communities without samples containing high C_N values and OTU X_11. A Hellinger transformed OTU-matrix was used to calculate a Bray-Curtis dissimilarity matrix which was used as response variable, with site, depth, moisture, pH and C-N ratio as explanatory variables. In A; the sites KH and OS, B; moisture gradient, C; show the depth. Arrows display the variables implemented in the model. The red arrow shows the moisture content. C_N shows the carbon nitrogen ratio. The 5 most abundant MOB OTU's are plotted and shown in red.

Abbreviations

ANOVA = Analysis of variance

atmCH_4 = Atmospheric CH_4

atmMOB = Atmospheric methane oxidizing bacteria

C:N = Carbon:Nitrogen ratio

FAME = Fatty Acid Methyl Ester

FISH = Fluorescent *In Situ* Hybridization

IPCC = Intergovernmental Panel on Climate Change

KH = Knudsenheia

MDM = Microbial Diagnostic Microarray

ML = Maximum Likelihood

MOB = Methane oxidizing bacteria

OM = Organic matter

OS = Ossian Sarsfjellet

OTU = Operational Taxonomic Unit

PCR = Polymerase Chain Reaction

pMMO = Particulate methane monooxygenase

RDA = Redundancy Analysis

MC = Moisture content

SLB = Signature Lipid Biomarkers

sMMO = Soluble methane monooxygenase

SOC = Soil organic carbon

TC = Total Carbon

TN = Total Nitrogen

Acknowledgments

Most of all I would like to thank my supervisor Prof. Mette Marianne Svenning for being supportive, giving me experienced guidance and the opportunity to participate in an international research project. I would also like to thank my co-supervisor, Postdoc. Christophe Victor Seppey for your patience, good mood and invaluable guidance.

A special tank you to Alena Didriksen for all your help and for teaching me to be methodical and efficient in the lab, and also for being a good travel partner.

I would also like to give my appreciation to Prof. Elie Verleyen, Dr. Bjorn Tytgat and PhD student Lotte De Maeyer from the Laboratory of Protistology and Aquatic Ecology at the University of Ghent for the learning experience, hospitality and guidance in Ghent. I would also like to thank all members of the Climarctic project for being an including, resourceful scientific collaborate.

Thank to Jeanette and Alicia for the good atmosphere and for making the office a good working environment.

Lastly, I want to thank my wife Lona and my two sons, Magnus and Peder for being more loving, caring and supportive than one could ask.

Abstract

Arctic soil microbiomes may have to face drastic climate changes in the coming century. Currently, the arctic tundra act as a carbon sink due to slow decomposition rates of soil organic carbon, which partly owes to low temperatures and poor water drainage. However, with elevated temperatures, large, latent carbon pools stored in arctic permafrost are exposed to mineralization by the active layer microbiota. This could cause increased emissions of potent climate gases, such as CH_4 and CO_2 to the atmosphere. Potentially changing the status of the arctic tundra into a net carbon source and further result in a positive feedback-loop to the climate system. Along with the climatic changes, altered precipitation regimes are predicted to cause higher water contents in some areas, while others are predicted to become drier. In turn, these changes are likely to trigger a response in the diversity and functioning of the soil microbial communities, which again might have an impact on biogeochemical cycles. Methane oxidizing bacteria (MOB) are bacteria that works as a filter for CH_4, mainly produced by anaerobic methanogenic archaea. Some MOB also possesses the ability to consume CH_4 from the atmosphere (atmMOB). Studies have shown that high water saturation might impede O_2 availability, which is demonstrated to lower CH_4 oxidation rates. Here we investigate how the bacterial biodiversity, and, in more depth, the MOB community changes along a moisture gradient in high-Arctic tundra, Svalbard. We have used next generation sequencing of the 16S rRNA gene, and the MOB functional gene, *pmoA*, to infer differences in community composition along the gradient. Statistical analyses were used to deduce the effect of environmental variables on the bacterial- and MOB community structure. Both moisture and pH were shown to have significant effects on the bacterial community composition. *Proteobacteria*, *Actinobacteria* and *Acidobacteria* were overall the most abundant phyla. *Cyanobacteria* had a high abundance in the top layer of wet soil, while *Chloroflexi* were abundant in the deep layers. Most interestingly, we found that the MOB community was dominated by members of the upland soil cluster γ (USCγ), a group of atmMOB not previously found in Svalbard. Our results demonstrate that dry, neutral to slightly alkalic upland cryosols could be a potential significant previously unrecognized CH_4 sink. An analysis of variance showed that in addition to pH, moisture had a significant effect on the MOB community, which also was shown by a lack *pmoA* product in the wet sites. This implies that the MOB communities in these soils are vulnerable to alterations in water saturation in future climate change scenarios.

1 Introduction

1.1 Arctic environment

Arctic tundra constitutes a variety of cryosols, which are soils affected by permafrost. Tundra is classified as a treeless terrain with a continuous vegetation, including lichens, mosses, sedges

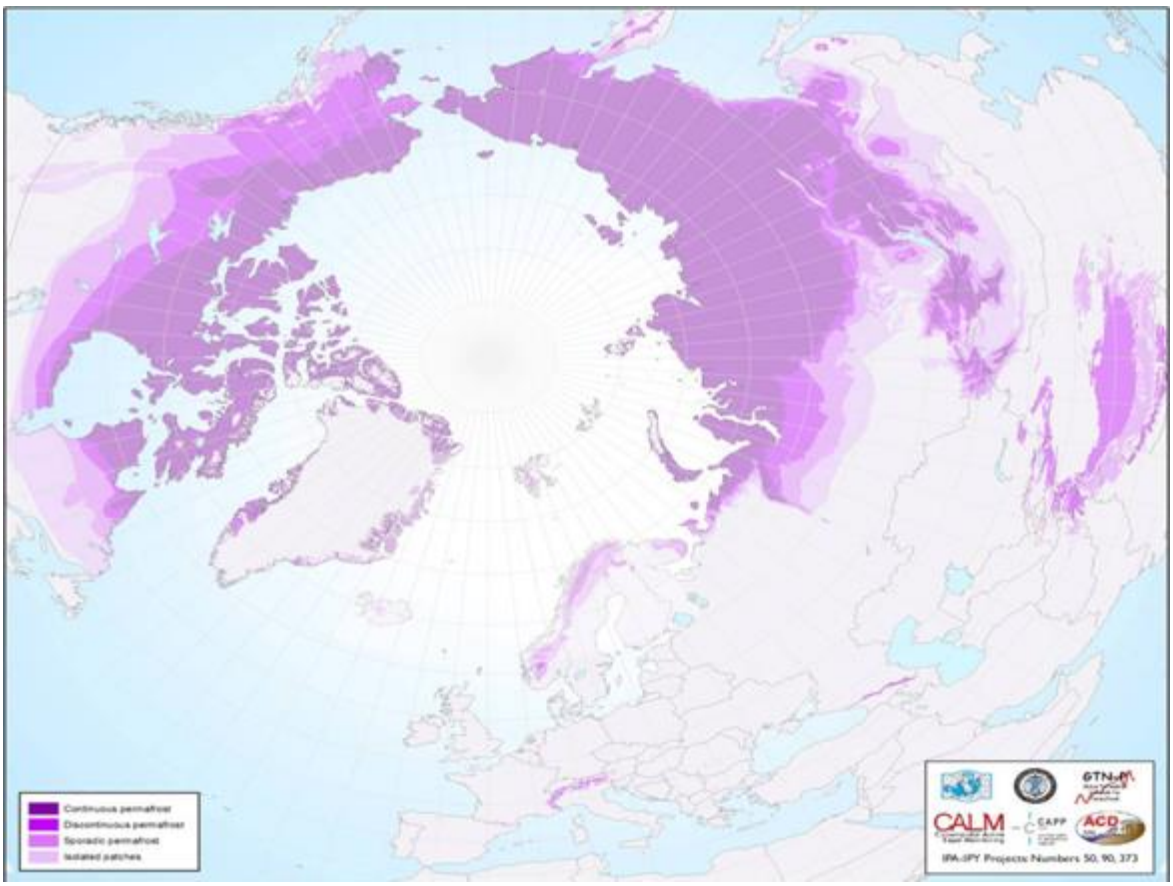

Figure 1: Geographical distribution of permafrost in the northern hemisphere. Illustration: International Permafrost Association. https://ipa.arcticportal.org/images/stories/permafrost%20map.jpg

grasses, forbs and low shrubs, found at both high latitudes and high altitudes (Everdingen, 1998, revised in 2005). Permafrost is defined as ground that remains below 0°C for at least 2 consecutive years (Everdingen, 1998, revised in 2005) and is overlain with a seasonally thawed active layer. Permafrost occurs either as continuous, discontinuous, sporadic or isolated patches of permafrost (Figure 1). Permafrost and cryoturbated soils are estimated to store 1034 ± 183 or 1104 ± 133 Pg of global below ground organic carbon in the top 3 m, which constitutes one third of earths below ground organic carbon (Hugelius et al., 2014).

1.2 Changing arctic environment

Soil organic carbon (SOC) decomposition rates are reduced at high latitudes owing to low temperatures and poor soil drainage (Davidson & Janssens, 2006). Over millennial timescales, SOC have accumulated on top of mineral layers, or been buried below ground due to cryoturbation (Bockheim & Tarnocai, 1998), creating abovementioned large pools of SOC in perennially frozen soil. As a consequence of these processes, arctic terrestrial ecosystems are considered to be important carbon sinks (Schuur et al., 2015). However, due to global warming and the polar amplification phenomena, temperatures in the Arctic has increased with double the rate of the global average, with an increase of approximately 0.6 C° per decade over the last 30 years (IPCC, 2013). Increases in temperature could expand the horizon that make up the active layer and make the vast pools of SOC available to mineralization into greenhouse gases such as carbon dioxide (CO_2) and methane (CH_4) by the decomposing soil microbiome (Liebner et al., 2015; Tveit et al., 2013). In turn, increased efflux of greenhouse gases might offset the balance of carbon uptake and release, shifting arctic into a carbon source. Conversely, a model prediction of permafrost made under the IPCC (Intergovernmental Panel on Climate Change) suggest that between 30 - 99 % of the permafrost in the top 3.5 m can be thawed within this century (Koven et al., 2013). The current state of CH_4 release per year is close to follow this model prediction, indicating a more accelerated efflux of greenhouse gases than suggested in Schuur et al. (2015).

Another effect of climate change in High-Arctic is an altered precipitation regime and/or increased evaporation during summer, altering the hydrology of biological systems, resulting in either a positive or negative soil moisture balance, depending on region and topography. Precipitation often comes as snow, and increased snowfall could lead to thicker snow cover, which could function as isolation and increase the temperature of underlying soil, and consequently also the activity of the microbiota. Then in turn this could result in a longer period of snow-covered soil and wetter spring and summer seasons. Further, elevated temperatures during spring could counteract the effect of longer periods with snow cover resulting in a more rapid melting of the snow cover, which prolongs the growing season. However, in some regions, climate models predict a less extensive snow cover and an prolonged growing season (Cooper, 2014), but as a consequence, colder soil temperatures could occur during winter. Shoulder seasons could have more profound effect than previously thought as climatic effects

may carry over to other seasons (Cooper, 2014). Higher temperatures could also lead to increased evaporation during summer and create drier soils which are less buffered to changes in temperature and could have profound impacts on the microbial community structure and activity. Notably, Fenner and Freeman (2011) showed that drying of peatlands induced carbon loss, as phenol oxidases were activated through higher levels of oxygen.

Future predictions of climate change effects on arctic terrestrial ecosystems are complex but needs to be investigated due to the potential global repercussions increased greenhouse gas emissions could have by causing a positive feedback loop to the global climate system, rapidly accelerating global warming.

1.3 Microbial communities

The biodiversity in arctic cryosols is shown to be comparable to soil in lower latitues (Chu et al., 2010). Arctic bacterial communities are often dominated by the bacterial phyla *Proteobacteria, Actinobacteria, Acidobacteria, Bacteriodetes, Chloroflexi* and *Cyanobacteria* (Chauhan et al., 2014; Koyama et al., 2014; Makhalanyane et al., 2016; Tveit et al., 2013). Biomass from arctic soils are dominated by bacteria, which are suggested to be at a 10-fold than of archaea, however, the archaea to bacteria abundance ratio increases with depth.

Nitrogen (N) availability is considered to be the main growth limiting factor in nutrient poor arctic tundra (Shaver & Chapin, 1980). *Cyanobacteria* are, in addition to being significant primary producers, considered to be the primary source of N input in arctic terrestrial ecosystems due to their capability to fix atmospheric N_2 (Liengen, 1999; Solheim et al., 2006; Stewart et al., 2011). *Cyanobacteria* can be either free living, or in symbiotic associations with a variety of eukaryotic hosts including lichens, mosses, liverworts and hornworts (Rai et al., 2000; Smith, 1984; Turetsky, 2003). N_2 fixation rates, and *Cyanobacteria* abundance, have been demonstrated to correlate with water availability, temperature and light (Chapin et al., 1991; Dickson, 2000; Solheim et al., 2006; Zielke et al., 2003). Studies have shown that the most abundant *Cyanobacteria* in arctic soils are members of the cyanobacterial order *Synechococccales, Oscillatores* and *Nostocales* (Kviderova et al., 2011; Liengen & Olsen, 1997; Pushkareva et al., 2015). Especially the *Nostoc commune* is demonstrated to display a

wide distribution in arctic terresterial ecosystems. The alphaproteobacterial class *Rhizobiales* is in addition to *Cyanobacteria* known to comprise many N-fixing members. Furthermore, several *Rhizobiales* families, i.e. *Rhizobiacea* and *Bradyrhizobiacea* are similarly associated with forming symbiotic relationships with plants.

Actinobacteria are considered to be prominent inhabitants of cold environments, as they are suggested to occupy several key functional processes both in SOC degradation and in the nitrogen cycle (Chan et al., 2013; Tveit et al., 2013). Moreover, *Actinobacteria* are suggested to possess DNA-maintenance abilities, which is considered to be a beneficial trait in freeze-thaw environments where DNA desiccation is prevalent (Johnson et al., 2008). *Actinobacteria* are also demonstrated to inhabit cold shock genes, which might enable them to cope with rapid changes in temperature (Chan et al., 2013).

Copiotrophic *Alpha-* and *Betaproteobacteria* are demonstrated to increase in abundance with increase in nutrient availability, while oligotrophic *Acidobacteria* decreases (Koyama et al., 2014). Moreover, there has been found a negative relationship between abundance of *Acidobacteria* and carbon mineralization rates, and a proposed classification into r- and K selected strategies based on oligotrophy and copiotrophy (Fierer et al., 2007). A study of soil microbial communities from Canadian, Alaskan and European arctic showed that the differences in communities composition highly correlated with pH and inversely correlated with the C:N ratio (Chu et al., 2010). The same study showed a strong positive correlation of *Alphaproteobacteria* with increasing pH, while *Acidobacteria* on phylum level demonstrated an equivalent negative correlation (Chu et al., 2010). In accordance to the findings in Chu et al. (2010), the microbial community composition in soil from the Kongsfjord (Ny-Ålesund, Svalbard) area are reported to be higher in abundances of *Proteobacteria*, and lower in abundances of Acidobacteria, than reported in the sites of Chu et al. (2010), due to higher pH levels (> pH 6) (McCann et al., 2016). Moreover, bacterial 16S rRNA gene copy numbers are reported to inversely correlate with pH (Gray et al., 2014). *Chloroflexi* comprises bacteria with a variety of different metabolic pathways, including phototrophs (green non-sulfur bacteria), lithotrophs, heterotrophs and are adapted to both oxic and anoxic environments (Woese, 1987).

Moreover, the fraction of *Chloroflexi* has been shown to be higher at increasing depths (Tveit et al., 2013).

Arctic microbial communities are important carbon sinks as low temperature and poor soil drainage minimalizes breakdown of SOC (Davidson & Janssens, 2006). In soils where anoxic conditions are predominant, such as peatlands, bogs and mires, high concentrations of phenolic compounds are considered to be a limiting factor in SOC degradation (Fenner & Freeman, 2011; Freeman et al., 2001). However, when subjected to drought, oxygen activates phenol oxidases which results in an increase in carbon loss (Fenner & Freeman, 2011). Degradation of SOC depend on the genetic repertoire of the soil microbial community. Initial step of carbon degradation includes the breakdown of major polymers such as cellulose and hemicellulose and requires expression of the extracellular enzyme cellulase (Kotsyurbenko, 2005). *Bacteriodetes*, *Actinobacteria* and *Verrucomicrobia* were found to be the most active taxa in conducting this step in an arctic peatland (Tveit et al., 2013). Further mineralization of SOC includes fermentation and methanogenesis, where the former step, in the same study (Tveit et al., 2013), was found to be conducted mainly by *Actinobacteria* and *Firmicutes*.

1.4 Methanogenesis

The origin of CH_4 could be a result of either biogenic or abiogenic processes. Degradation of organic compounds to yield CH_4 is termed biogenic while CH_4 derived from processes involving inorganic compounds is termed abiogenic (Schoell, 1988). Biogenic production of CH_4 mainly results from the activity of methanogens, archaea that produces CH_4 through several metabolic pathways. However, biogenic production of CH_4 also include degradation of relic organic compounds on geological timescales through elevated levels of heat and pressure, termed thermogenic CH_4 production, and the incomplete combustion of biomass, i.e peat fire and biofuel burning, termed pyrogenic CH_4 production (Saunois et al., 2016). Several anthropogenic entities are major sources of biogenic CH_4, namely, livestock farming, rice agriculture, fossil fuel exploitation, waste management, biomass burning, landfills and coal mining. In addition, inorganic pathways of CH_4 production, involving water-rock-gas reactions, or magmatic processes, are also significant sources of natural occurring CH_4, i.e. from hydrothermal vents (Etiope & Lollar, 2013). Methane hydrates, clathrates, constitutes the

largest reservoir of CH_4, of which the methane could origin from either methanogenic archaea or thermogenic processes (Wallmann et al., 2012).

CH_4 concentrations in the atmosphere have increased by a factor of 2.5 since pre-industrial times (Etheridge et al., 1998). In the period 2003-2012, CH_4 emissions from anthropogenic sources comprised approximately 352 Tg CH_4 yr^{-1} of global CH_4 emission, while contributions from natural sources constituted 384 Tg CH_4 yr^{-1} of CH_4, considering bottom-up models (inventories and data-driven approaches), with estimated total global emission of 736 Tg CH_4 yr^{-1} (Kirschke et al., 2013; Saunois et al., 2016). CH_4 has a short lifetime of approximately 9 years, yet the radiative forcing contribution is significant and CH_4 has a global warming potential 28-34 times higher, over a 100-year time period, than CO_2 (Shindell et al., 2009). Removal of atmospheric CH_4 ($atmCH_4$) is mainly caused by reactions with hydroxyl (OH) radicals, in the tropos- and stratosphere, reaction with atomic chlorine in the marine atmospheric boundary layer and minor reactions with electronically exited oxygen atoms in the stratosphere (Dlugokencky et al., 2011). Additionally, a substantial amount is removed through oxidation by methane oxidising bacteria (MOB). From natural sources, wetlands constitute the largest contributor to global emissions, due to the anaerobic production of CH_4 by methanogens. However, emission rates from wetlands have the highest level of uncertainty in global models (Kirschke et al., 2013), partly owing to difficulties in defining wetland CH_4-producing area and parameterization of anaerobic sources and oxidation rates (Wania et al., 2013). Emissions from wetlands varies, depending primarily on water table position, substrate availability and temperature (Saunois et al., 2016; Wania et al., 2013).

CH_4 emission from high latitudes (60-90°N) contributes only ~4% to global CH_4 emissions, however the potential in the large amounts of carbon sequestered in perennially frozen soil is substantial (Saunois et al., 2016). Moreover, an increasing number of studies has been conducted on CH_4 oxidation in carbon-rich peatlands, however, CH_4 oxidation from mineral (carbon-poor) cryosols, despite its spatial predominance, is not thoroughly described, but is starting to get more attention (Lau et al., 2015).

1.5 Methanogens

Methanogenic archaea are the most substantial source of natural occurring CH_4. They are on the bottom of the thermodynamic hierarchy and consequently close to the limits of life. Anaerobic methanogens conduct the last step in degradation of SOC by utilizing mainly H_2/CO_2, formate or acetate as substrates to produce CH_4 (Tveit et al., 2013), however, they can also use C1 compounds, i.e. methanol, mono-, di- and tri methylamines (Whitman et al., 2006). Phylogenetically, the methanogens are members of the *Euryarchaeota* phylum, and constitute seven distinct orders (Adam et al., 2017; Hug et al., 2016), whereof five are considered obligate hydrogenotrophs namely, *Methanobacteriales, Methanopyrales, Methanococcales, Methanomicrobiales* and *Methanocellales* (Buan, 2018). The order of *Methanomasiliiicoccales* constitutes the as-of-now only group that are obligate methylotrophs, while the order of *Methanosarcinales* are the most versatile group, having members that are either obligate acetoclastic or obligate hydrogenotrophic or members capable of utilizing several substrates for metabolism (Buan, 2018). Production of methane depend on water saturation (water table), and temperature. However, methane production is also reduced at higher levels of ferric iron (Fe (III)), due to Fe (III) reducing organisms utilizing H_2 and acetate for metabolism at a lower concentration then methanogens (Lovley & Phillips, 1987). Moreover, methane production is shown to increase in sulfate depleted sediments (Winfrey & Ward, 1983). Increases in temperature induced CH_4 production and in addition, revealed a shift in abundance of active methanogens from formate and H_2 consuming *Methanobacteriales* to *Methanomicrobiales* and from acetoclastic *Methanosarcinaceae* to *Methanosaetaceae* (Tveit et al., 2015).

A conserved phylogenetic marker gene, *mcrA*, is frequently used in addition to the 16S rRNA gene to assess the presence and phylogeny of the methanogens. This gene encodes the α-subunit of the methyl coenzyme-M reductase gene and is ubiquitous and found in all methanogens (Thauer, 1998).

1.6 Methane oxidizers

MOB oxidizes CH_4 and converts it into CO_2 or biomass, and function as methane catalysts.

Generally, MOB have phylogenetic affiliations to the proteobacterial subclasses Alpha and *Gammaproteobacteria* (Type II and Type I respectively) mainly based on differences in

metabolic pathways (Semrau et al., 2010). In addition, there have been discovered acidophilic MOB with phylogenetic association to the *Verrucomicrobia* phylum (Op den Camp et al., 2009) and to the novel NC10 phylum (Ettwig et al., 2010). Aerobic oxidation of CH_4 is carried out by MOB primarily via either the RuMP pathway (type I), or the Serine pathway (type II), both with CO2 as an end product (Hanson & Hanson, 1996). Anaerobic oxidation of CH_4 however, is also known to play an important role in mitigating CH_4 emissions. Methanotrophic archaea have been shown to oxidize CH_4 by conducting reverse methanogenesis in the presence of iron, manganese, nitrate and sulfate (Beal et al., 2009; Boetius et al., 2000; Haroon et al., 2013). Also, more recently, there has been provided evidence contradicting the 'strictly aerobic' nature of MOB, suggesting that MOB also are capable of oxidizing CH_4 anaerobically. The bacterium *Methylomirablis oxyfera* in the phylum NC10 is shown to have the ability to oxidize CH_4 by producing its own oxygen via the reduction of nitrite (NO_2^-) (Ettwig et al., 2010). Moreover, Martinez-Cruz et al. (2017) suggests that anaerobic oxidation of CH_4 can be performed by MOB using several different electron acceptors such as nitrate (NO_3^-), nitrite (NO_2^-), ferric iron (Fe^{3+}) or manganese (Mn^{4+}) and/or involve reactions providing O_2 for the aerobic MOB.

Methanotrophs are ubiquitous in nature and are found at high and low latitudes and- altitudes, which includes, marine systems, the atmosphere, aquatic environments, and terrestrial habitats. Moreover, induced MOB abundances are found in anthropogenic sites, such as, landfills, wastewater treatment sites, coal mines, livestock farms and rice fields.

All MOB harbours the particulate methane monooxidase (pMMO) enzyme gene for oxidation of CH_4 (Semrau et al., 1995), except a few genus that only possesses the gene for soluble methane monooxidase (sMMO) (Dedysh et al., 2000; Dunfield & Dedysh, 2014; Vorobev et al., 2011). Hence, a gene that encode a subunit of the pMMO gene, namely *pmoA*, is used as a phylogenetic marker gene to assess the diversity of MOB in microbial communities (Liebner et al., 2009; McDonald & Murrell, 1997; Semrau et al., 1995). It has been shown that type I MOB rRNA gene abundance correlates with phosphorous (Gray et al., 2014).

1.6.1 Atmospheric CH_4 oxidizers

Consumption of atmospheric methane (atmCH_4) in cold environments is not a novel phenomenon, and has previously been described (Flessa et al., 2008; Lau et al., 2015; Martineau et al., 2014; Nauer et al., 2012; Whalen et al., 1990). Initially, atmMOB was found in upland soils, and were termed upland soil cluster (USC) α and γ, and constitutes clades within the *Alpha-*, and *Gammaproteobacteria* respectively (Holmes et al., 1999; Knief et al., 2003). Responsible for the atmospheric CH_4 consumption are methane oxidizing bacteria (MOB) that comprises a high affinity version of the particulate methane monooxygenase (pMMO) enzyme (Baani & Liesack, 2008). More recently, members of *Methylocystis* and *Methylosinus*, has been found to, in addition to the low affinity pMMO, have a high affinity version of the pMMO enzymes which enables them to uphold cell maintenance under periods with low CH_4 availability (Cai et al., 2016).

USCα

Recently a cultivated member of the USCα clade, *Methylocapsa* gorgona MG08 (Tveit et al., 2019) has given more insight into the biology and phylogeny of the USCα clade. Phylogenetically, USCα is classified as type IIb (*Beijerickiaceae*) methanotrophs, and the recent discovery of *M. gorgona* suggest that by extension, all members of the USCα are of the genus *Methylocapsa* (Tveit et al., 2019). Members of the USCα has been identified as the dominant MOB in upland soils with acidic to neutral pH (Degelmann et al., 2010; Kolb et al., 2005). A screening of the 16S rRNA sequence of *M. gorgona* through all publicly available 16S rRNA datasets showed that the *M. gorgona* was globally widely distributed, ranging from the high latitudes of the Arctic, till Australia and New Zealand (Tveit et al., 2019). This includes hydromorphic soils (Knief et al., 2006; Shrestha et al., 2012), Arctic acidic upland soil (Lau et al., 2015; Martineau et al., 2014), and a glacier forefield (Chiri et al., 2017)

USCγ

USCγ, belongs to the class of Gammaproteobacteria and is classified as type Id MOB, a group comprised of the clade of *Nitrosococcus* and related uncultivated clusters (Knief, 2015). However, in some literature sited in this thesis, the USCγ is classified as type Ic (e.g. in Chiri et al. (2017)). MOB of the USCγ is mostly found in neutral to alkaline soil, hereby an alpine

meadow (Zheng et al., 2012), a former lake (Serrano-Silva et al., 2014), glacier forefields (Chiri et al., 2017; Nauer et al., 2012), a karst cave (Zhao et al., 2018), and an arid desert ecosystems (Angel & Conrad, 2009). The distribution of the two USC groups is thereby assumed to be highly determined by pH (Knief et al., 2003; Martineau et al., 2014). However, Nauer et al. (2012) reports USCγ to be the dominant MOB in the top soil of a 20 year old siliceous glacier forefield in the Swiss Alps with pH of 4.88, contradicting the perception of USCγ being solely constrained to neutral and alkaline environments. Further, the presence of the USC at sub atmospheric CH_4 concentrations down to 0.65 ppm (Zhao et al., 2018), suggest an adaptation to highly oligotrophic environments, with minimal CH_4 supply.

Notably, a potential pit fall in determining USC abundance is that the primer pair A189f/mb661r is known to highly discriminate USCα, and is in general less efficient in amplifying *Alphaproteobacteria* methanotrophs (Bourne et al., 2001). Therefore, the abundance of USCα can be underestimated if only the above-mentioned primer pair is used. To get the best coverage of the MOB community, a combination of the forward primer A189f with each of the three reverse primers A682r, mb661r and A650r has been recommended (Bourne et al., 2001; Knief, 2015).

Moreover, as for methanotrophs in general, the USCγ and α abundance is demonstrated to be reduced when the ecosystem is subjected to anthropogenic disturbance such as deforesting, nitrogen deposition, fertilization and acidification (Abell et al., 2009; Dorr et al., 2010). Reoccurs when nitrogen fertilization is reduced (Shrestha et al., 2012).

1.7 Methods for studying microbial biodiversity

Microbial ecology studies was revolutionized with Woese and Fox (1977) discovery of the 16S rRNA gene as a phylogenetic marker gene and a distinction of the three domains (Bacteria, Archaea and Eukarya) we refer to today. The characteristics of the 16S rRNA gene, being conserved through evolution, yet possess hypervariable regions, allows for species specific identification of bacterial and archaeal taxa (Kolbert & Persing, 1999; Pereira et al., 2010). In addition to the 16S rRNA gene, several conserved genes for functional traits show similar

characteristics as the 16S rRNA gene and are frequently used as functional marker genes for the respective functional guilds. Functional genes include the abovementioned *pmoA* and *mcrA* genes for MOB and methanotrophs respectively. In addition the whole nitrogen cycle could be targeted by the *nifH* gene for nitrification, *amoA* for ammonia oxidizing bacteria and archaea (AOB, AOA), *narG* gene targeting denitrifiers, *nirS* which encodes the gene for nitrite reductase and *nosZ* the gene for nitrous oxide reductase (Braker et al., 1998; Francis et al., 2005; Henry et al., 2006; Holmes et al., 1995; López-Gutiérrez et al., 2004; Okano et al., 2004; Rösch & Bothe, 2005).

Studying microbial communities is a study of soil microbial diversity, which includes, species-, genetic and ecosystem diversity. Species diversity is based on species richness, species evenness, total number of species present and species distribution (Øvreås, 2000). Dependency on cultivation and/or their expression of phenotypic traits has been a limitation with traditional methods. However, there are several biochemical and molecular methods that overcome this limitation.

1.7.1 Biochemical methods

Mainly, biochemical analysis is mainly analysis of signature lipid biomarkers. A limited number of bacteria and archaea have proven to be cultivable and it is estimated that only between 0.1% to 1% of the bacterial diversity is cultivated (Torsvik et al., 1998). Efforts to cultivate bacteria is however important as it is key to revealing the metabolic, physiological and biochemical properties of an organism and related taxa. A biochemical method that avoids cultivation efforts is analysis of signature lipid biomarkers (SLB). Fatty acid methyl ester (FAME) relies on signature fatty acids in the relatively homogenous proportion of fatty acids in cell biomass (Kirk et al., 2004). Differences in microbial biomass would be represented by changes in the fatty acid profile. Analysis of phospholipid fatty acid (PLFA) fingerprints is often used to highlight adaptation strategies activated by microorganism to environmental changes (Zelles, 1999).

1.7.2 Molecular methods

Fluorescent In-Situ Hybridization (FISH) relies on fluorescent probes to target a region of interest. The FISH technique is versatile and can target both archaea and bacteria, active cells can be identified by probes targeting mRNA. Probes for functional groups is also frequently used. A mixture of probes can be applied to identify specific combinations, i.e. active part of a certain fraction of the microbial community. FISH is a visual identification method and cells can be quantified by counting. It is a fast and easy way of detecting and quantifying certain groups in the environment, taxonomical classification by FISH, however, often depend solely on morphology and is highly challenging.

Microbial diagnostic microarray (MDM) utilizes DNA hybridization technologies to analyse environmental samples by applying environmental DNA or RNA to a matrix of functional gene specific probes (i.e *pmoA*), and analysing hybridization signal strength to infer phylogenetic affiliations (Wu et al., 2001). Bodrossy et al. (2003) developed a MDM containing 59 probes for detecting MOB from environmental samples, later Stralis-Pavese et al. (2011) extended this to account for 199 probes targeting approximately 50 species-level clades. Efforts have been made to be able to simultaneously quantify the detected microorganisms, but this proved problematic when using oligonucleotide probes, since it requires a twocolored quantification approach, hybridizing the samples with one colour against a hybridized reference set of strains/clones with another colour and determine quantification data from the ratios between the two colours (Bodrossy et al., 2003).

Metagenomics include amplicon sequencing and shotgun sequencing. Shotgun sequencing amplifies and sequences all environmental DNA or RNA (cDNA), and thereby accesses the whole genomic potential (DNA) and the activity (RNA) of microbial communities. Amplicons are PCR-amplified genes from environmental DNA or cDNA. Amplification of the 16S rRNA gene has been widely used in metagenomics to assess the prokaryotic diversity and abundance in all types of environments including soil (Bach et al., 2018; Borsetto et al., 2019). Conserved functional genes that have diverged sufficiently to possess hypervariable regions that can be utilized to elucidate phylogenetic relationship are also frequently used. Amplicons are subjected to hi-throughput sequencing by a next generation sequencing platform, for example the

sequence by synthesis platforms Illumina HiSeq and Illumina MiSeq or the pyrosequencing platform 454 Life Sciences by Roche. Sequencing of environmental DNA allows for species-specific identification through bioinformatic analysis of the hypervariable regions of either the 16S rRNA gene or a functional gene. Moreover, taxonomic identification and the possibility to deduce abundance data from amplicon sequencing, makes it a powerful tool to infer community structure in microbial ecology.

Stable isotope probing is often used in combination with sequencing techniques to highlight the link between microorganisms and its ecological function (Dumont & Murrell, 2005). DNA or RNA extractions from soil incubated with a stable isotope labelled (often C^{13}) substrate are separated by centrifugation in a density gradient. Then, when separated, amplicon sequencing of isotope labelled DNA can be used to identify which microorganisms that has been active and assimilated the isotope substrate (Leake et al., 2006).

Denaturing gradient gel electrophoresis (DGGE) and temperature gradient gel electrophoresis (TGGE) are two frequently used methods, often termed DNA fingerprinting. DNA fragments are subjected to a denaturing gradient gel electrophorese which denatures and separates DNA based on base composition and the GC content of the fragment. This produces a DNA profile (DNA fingerprint) of the sample and is a representation of the community composition (if using 16S rRNA gene), band intensities can give an indication of abundance. Further, the DNA fragments can be excised and sequenced. The difference between TGGE and DGGE is that TGGE uses temperature to denature the DNA fragments.

Aims

We aim to study the biodiversity and structure of the terrestrial microbial community along environmental gradients in the Arctic. A comprehensive sequence dataset was used to analyse the bacterial community structure and more specific, the methane oxidising community. These results are the platform for further studies of the microbial community related to seasons and longer-term perspectives. Ultimately, we aim to obtain data that allows us to make predictions on how these communities will be affected by future climate change scenarios and the potential feedback mechanisms to the climate system. In addition, the purpose of this thesis was to learn

bioinformatical processing of sequence data and statistical methods used in microbial ecology. Here we use amplicon sequencing of the 16SrRNA gene and the MOB specific gene, *pmoA* to map both the bacterial community, and the methane oxidizing community.

2. Materials and methods

Data

This thesis is written in agreement with a BiodivERsA project termed Climarctic. The rights to use data acquired in the project was given by the project leaders. All data on physical and chemical soil properties was obtained by project collaborates. The bioinformatic processing of sequence data was done by Postdoc Christophe Victor Seppey. Thus, mainly library preparation of the *pmoA* gene and statistical analysis of sequence data from both the 16S rRNA gene and *pmoA* gene, in addition to DNA extractions of some samples were done by this thesis author. However, the material and methods section describe all steps done to obtain the data presented in this thesis.

2.1 Study sites

This study was conducted at Kongsfjorden International Research Base in Ny-Ålesund (Svalbard, Norway, 78°55′26.33’’N, 11°55′23.84’’E). The research station is a model system for the High Arctic with many institutions and countries contributing to arctic science and surveillance of the arctic environment. Environmental characteristics in Ny-Ålesund includes a variety of different soil and glacier types, geological features, and hence habitats such as polar

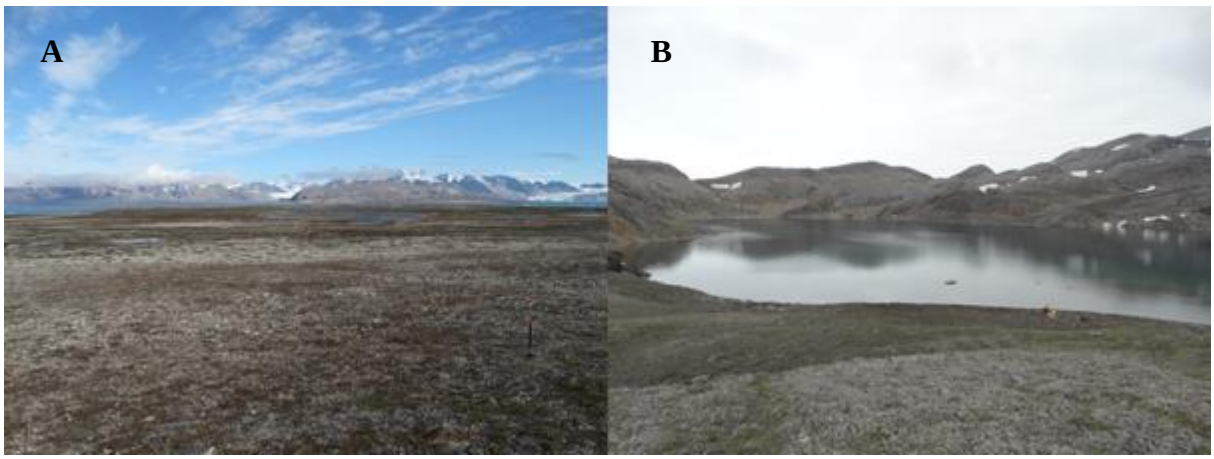

Figure 2: The two study sites, A; Knudsenheia (KH) and B; Ossian Sarsfjellet (OS)

semi-desert, wet moss tundra, and ornithogenic soils, due to its coastal terrestrial nature. Ny-Ålesund demonstrate relatively mild climatic conditions compared to other regions at the same latitudes, caused by input of warm Atlantic water masses, transported by the West-Spitsbergen Current into the Arctic Ocean. This results in relatively mild mean summer and winter temperature of 5°C and -15°C, respectively (Statistisk Sentralbyrå, SSB). However, during winter, prolonged periods with low temperatures between -20°C and -35°C can occur, typically between December and April. The precipitation is quite low, averaging at 470 mm annually with 70% typically falling between October and May, when snow cover is usually complete (Norwegian Meteorological Institute). Two study sites with clear moisture gradients were chosen in the study area: (1) Knudsenheia (KH) a wetland located approximately three km north-east of Ny-Ålesund (Figure 2A) and (2) Ossian Sarsfjellet (OS) a Nature Reserve approximately 12 km north-west of Ny-Ålesund across the Kongsfjorden (Figure 2B).

2.2 Experimental design and sampling

The KH moisture gradient was established from the north, north-eastern littoral zone of a wide, shallow pond towards decreasing soil moisture in a south-southwestern orientation. In OS, the transect decreases in soil moisture from the shore of Sarsvatnet towards an elevated ridge in a north by western orientation (Figure 2). In both study areas the soil moisture gradient constituted three subsites: dry, intermediate and wet, each with three 1m^2 replicate plots. Each

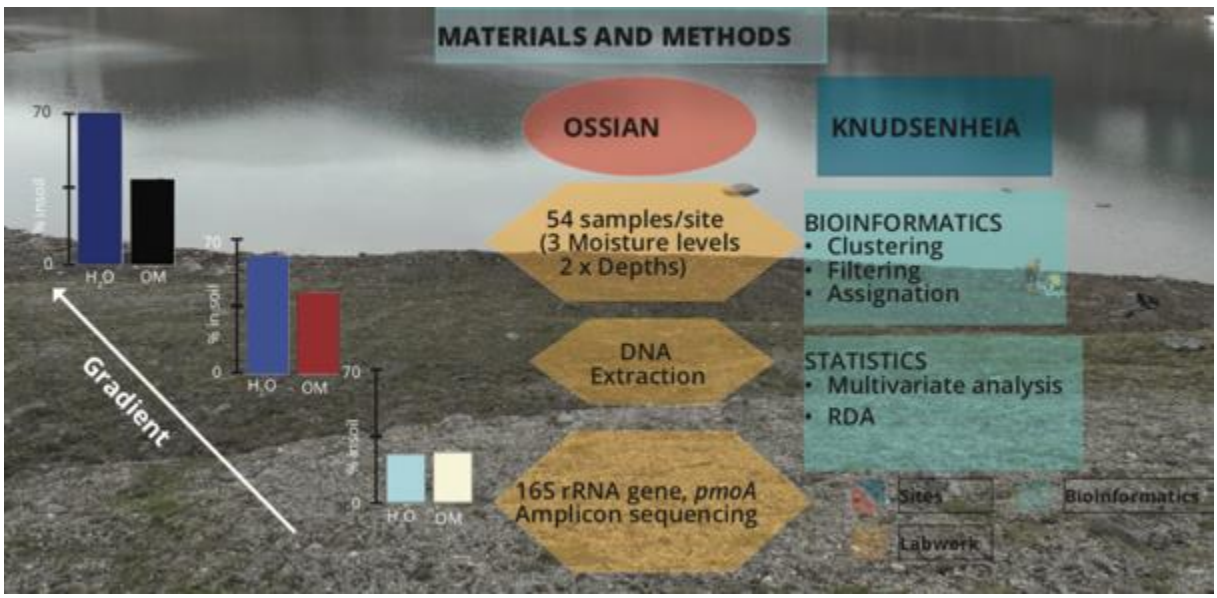

Figure 3: Overview of materials and method section. Illustration of the gradient selected in OS with the soil moisture content in percentage per moisture level. In yellow is the work done in laboratory, while light blue illustrate the work done in silico.

plot was divided into 4 sub quadrats, whereof 3 were selected for sampling. Furthermore, soil was collected at two different depths: the top layer (0-1 cm) and the deeper layer (5-10 cm). In total, 54 soil samples (3 subsites x 3 plots (replicates) x 3 sub quadrats x 2 soil depths) were collected per site. Each sample was homogenized by hand in a plastic bag to obtain representative samples. Subsamples were taken from homogenised soil and dried at 60°C within 24h after collection designated for soil analysis. Samples for molecular analysis were kept in - 80 °C until nucleic acid extraction in home laboratory. The sample campaign took place in July 2017. All plot details concerning GPS, altitude, and physical-chemical soil parameters are summarized in (Kern et al., 2019).

2.3 Physical and chemical soil analysis

To determine soil moisture content (MC), about 20 g of fresh soil of each sample, were sieved (2 mm) and weighed while fresh and then re-weighted after soils were dried at 105°C. The weight difference between wet and dry soil was used to calculate the gravimetric soil water content, expressed as percentage of fresh weight (Eq.1).

$$\%\, H_2O = \frac{Fresh\ weight - Dry\ weight}{Wet\ weight} \times 100 \qquad \textbf{(Eq. 1)}$$

Thereafter a combustion step followed at 450°C for 5 h to assess the amount of organic matter. The organic matter content was expressed as percentage of total dry mass (Eq. 2).

$$\%\, Organic\ matter = \frac{Dry\ weight - Combusted\ weight}{Dry\ weight} \times 100 \qquad \textbf{(Eq. 2)}$$

The pH was measured for each soil sample with a glass electrode connected to a pH meter in aqueous soil-extract (soil:aqua regia ratio of 1:2) (FEP20-FiveEasy Plus, Mettler-Toledo GmbH, Switzerland).

Dried soil subsamples (see above) were sieved (2 mm) and stored at room temperature prior to

nutrient analysis. Total carbon (TC) and total nitrogen (TN) were determined by dry combustion after grinding dried subsamples using a CNS VARIO EL analyser (Elementar Analysensysteme GmbH, Germany).

2.4 Soil grinding and DNA extractions

Subsamples from KH and OH were manually grinded in liquid nitrogen using a pestle and mortar. Finely grinded soil was transferred to 15 ml Falcon tubes and stored in -80°C, prior to DNA extractions. The DNA extraction and purification steps were performed using Qiagen RNeasy® PowerSoil® Total RNA Kit (Qiagen) coupled with the RNeasy® PowerSoil® DNA Elution Kit (Qiagen) with following modifications: the protocol suggested that 2.0 g of soil is adequate to provide a sufficient amount of DNA for analysis. However, based on personal communication with laboratory technician Alena Didriksen, a decision was made to use up to 4.0 grams of soil from the deeper layers to get sufficient amount of DNA for PCR. In the 12th step of the protocol, an incubation at 45°C followed by vortexing was needed to resuspend the pellets. This was to be repeated until pellets were completely resuspended. However, if the pellets were hard to resuspend after repeating the incubation and vortexing process, the vortexing step was replaced with dragging the bottom of the tubes in a slight angle up and down along a tube-rack to detach the pellet from the collection tube surface and fully resuspend it in Solution SR5. Following the step of washing the JetStar Column with Solution SR5 to remove unbound contaminants (step 15), the protocol for the DNA Elution Kit was followed herein according to kit protocol. Final elution of DNA was done in H_2O to a volume of 50µl instead of 100µl to increase DNA concentration. The kit required a phenol/chloroform/isoamylalcohol solution which was made by mixing the reagents in the ratio 1:1:24 (pH 6.5 – 8) to a final volume that covered the samples designated for DNA extraction. To ensure RNA free DNA isolation, the samples were treated with 10 µg/ml RNase-A. The quality of the extracted DNA was measured by applying 1µl of sample to a Nanodrop 1000 spectrophotometer (Thermo Fischer).

2.5 Library preparation 16S and *pmoA*

The library preparations followed the instructions given in Ilumina 16S Metagenomic Sequencing Library Preparations (Amplicon PCR, 2013) with modifications for the

A189f/mb661r primers (Table 1) and A189f/A682 (Table S2) for amplifying the *pmoA* gene and the primers for *mcrA* for methanogens (Table S2). The modifications were; specific PCR programs for the respective primers to maximize template for sequencing. During the clean-up, the concentration of AMPure Beads was specified to target the *pmoA* length fragments from the PCR. The general steps of the library preparation is: 1. an initial PCR, followed by a PCR clean-up to obtain pure amplicon DNA, which is run on a agarose gel to confirm PCR product, 2. a quantification by Qubit and normalization, 3. a second PCR to attach indices, followed by 4. a final quantification and normalization before sequencing.

Table 1: Primers and adapters used for amplifying the *pmoA* and 16S rRNA genes in PCR reactions.

Primers	**Primer sequence**
A189f (*pmoA*)(Holmes et al., 1995)	5'-GGNGACTGGGACTTCTGG-3'
mb661r(*pmoA*)(Costello & Lidstrom, 1999)	5'-CCGGMGCAACGTCYTTACC-3'
A682r (*pmoA*)(Holmes et al., 1995)	5'-GAASGCNGAGAAGAASGC-3'
pA (16S rRNA gene)(U. Edwards et al., 1989)	5'-AGAGTTTGATCCTGGCTCAG-3'
BKL1 (16S rRNA gene)(Tytgat et al., 2014)	5'-GTATTACCGCGGCTGCTGGCA-3'

Adapters	**Adapter sequence**
Forward overhang	5' TCGTCGGCAGCGTCAGATGTGTATAAGAGACAG-3'
Reverse overhang	5' GTCTCGTGGGCTCGGAGATGTGTATAAGAGACAG-3'

2.5.1 PCR Amplification of pmoA gene with A189f/mb661 and A189f/A682 primers

Separate PCR reactions were conducted for the reverse primers mb661r and A682 in combination with forward primer A189f. A PCR reagent mix from FastStart High Fidelity PCR system by Roche was used. In a 25 µl PCR reaction, the following reagents were combined, 2.5 µl reaction buffer (with $MgCl_2$), 2.5 µl dNTP (2mM to a concentration of 0.2 mM in the reaction), 0.25 µl taq FastStart enzyme, 1 µl primers (10µM to a concentration of 0.4 µM in reaction) 1 µl soil DNA template (15ng μl^{-1}), and 16.75 µl H_2O. The reagents were added in decreasing order according to volume. The PCR reaction was initialized with a 4 min initial denaturation step at 94°C, followed by 35 cycles of 30 sec denaturation at 94°C, 1 min

annealing, 3 min elongation at 72°C, and a final elongation step of 20 min at 72°C. Duplicates of PCR were performed for each sample and pooled prior to the clean-up step.

2.5.2 PCR Amplification of 16Sr RNA gene

Primers pAf and BKL1 (Table 1) was used to amplify the 16S rRNA gene region V1-V3 (Tytgat et al., 2014). The amplicon library preparation process of the 16S rRNA gene was conducted by Climarctic project collaborators, at the University of Ghent (Belgium), Department of Biology by the Protistology and Aquatic Ecology research group.

2.5.3 PCR Amplification of mcrA gene

To optimize PCR product for the *mcrA* gene, several PCR protocols were tested on samples from wet soil (T31, T37, T39, T43, T44, T45, T47). A initial PCR was performed using FastStart High Fidelity PCR system (Roche) with 2.5 µl reaction buffer (with $MgCl_2$), 0.2 mM dNTP's, 0.4 µM primers (mlasf, mcrArev, see Table S2) (Steinberg & Regan, 2008), 2.5 U taq FastStart enzyme, 1 µl soil DNA template (15ng μl^{-1}) and filled with dH_2O to obtain a 25 µl reaction. The PCR program was as described in Steinberg and Regan (2008) using an Biometra TProfessional Standard Thermocycler. A second PCR was performed on the same samples as above using the same amount of PCR reagents as described above, except with primers from Luton et al. (2002) (MLf and MLr, see Table S2). The PCR cycle was performed according to the program given in Frey et al. (2011) with a 60 sec denaturation step in the cycles. A third 25 µl test PCR reaction was set up for the abovementioned samples using 30 ng template DNA, 1 x PCR buffer (without $MgCl_2$), 2 U taq enzyme blend, 2 mM $MgCl_2$, 20 pmol of each primer, and 0.4 mM dNTP's (Frey et al., 2011). The PCR program was the same as described in Frey et al. (2011). Of the PCR product, 15µl was run on a 0.8 % agarose gel to check for product.

2.5.4 PCR cleanup

Clean-up of PCR product was done using Solid Phase Reversible Immobilization (SPRI) beads, AMPure XP beads (Agencourt), magnetic beads coated with negative carboxyl groups, which binds aggregated DNA in a NaCl, PEG buffer. It binds a certain length of DNA fragment based

on the concentration of AMPure beads used in the clean-up and releases it during a rinsing step with Tris ph 8.7 (10mM) or molecular biology grade H_2O.

Beads that had obtained room temperature was vortexed to evenly disperse the beads in the solution. Using a pipette, 35µl of AMPure XP beads were distributed to the PCR tubes containing PCR-product to obtain a concentration of 0.7X AMPure XP beads. After aliquoting the AMPure XP beads, the entire sample solutions were pipetted up and down 10 x times, then the tubes were incubated for 5 min at room temperature. The tubes were thereafter put on a magnetic stand and let adhere for two minutes or until the supernatant had cleared, then the supernatant was discarded. Thereafter, two washing steps with 80% ethanol (EtOH) followed; while on the magnetic stand, 200µl 80% EtOH was added to the tubes, and incubated at room temperature for 30 sec, and carefully discarded. This was repeated a second time with an extra removal of excess EtOH with a fine pipet tip. The beads were let air dry for approximately 10 min at room temperature. The tubes were then removed from the magnetic stand and added 26.25µl of RNase free water and pipetted up and down until the AMPure XP beads were fully resuspended. Then the plate was put on a magnetic stand and let stay until supernatant cleared. A pipette was used to transfer 25µl of the DNA-supernatant to new PCR tubes.

2.5.5 Gel-electrophoresis

Following the clean-up process, 0.8 % agarose gels were made by measuring 32 mg agarose (Sigma-Aldrich) in a plastic measuring ship and allocating to a clean Erlenmeyer flask. Thereafter, 40 ml of TAE buffer was poured into the flask and put in a Microwave oven on 700W until the agarose was fully dissolved. The hot agarose liquid was cooled down to 60°C in room temperature and added 4 µl of GelRed with a pipette and mixed carefully before it was poured into a gel-mould with 20 wells and let set for approximately 20 min. Of the cleaned PCR product, 10µl was mixed with 2µl loading dye by pipetting carefully up and down until fully suspended and loaded to the wells. A 1kb DNA ladder (GeneRuler, Thermo Scientific) was used in 2 µl to get fragment length. Gels were run for 20 min at 100V. After running the gels, the gels were placed on a GelDoc (Bio-Rad, ChemiDoc™ MP) imaging system and the program was manually set to nucleic acid, with automated exposure time. Gel pictures of *pmoA*

amplicons generated by the reverse primers mb661r and A682r are shown in Appendix (Figure S2-S8).

2.5.6 Quantification of amplicon DNA by Qubit™.

A fluorometric quantification of amplicon DNA was estimated with a Qubit™ ds DNA High Sensitivity Assay executed according to manufacturer's description on a Qubit™ 3.0 fluorometer (Qubit™ Invitrogen, www.invitrogen.com/qubit). The Qubit working solution was made by mixing 1µl Qubit™ Reagent per sample plus two standards with 199 µl Qubit™ buffer per sample and standard. Two Assay Tubes for the standards were set up by allocating 190µl of buffer per standard into the AssayTubes and adding 10µl of standard solution I and II to the respective tube to a final volume of 200µl. For the samples, 1µl of sample was mixed with 199µl of buffer to a final volume of 200µl. Standards and samples were then vortexed for 2-3 seconds and incubated at room temperature for 2 minutes prior to analysing. The Qubit™ 3.0 fluorometer was set to the ds DNA Hi-Sensitivity setting. On the fluorometer the standards were read in order I and II, before the samples were analysed.

2.5.5 Illumina sequencing

The final steps of library preparations, including, index PCR and normalization, was performed at the University of Ghent (Belgium), Department of Biology by the Protistology and Aquatic Ecology research group prior to sequencing with Illumina MiSeq.

2.6 Bioinformatics pipeline

Raw sequences were received demultiplexed from the sequencing facility. The bioinformatics pipeline was performed in three steps: a pre-processing step, a clustering step and an assignation step. The pre-processing step was initialized by merging of paired end reads with the program PEAR (PEAR - Pair End reAds mergeR, https://cme.h-its.org/exelixis/web/software/pear/). This was followed by a filtering step were the reads were filter by size, 400 – 650 bp for 16S DNA (V1-V3 region), 500-510 bp for *pmoA* (A189f/mb661r) and 530-535 bp for *pmoA* (A189f/A682r). Further, a truncation by quality, were the reads were truncated if 2 nucleotides in a row had a phred-score below 30, and a max expected error = 1. Chimeras were removed

with the UCHIME algorithm in the open source tool suite vsearch (Rognes et al., 2016). Reads including a stop codon or not having a nucleotide number divisible by three were discarded in order to avoid frameshift errors. The clustering was done in vsearch with an OTU cut-off for 16S at 97% and 86% for *pmoA* (Wen et al., 2016). The classification was done based on the Silva database for 16S rRNA gene data and Wen et al. (2016) for the *pmoA* OTUs using a RDP classifier, a Näive Bayesian classifier to assign OTUs from domain to genus (Wang et al., 2007).

2.7 Statistics and phylogenetics

A standard Pearson correlation test was used to test for linear relationships among the measures soil variables (Pearson, 1931). Species richness (Shannon indices) was calculated from a relative abundance OTU-table using the *diversity* function in the *vegan* package (Oksanen et al., 2007).

2.7.1 Redundancy analysis

Investigations into the response of the bacterial communities to different factors and environmental variables was conducted using a multivariate analysis termed distance based-redundancy analysis (db-RDA)(Legendre & Legendre, 2012). A Hellinger transformed OTU table (Eq. 1) was made with the *decostand* function in the package *vegan* (Oksanen et al., 2007). All statistical analysis were performed in R (R Core, 2019).

$$y'_{ij} = \sqrt{\frac{y_{ij}}{y_{i+}}} \qquad \textbf{(Eq.3)}$$

In Eq. 1, the Hellinger transformed number (y'_{ij}) is the square root of the number of reads from an OTU in a sample (y_{ij}) divided by the row sum of the respective sample y_{i+}. Thereafter, the db-RDA was computed, using the *capscale* function in the R package *vegan,* on a Bray-Curtis dissimilarity matrix (Eq. 2) (Bray & Curtis, 1957) calculated from the Hellinger transformed OTU-matrix by selecting the option *distance = 'bray'*.

$$BC_{ij} = 1 - \frac{2C_{ij}}{S_i + S_j} \qquad \textbf{(Eq. 4)}$$

In Eq. 2, BC_{ij} is the Bray-Curtis distance, C_{ij} is the sum of lesser values only for species shared by the two compared communities and S_i and S_j are the total number of reads per OTU at each site. An ANOVA like permutation test in the *vegan* package, *anova.cca*, was executed with 1000 permutations on the db-RDA to assess the significance of the effect of factors and variables implemented in the db-RDA on both the whole bacterial community (16S rRNA gene) and the MOB-community (*pmoA* gene).

2.7.2 Phylogenetics

Tree-building

Evolutionary relationship of the MOB-OTU's, was inferred by constructing phylogenetic trees in MEGAX (Kumar et al., 2018). Fasta files of *pmoA* amino acid sequences were retrieved from NCBI (Sayers et al., 2019)(https://www.ncbi.nlm.nih.gov). Separate trees were built for the alphaproteobacterial and gammaproteobacterial MOB. Multiple sequences were aligned using ClustalW. For the pairwise sequence alignment the gap opening penalty and gap extension penalty had the default settings of 10.00 and 0.10 respectively. However, for the multiple alignment of amino acid sequences, the gap opening penalty was set to 3.0 and the gap extension penalty set to 1.8 as suggested by Hall (2013). Sequences were manually truncated after alignment to obtain equal length sequences for further analysis. An assessment of the best combination of amino acid substitution model and distribution of rate differences among sites were performed in MEGAX. It compares the combination of 16 substitution models and 4 distribution models to compute the best combined model for the given data. The combination of amino acid substitution model and suggested distribution of rate differences among sites with the lowest Aikaike criterion (AIC) score was chosen. The maximum likelihood (ML) tree was calculated based on initial trees constructed automatically by using Neighbor-Join and BioNJ algorithms to a pairwise distance matrix estimated from a Jones Taylor Thornton amino acid substitution model (Jones et al., 1992), selecting the topology with a superior log likelihood value. Further, the Le and Gascuel (2008) model was applied to infer the evolutionary history assuming a discrete Gamma distribution with 4 categories of the evolutionary substitution rate differences between sites. To ensure a sufficient robustness of the trees, a bootstrapping with

1000 re-samplings was performed. For the gammaproteobacterial MOB tree, the sequences of the alphaproteobacterial *Methylocystis* sp. SC2, *Methylosinus trichosporium* OB3b and *Methylosinus sporium* M242 were used to root the tree. For the alphaproteobacterial MOB tree, sequences of the gammproteobacterial *Methylococcus capsulatus* Bath, *Methyloparacoccus murellii* R-49797 and *Methylogaea oryzae* JCM were used to root the tree.

3. Results

Soils were characterized based on chemical and physical soil properties. Gravimetric water content (MC), pH, organic matter (OM), total carbon (TC) and total nitrogen (TN) constitutes the chemical soil parameter. Grain coarseness, divided into sand, silt and clay, constitutes the physical soil properties. Data from the top layers are presented in (Kern et al., 2019). A table of data for all samples are shown in Table S1.

3.1. Soil characteristics

3.1.1 Gravimetric water content

Moisture content (MC), ranges from 15.1 ± 3.7 % to 70.0 ± 10.0 %, where the former represents the deep layer of the KH intermediate site, and the latter represent the top layer at the wet site at KH (Table 2). A natural moisture gradient was observed at each site within the top layers and within the combined mean values for top and deep layers. However, when considering only the deep layers, the moisture content at the intermediate site at KH is slightly lower than the dry site. In contrast, the intermediate site at OS is considerably higher in water content than the wet site. Overall, the combined mean value for MC at each site, show that KH has a higher mean water content than OS, with 36.2 ± 23.3 % at KH, compared to 29.9 ± 11.0 % at OS, albeit with higher variation at KH. Further, the top layers were consistently more humid than the deep layers at both sites and all sites. The largest difference in mean water content between layers within a moisture level was measured at the KH, wet site, ranging from 21.5 ± 2.3 % in the deep layer to 70.0 ± 10.0 % in the top layer. Largest variation in water content was observed at the top layers at KH, while the least variation was overall observed in the deep layers. Differences in water content between the top and deep layers were not as profound in OS as in KH. Generally, OS showed less variation in measured water content in the top layers than in KH.

3.1.2 pH

Mean values for pH along the gradient ranges from 5.5 ± 0.2 in the top layer of the dry site at KH to 7.4 ± 0.2 in the deep layer of the intermediate site at KH (Table 2). However, the pH in the top layer of the dry site at KH (5.5 ± 0.2) is substantially lower than measured for remaining samples, which more constant (6.4 ± 0.1 to 7.4 ± 0.2). Consistently, the top layers within the moisture levels exhibit slightly lower mean pH values than their respective deep layers, with the largest difference measured at the KH dry site. There is a slight negative trend of pH in relation to moisture content (MC), however the correlation does not meet the requirements of being statistically significant (correlation coefficient = -0.2, p-value = 0.056).

3.1.3 Organic matter, total carbon, total nitrogen and carbon nitrogen ratio

There is a considerable difference in the OM content of the top layers and down layers. Overall the OM content in the top layers vary from 12.9 ± 5.1 to 43.8 ± 23.3, while it varies from 2.3 ± 0.4 to 13.9 ± 7.9. Except for the deep layers at the intermediate and wet sites, OS show overall lower levels of OM (Table 2). Moreover, for both KH and OS, the top layer at the intermediate site contains most OM. In the deep layers in all sites, the mean OM content is < 5 % except for the deep layer in the intermediate site (13.9 ± 7.9 %).

Except for in the deep layer of the intermediate site at KH (1.4) and in the deep layer of the wet site at OS (1.5) TC is approximately a factor of 2 less than OM. Consequently, the same trend as for OM is observed in the TC content. The lowest content TC is observed at the wet site and in the deep layer at KH, while the highest content of TC is found at the top layer in the intermediate site in KH. As for OM, there are generally higher proportions of TC at the KH site, than in OS. TC content is similarly to OM higher, at both KH and OS, in the top layer at the intermediate site at OS, resembling that of mineral soils. The same trend for the total nitrogen content as for the OM and TC contents was demonstrated. Highest content of TN for both sites was observed at the intermediate site and in the top layer (1.2 ± 0.4 % and 1.0 ± 0.2 % for KH and OS respectively). For all moisture levels at both KH and OS, the deeper layers exhibited lower contents of TN compared to the top layers. Notably, OM, TC and TN demonstrated strong positive correlations to MC (correlation coefficient = 0.81 – 0.84, p-value < 0.001).

Table 2: Table of soil properties along the moisture gradient from KH and OS. Values from the top sites are presented in (Kern et al., 2019)

			Soil properties					
Site	Site	Layer	MC (%)	pH	TC (%)	TN (%)	OM (%)	C:N
Knudsenheia	Dry	Top	28.1 ± 10.5	5.5 ± 0.2	13.2 ± 4.5	0.7 ± 0.2	29.4 ± 9.7	19.7 ± 1.3
		Deep	19.2 ± 1.6	7.2 ± 0.2	1.8 ± 0.2	0.1 ± 0.0	4.4 ± 0.4	12.5 ± 0.5
	Intermediate	Top	63.4 ± 10.2	6.8 ± 0.1	22.8 ± 10.8	1.2 ± 0.4	43.8 ± 23.3	19.1 ± 2.7
		Deep	15.1 ± 3.7	7.4 ± 0.2	1.9 ± 0.2	0.1 ± 0.0	2.5 ± 0.9	26.9 ± 18.5*
	Wet	Top	70.0 ± 10.0	7.0 ± 0.2	18.5 ± 2.9	1.1 ± 0.1	39.2 ± 12.6	17.5 ± 0.5
		Deep	21.5 ± 2.4	7.3 ± 0.3	1.2 ± 0.2	0.1 ± 0.0	2.3 ± 0.4	13.8 ± 1.2
Ossian-Sarsfjellet	Dry	Top	23.5 ± 3.6	7.3 ± 0.5	6.2 ± 1.0	0.3 ± 0.0	12.9 ± 5.1	17.8 ± 1.6
		Deep	18.6 ± 1.9	7.4 ± 0.2	1.8 ± 0.2	0.1 ± 0.0	3.6 ± 0.8	14.2 ± 0.6
	Intermediate	Top	34.2 ± 6.6	6.4 ± 0.1	17.7 ± 3.6	1.0 ± 0.2	31.4 ± 10.7	18.0 ± 0.7
		Deep	31.8 ± 5.5	6.6 ± 0.2	6.1 ± 1.5	0.4 ± 1.0	13.9 ± 7.9	14.4 ± 0.2
	Wet	Top	48.3 ± 5.7	6.9 ± 0.5	8.0 ± 0.3	0.5 ± 0.1	15.8 ± 3.2	15.4 ± 1.7
		Deep	22.8 ± 5.5	7.2 ± 0.3	2.7 ± 0.8	0.1 ± 0.1	4.1 ± 2.2	18.3 ± 4.1

Shown are calculated means of the respective soil parameters. Mean values for MC are based on 9 datapoints representing the replicates for each combination of site, site and layer. Mean values for pH, TC, TN, OM and C:N are calculated from 3 datapoints representing 1 datapoint from each plot for the combination of site, site and layer. Notably, values for TC, TN and C:N in the OS, intermediate, deep layer are based on 2 datapoints owing to missing values from one plot. The value for pH in the KH, wet, top layer are based on 2 datapoint as there are missing values from one plot.

MC = Moisture Content (percentage of fresh weight)

TC = Total Carbon (percentage of dry weight)

TN = Total Nitrogen (percentage of dry weight)

OM = Organic matter (percentage of dry weight after combustion at 450°C)

C:N = Carbon Nitrogen ratio (TC/TN)

* Data from one plot used to calculate the value was inflated due to a very low measured TN value, this resulted in a high standard deviation.

3.1.4 Physical soil properties

Sand represents the highest granulometric fraction, for each combination of site, moisture and depth (Figure 4). Except for in the deep layer at the wet site at KH (3.8 %), proportions of clay were more or less consistent between both sites and layers, ranging from 6.3 to 12.1 % at KH, and from 9.1 to 14.8 % at OS (Table S1). Still, there was a positive correlation between proportion of clay and WC (Pearson correlation coefficient = 0.46, p-value < 0.001). Differences in soil grain coarseness between sites became more apparent considering proportions of sand and silt. Overall, there was a higher proportion of sand at the KH site (65.5 % to 88.1 %) compared to OS (54.4 % to 71.7 %). In contrast, there was a lower proportion of silt at KH (6.5 % to 25.6 %) compared to OS (19.4 % to 35.5 %). Moreover, a Pearson correlation test showed that there was a moderate negative correlation between proportion of silt and moisture content (WC) (correlation coefficient = - 0.28, p-value = 0.0034).

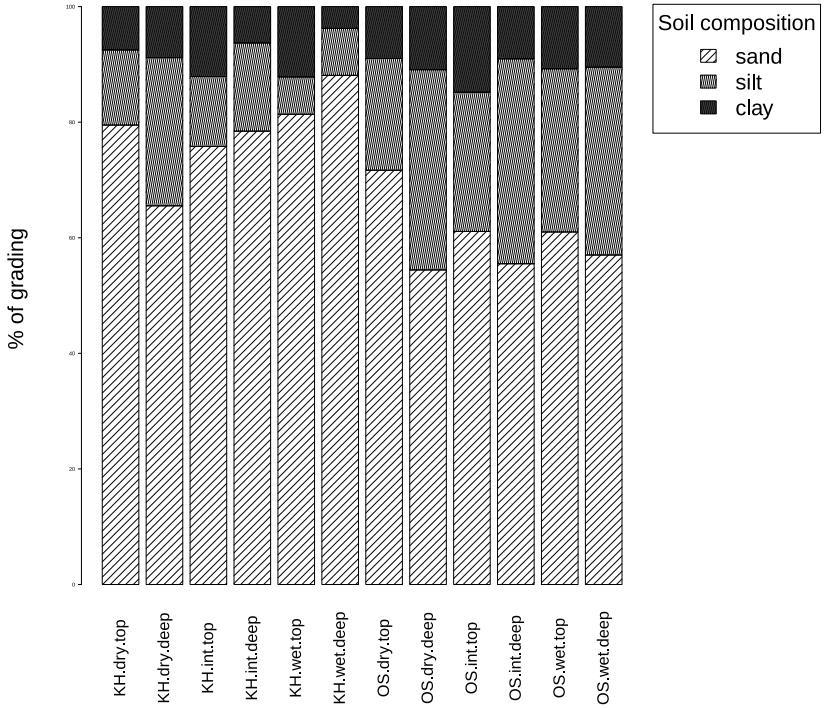

Figure 4: Figure shows the mixture of sand silt and clay at KH and OS along the moisture gradient and at the top and deep layer

3.2 Bacterial community structure (16S rRNA gene)

PCR amplification of the 16S rRNA gene gave product for a total of 94 samples out of totally 108. These samples representing both sites (KH and OS), all moistures (dry, intermediate and wet), and both depths (top and deep). There were 14 samples that did not give any PCR product, whereby the majority (6 samples) represented the wet site at KH (3 top layer, 3 deep layer), 2 samples (1 top layer, 1 deep layer) represented the KH intermediate site. For OS, 6 samples

gave no product, which 3 were from the dry site (1 top layer, 2 deep layer), 2 from the top layer of the wet site and 1 representing the top layer at the intermediate site (Table S1).

3.2.1 Species richness and evenness

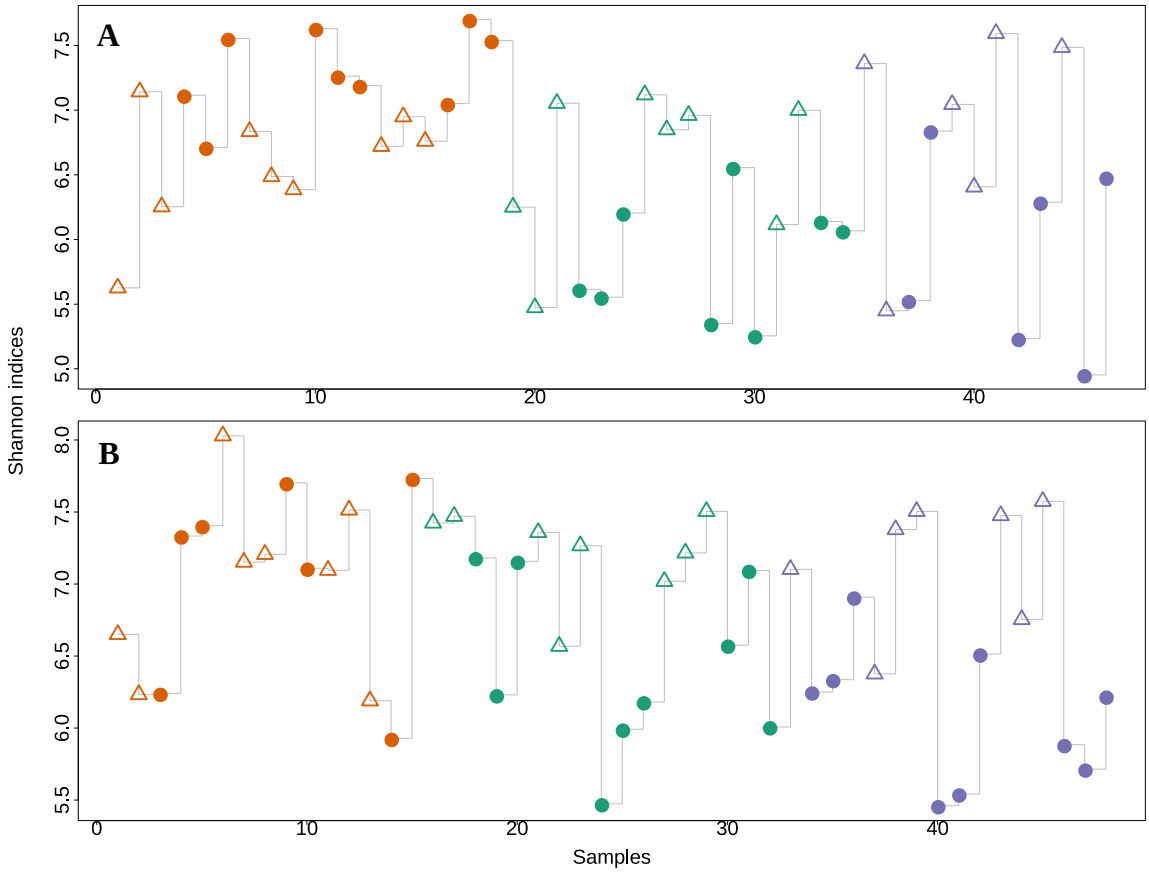

Figure 5: The figure show the Shannon-Wiener indices (richness and evenness) based on relative abundance of OTU's in 94 samples from **A;** Knudsenheia, and **B;** Ossian Sarsfjellet. Top layers are shown by the open triangles, and the deep layers are shown by the filled circles. Colours represent different moisture levels; orange = dry site, green = intermediate, blue = wet.

The nonparametric Shannon-Wiener indices show that there is no apparent relationship between the moisture gradient and the bacterial biodiversity. Plotted in Figure 5 are the calculated species diversity indices from a total of 94 samples (46 KH, 48 OS). The result show that there is great variation in species richness between samples from the same site and layer. However, samples representing the dry site and the deep layer show the highest degree of diversity at KH. Similar trend is observed at OS, where the greatest species diversity seems to be demonstrated in the top layer at the dry site. There are no apparent differences in species richness and evenness between moisture levels, however there is a large variation between samples

3.2.2 Pie charts

When reporting differences in community structure based on the 16S rRNA gene, only the observed differences between the dry and the wet sites (Figure 7 and Figure 8) will be presented. Bacterial community data based on the 16S rRNA gene for the intermediate sites is not included in this thesis. For the MOB community based on the *pmoA* gene, all sites are.

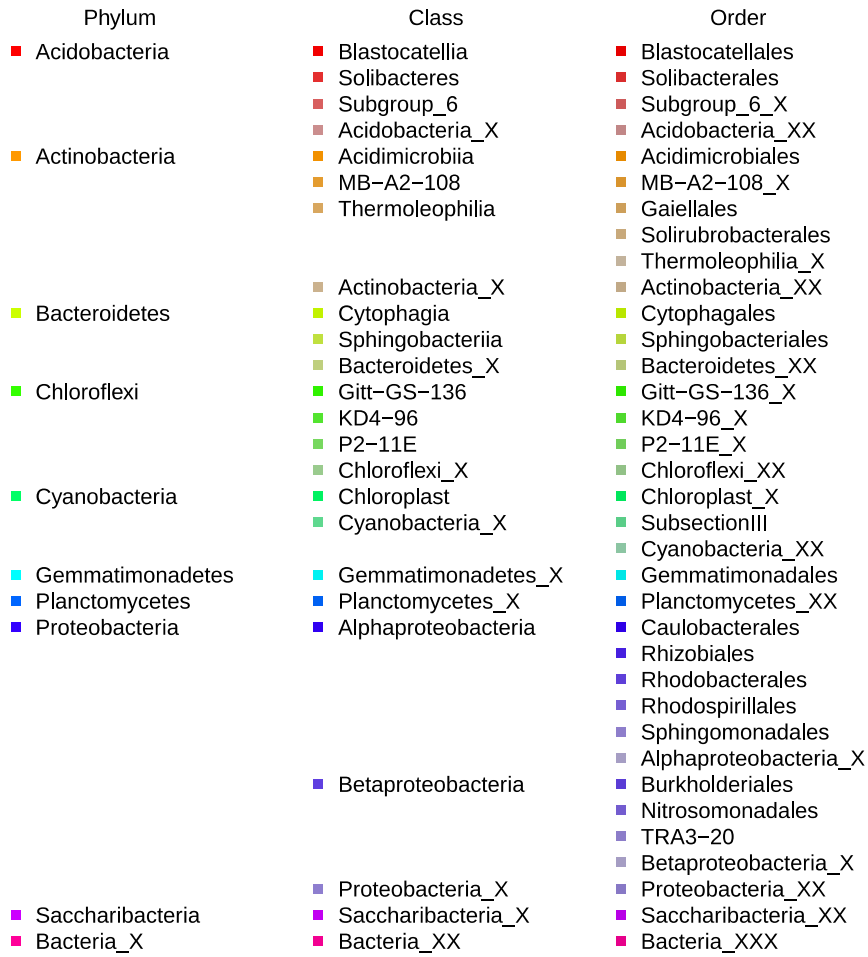

Figure 6: A list of colour codes representing the taxa showed in pie chart (Figure 7 and 8)

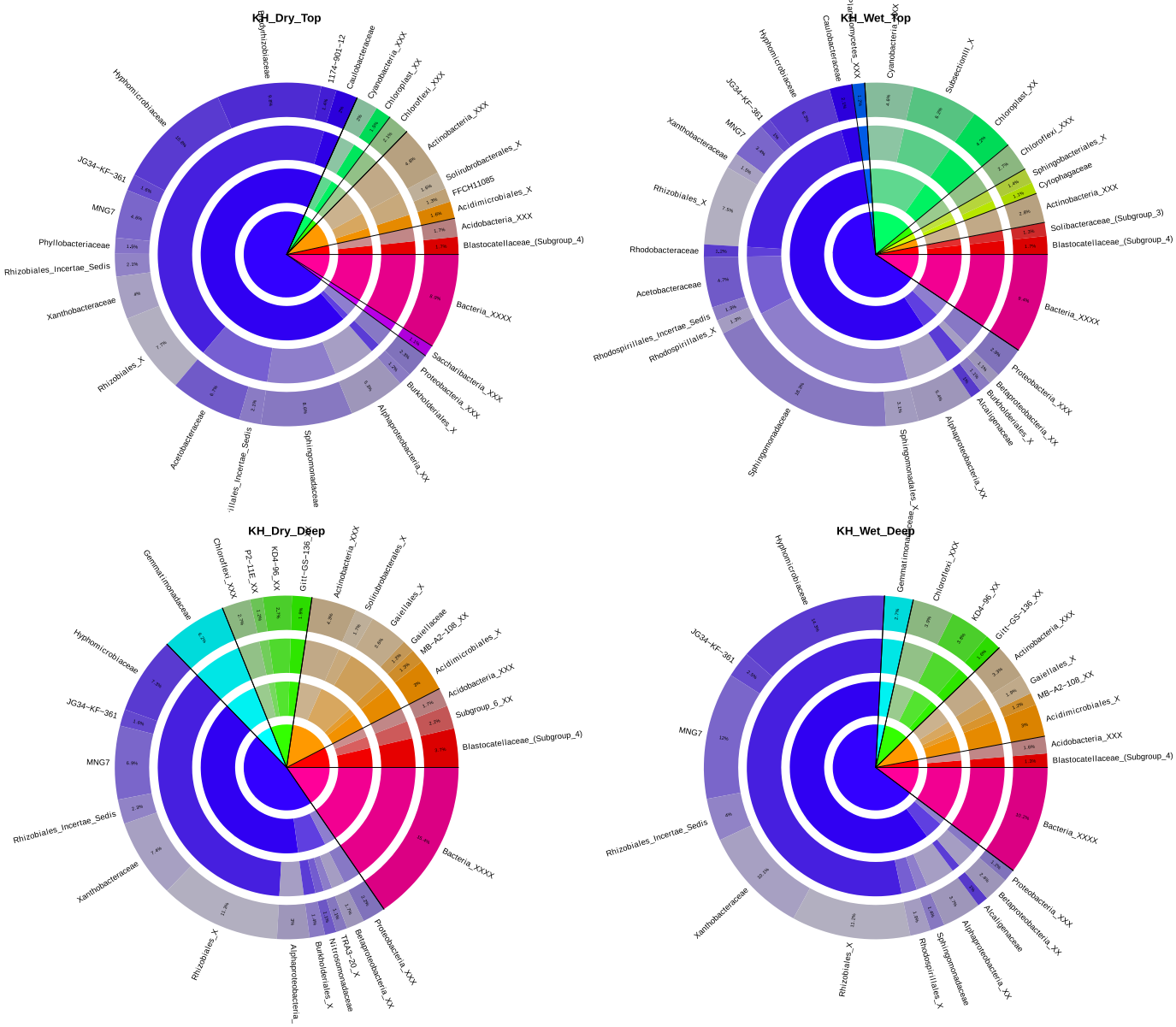

Figure 7: The pie charts show the microbial communities in the top and deep layer of the dry and wet sites for KH. The circles from inner to outer represents the taxonomic levels in the following order: Domain, Phylum, Class and Order, while the text outside diagram represents the Family level. Colours indicating respective taxa are given in the legend. Figure show taxa that make up >1% of the community. Taxa representing <1% of the community is grouped into higher level taxa.

The most dominant phylum is the *Proteobacteria* (47 – 72% of sequences), with *Alphaproteobacteria* (84 – 95 % of *Proteobacteria*) being the most dominant class. The highest relative abundance of *Alphaproteobacteria* is found in the KH dry top layer (Figure 7). The phyla *Actinobacteria* (3 – 15 %), *Chloroflexi* (2 – 14 %), *Acidobacteria* (2 – 7 %) and *Cyanobacteria* (up to 17 %) are present at all sites in various relative abundances. Among the *Alphaproteobacteria*, the order *Rhizhobiales* (34 – 92 %), is the most abundant order in all communities and is mainly represented by the families *Hyphomicrobiaceae* (16 – 32 %), *Xanthobacteriaceae* (8 – 23 %), *Bradyrhizobiaceae* (1 – 23 %) and MNG7 (8 – 22 %). The

proportion of *Hyphomicrobiacea* is relatively similar at KH and OS in both moisture levels and depths. However, the highest relative abundance is found in the top layer of the wet site in KH (14.8% of total community). *Bradyrhizobiaceae* are only found above the 1% threshold in the top layers at the dry sites of both KH and OS, where they constitute a considerable proportion of the community at KH (9% of total community), and slightly less at OS (2.2% of total community). Members of the *Xanthobacteraceae* are found to exhibit higher relative abundance

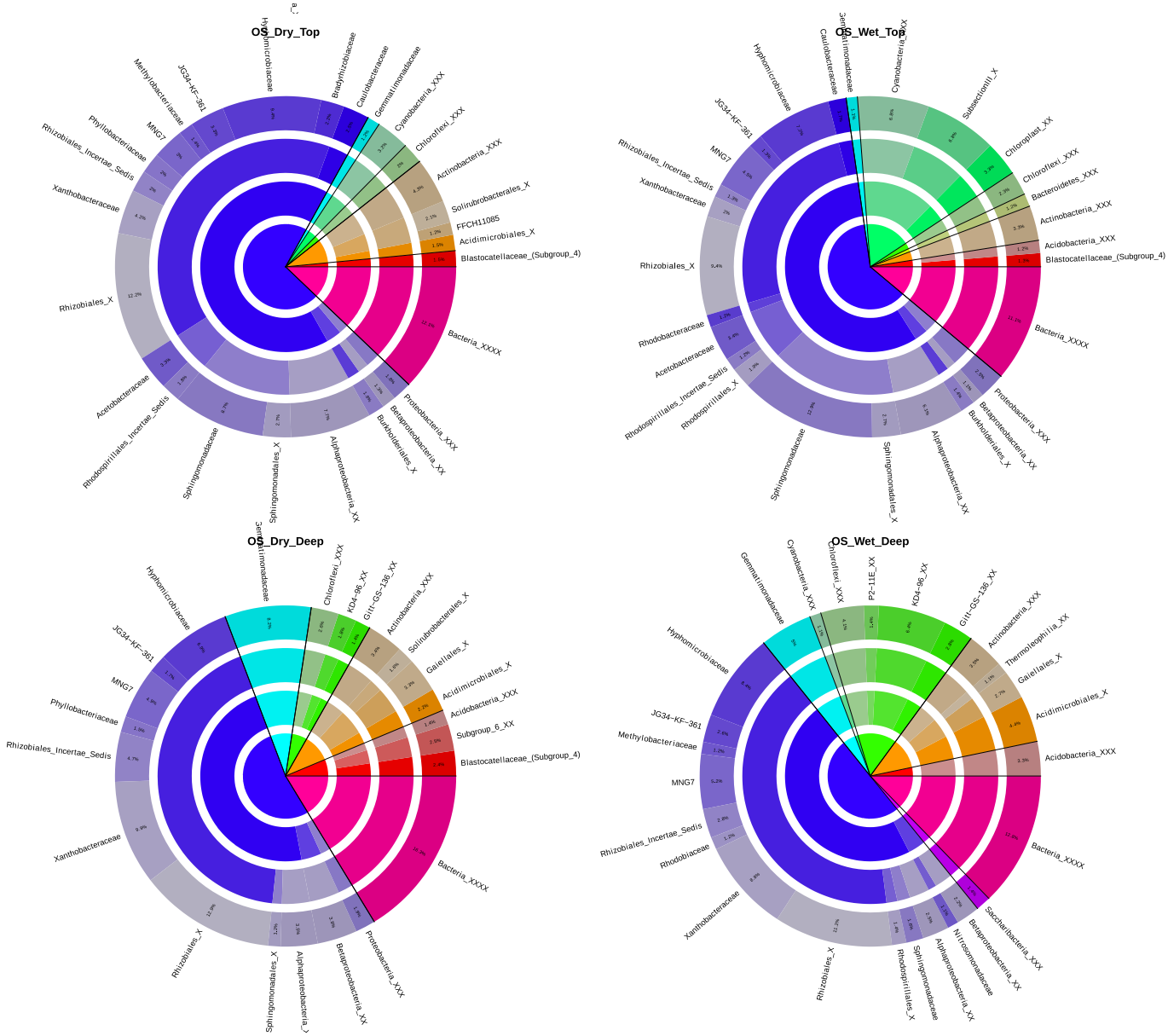

Figure 8: The pie charts show the microbial communities in the top and deep layer of the dry and wet sites for OS. The circles from inner to outer represents the taxonomic levels in the following order: Domain, Phylum, Class and Order, while the text outside diagram represents the Family level. Colours indicating respective taxa are given in the legend. Figure show taxa that make up >1% of the community. Taxa representing <1% of the community is grouped into higher level taxa.

in the deeper layers than in the top layers at both KH and OS (Figure 7 and Figure 8). In contrast, members of the order *Sphingomonadales* and *Rhodospirillales*, mainly represented by the

families *Sphingomonadaceae* and *Acetobacteraceae* respectively, exhibits higher proportions in the top layer communities at both moistures and both sites (KH and OS).

There is a strong positive correlation between the cyanobacterial 16S rRNA gene read counts with MC (correlation coefficient = 0.56, p-value < 0.001). This reflects observed differences in Figure 7 and Figure 8, showing that the relative abundance of *Cyanobacteria* is higher in the top wet site, than in the top dry site. In these sites, the genus *Leptolyngbya* of the order *Oscillatoriales* comprises between 14-22 % of the assigned cyanobacteria reads (not shown). Notably, a small proportion of cyanobacteria sequences are assigned to chloroplast. Further, a shift to *Chloroflexi* with depth is also evident (Figure 7 and Figure 8). Moreover, the *Gemmatimonadetes* are more abundant in deeper soils, and slightly more numerous in drier soil. There was also a significant log linear correlation between the *Alfaproteobacteria*:*Acidobacteria* ratio and the C:N ratio (correlation coefficient = 0.35, p-value = 0.04)(Figure S1). The proportion of unassigned *Bacteria* make up approximately 8-15 % of the communities, with the highest proportion of unassigned *Bacteria* in the deep layer of the dry site at KH (15%) and the lowest proportion of unassigned *Bacteria* in the top layer at the dry site in KH.

No MOB related families represented at least 1% of the community in any combination of site moisture and depth. Further investigations into the 16S rRNA gene sequence data revealed that MOB related sequences make up 0.06% of the total read count. All sequences assigned to MOB taxa are members of the *Rhizobiales* family. Consequently, all MOB identified by 16S rRNA gene sequence data are members of the *Alphaproteobacteria* (type II) MOB. The most abundant of MOB identified were assigned to the *Methylocystaceae* and *Beijerinkiaceae* families. The only recognized OTU's on genus level were members of the *Methylocella*, *Methylovirgula* and *Methylorosula* genera.

3.2.3 Redundancy Analysis (RDA) 16S rRNA gene

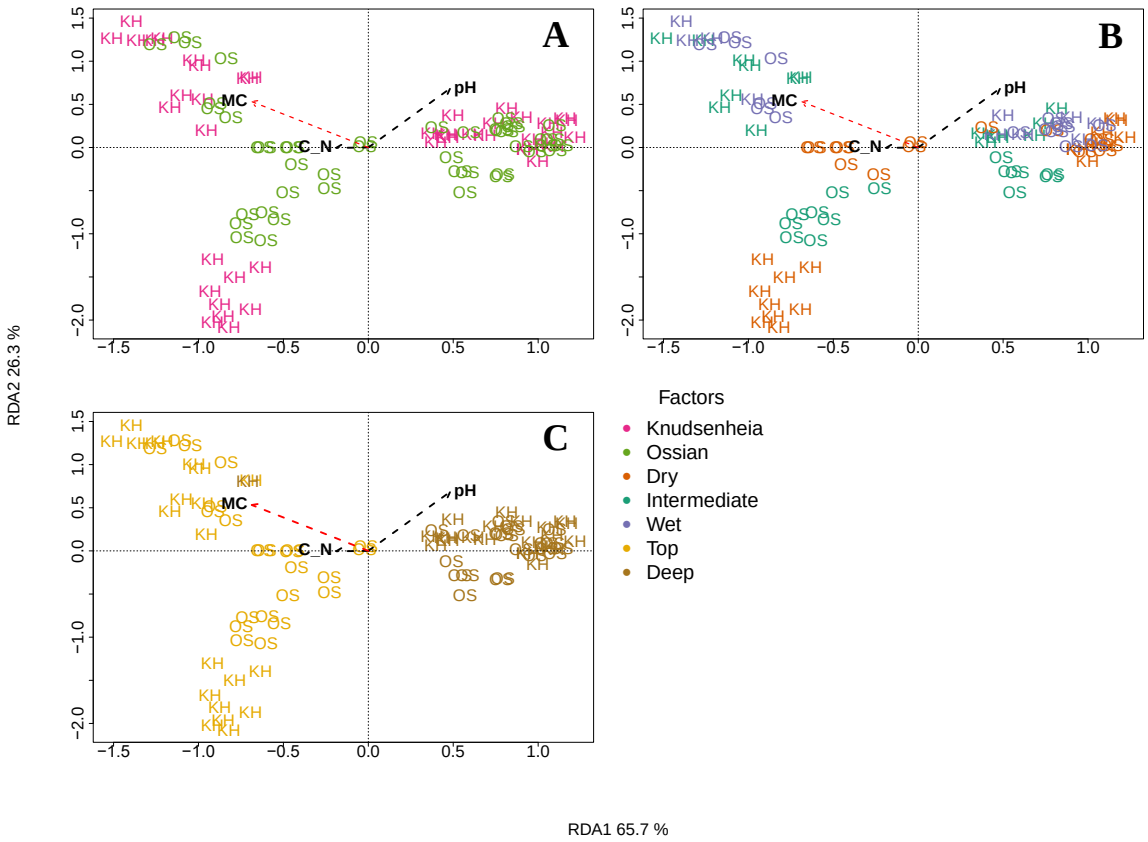

Figure 9: Plot of a distance based redundancy analysis (dbRDA) performed on the bacterial communities. A Hellinger transformed OTU-matrix was used to calculate a Bray-Curtis dissimilarity matrix which was used as a response variable, with site, depth, moisture, pH and C-N as explanatory variables. In **A;** the sites KH and OS, **B;** moisture gradient, **C;** shows the depth. Arrows display the variables implemented in the model. The red arrow shows the moisture content (MC). C_N shows the carbon nitrogen ratio.

Redundancy analysis of the bacterial community highlighted that depth is the factor that has the strongest influence on the community structure ($F=35.71$, p-value<0.001)(Table 3 and Figure 9). In addition, moisture (MC), pH, carbon-nitrogen ratio (C:N) and sites are significant factors and variables in explaining the variation in community composition (Table 3). Site also explained some of the variation community composition (Table 3). The top layer samples from KH display the largest variation along the y-axis of the ordination space with regards to moisture, which is consistent with the reported variation in water content for the top layers at KH (Table 2). Further, both sites show a clear separation according to moisture (Figure 9). KH top intermediate and top wet sites clusters closely in the ordination space with high correlation to water content, which is confirmed by the similar water content shown in Table 2.

ANOVA community				
	Df	**Sum Of Sqs**	**F**	**Pr(>F)**
site	1	0.67	4.71	<0.01
depth	1	5.1	35.71	<0.01
MC	1	1.02	7.12	<0.01
pH	1	0.93	6.54	<0.01
C-N	1	0.50	3.53	<0.01
Residual	83	11.85		

Table 3 Table showing the results from an Analysis of Variance (ANOVA), performed on a Hellinger transformed 16S rRNA gene OTU matrix as response variable, and site, depth, moisture (MC), pH and C-N as explanatory variables. The Pr(>F) column shows the p value, the test statistics are shown in column F. To calculate the test scores, 1000 permutations were performed.

3.3 Methane biocenosis

3.3.1 Methanogens

PCR of the *mcrA* gene was used to analyse for methanogens in the soil samples. Few samples gave product and therefore amplicon sequencing of the methanogen community was not done. However, an effort was made to optimize the PCR protocol prior to deciding that the sample foundation was not sufficient to go forward with sequencing of amplicons. The main conclusions from this effort will be included in the thesis.

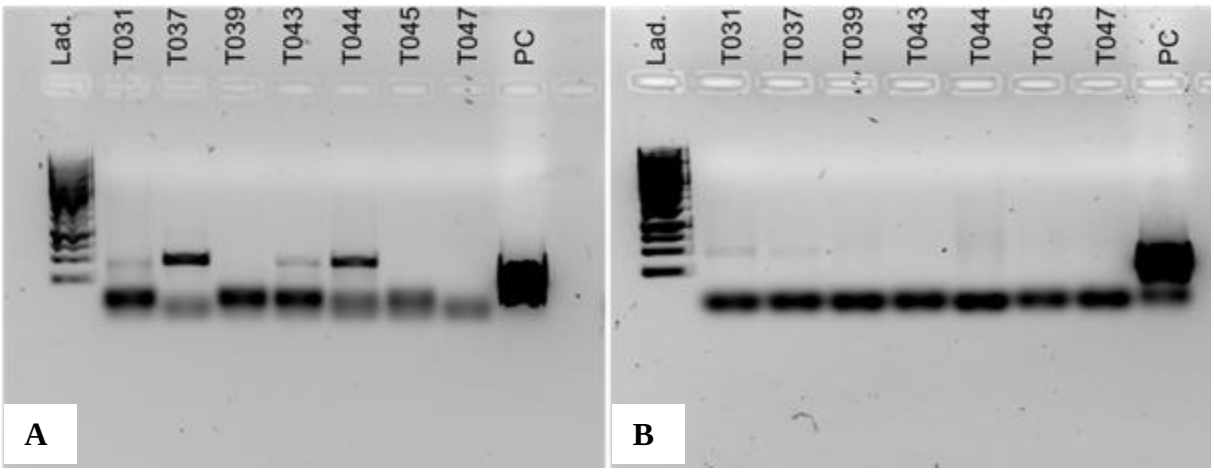

Figure 10: Comparison of two PCR protocols performed on the mcrA gene. A; Primers from Luton et al. (2002) and the PCR program described in Frey et al. (2011), B; PCR performed with primers and program from Steinberg and Regan (2008). Lanes are labelled with sample number. Lad = Ladder, PC= Positive control

Samples from the same plots that previous had yielded a PCR product (T045, T039) and those samples that had given a product (T031, T037, T043, T044) were selected in addition to one sample from the deeper layers (T047). In Figure 10, bands in A has a darker colour and is clearer than in B. Therefore, combination of primers and program used to generate the results in A is to be preferred. Importantly, PCR product shows a presence of methanogens at the KH site.

3.3.1 Methane oxidizing bacteria

MOB data are obtained from use of the primer pair A189f/mb661r for the *pmoA* gene in the CAB operon for methane monooxygenase. PCR amplification and sequencing was also done with the A682r primer, but these results were considered to be of poor quality and will therefore not be presented in this thesis. Taxonomical assignations of all OTU's from the bioinformatic pipeline and respective read counts for each combination of site, site and layer are shown in Table 5. PCR products of the *pmoA* gene (A189f/mb661r) were obtained for 64 of 108 samples. The KH wet site (16 samples, including all representatives for the deep layer) and OS (15 samples) constituted the largest proportion of no-PCR-product samples. Lack of PCR product was also observed for the intermediate site (10 samples, 7 top layer, 3 deep layer) and dry (1 sample from deep layer) sites at KH. Consequently, these sample were not sequenced

Except for the X_11, X_14 and X_6, all OTU's clusters within the USCγ/USCγ-like clade. The X_1 OTU, which is both assigned to USCγ via the RDP classifier and clusters in the tree to USCγ, is highly dominating at both sites (KH and OS), in all sites and both layers (Table 4, Figure 11). Moreover, the closest evolutionary relatives to X_1 in is an environmental sequence representing a USCγ from the Tibetan Plateau, and an alpine grassland at high altitude (Zheng et al., 2012). Further, OTU X_5, OTU X_13, X_19 and X_2 are evolutionary close to the USCγ yet constitutes separate branches. Similarly, sequences representing OTU X_4, X_3 and X_7 clusters with USCγ like sequences (Figure 11). OTU X_11 is closely related to the *Methylobacter tundripaludum* SV96^{T} (Wartiainen et al., 2006) type strain with high bootstrap value. *M.tundripaludum* is previously identified as an active MOB and a key player in the biochemistry of arctic peatland Svalbard (Graef et al., 2011; Tveit et al., 2013). OTU X_14 clusters to *Methylovulum psychrotolerans* Sph1 an isolate from cold methane seeps in a

floodplain of a West-Siberian river (Oshkin et al., 2016). The X_6 OTU clusters inside the *Methylobacter* genus and is closely related to both *M.psycrophilus* and *M.tundripaludum*.

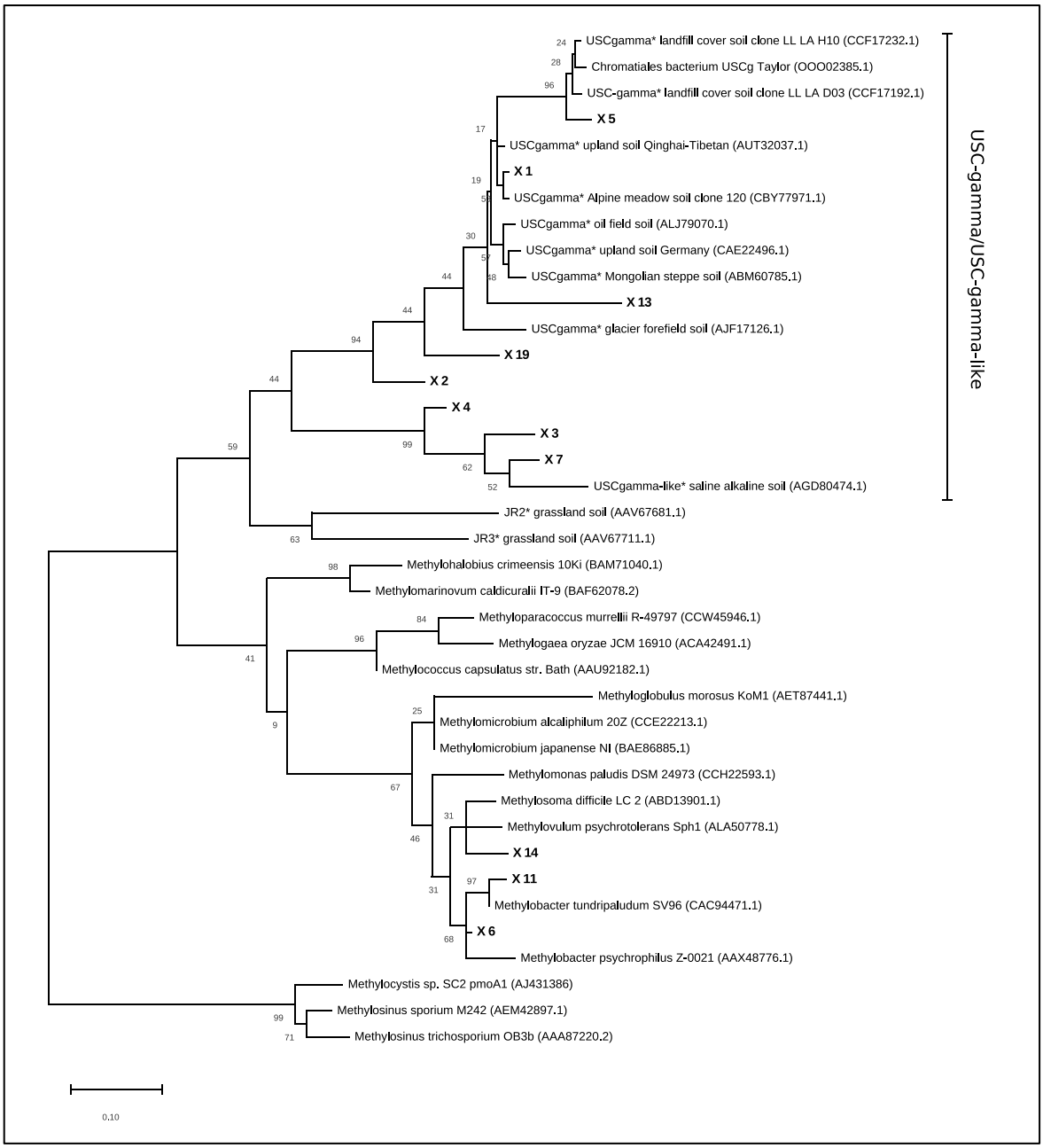

Figure 11: A Maximum Likelihood (ML) tree of the gammaproteobacterial MOB based on the Le and Gascuel Le and Gascuel (2008) model of amino acid substitution. A discrete Gamma distribution was applied to model evolutionary rate differences among sites The Neighbor-Join and BioNJ algorithms was applied to a matrix of pairwise distances estimated using a Jones-Taylor-Thornton (JTT) (Jones et al., 1992) model and selecting the topology with greater log likelihood. Involved in the analysis were 39 amino acid sequences with a total of 157 positions included in the final dataset. The three was rooted with an alphaproteobacterial outgroup. Environmental sequences are marked with an asterix, while others are type strain MOB. Highlighted in bold are environmental sequences acquired in this study. Scale bar indicate number of substitutions per site. In parentheses are the NCBI accession numbers. The program MEGAX was used for analysis (Kumar et al., 2018)

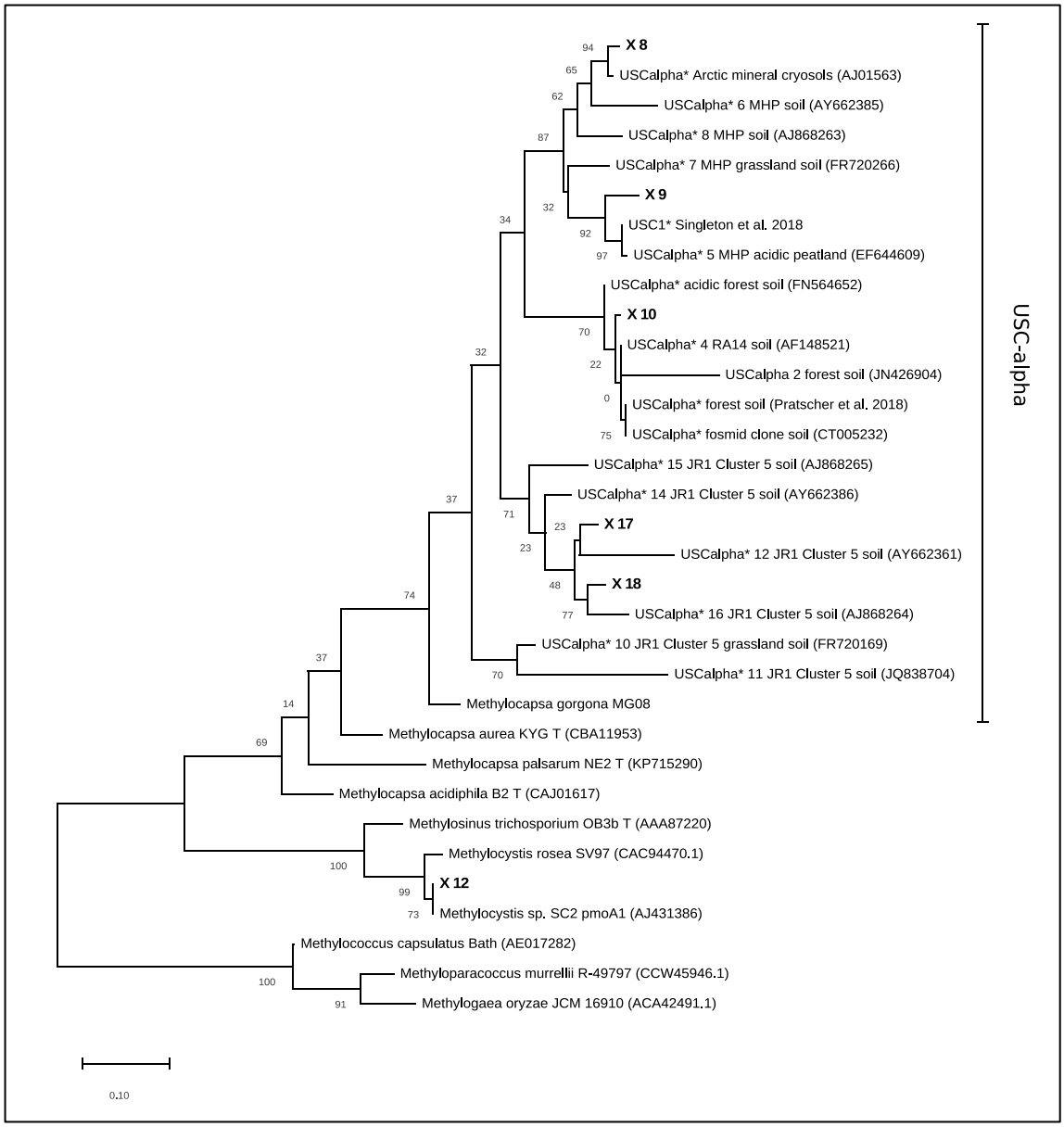

Figure 12: A Maximum Likelihood (ML) tree of the alphaproteobacterial MOB based on the Le and Gascuel (2008) model of amino acid substitution. A discrete Gamma distribution was applied to model evolutionary rate differences among sites. The Neighbor-Join and BioNJ algorithms was applied to a matrix of pairwise distances estimated using a Jones-Taylor-Thornton (JTT) (Jones et al., 1992) model and selecting the topology with greater log likelihood. Involved in the analysis were 33 amino acid sequences with a total of 155 positions included in the final dataset. The program MEGAX was used for analysis (Kumar et al., 2018). Environmental sequences are marked with an asterix, while others are type strain MOB. Highlighted in bold are environmental sequences acquired in this study. Scale bar indicate number of substitutions per site. In parentheses are the NCBI accession numbers.

Highest number of reads for the USCγ affiliated X_1 OTU was observed in the deep layer of the dry site at OS (63921 reads, Table 5). However, the highest relative abundance was observed in the deep layer in the wet site at OS (99.65%), albeit based on few reads (704/735). The deep layer in the intermediate site at KH differs somewhat from the other sites, with a X_1 relative abundance of 79.22 %, owing to a substantial proportion of the *M. tundripaludum* related

sequence of X_11 (10.56%). This also impacts the redundancy analysis (RDA) performed (Figure 13). Alphaproteobacterial MOB are dominated by OTU's clustering to the USCα clade. However, the overall abundance is quite low compared to the abundance of the gammaproteobacterial MOB (Table 5). The USCα clade branches out from the *Methylocapsa acidophila* B2 T, emphasising their evolutionary relationship. The closest related OTU's comes from a variety of different environments, ranging from beech forest acrylic soils (Roslev & Iversen, 1999) to acidic arctic cryosols (Lau et al., 2015). Only one OTU, X_12, clusters to a non-USCα sequence, the *Methylocystis* sp. SC2, an isolate from an aquifer in Germany. Conversely, *Methylocystis* sp SC2 have the ability to express two isozymes (*pmoA*1, *pmoA*2) (Dam et al., 2012), the sequence included in the tree is *pmoA*1. Interestingly, the *Methylocapsa gorgona* MG08 does not cluster inside USCα clade (Figure 12) as previously shown in (Tveit et al., 2019), but the closest related sequences are similar. Bootstrap values for both the α-tree and the γ-tree are at some branch point relatively low, despite a number of bootstraps (1000 re-samplings). The tree was rooted with sequences *Methylococcus capsulatus* Bath, *Methyloparacoccus murellii* R-49797 and *Methylogaea oryzae* JCM.

Table 4: Table showing the results from an Analysis of Variance (ANOVA), performed on a Hellinger transformed *pmoA* gene community matrix as response variable, and site, depth, moisture (MC), pH and C-N as explanatory variables. The Pr(>F) column shows the p value, the test statistics are shown in column F. To calculate the test statistics, 1000 permutations was performed.

ANOVA								
	MOB community				**Without high C_N samples**			
	Df	**Sum of sqs**	**F**	**Pr(>F)**	**Df**	**Sum of sqs**	**F**	**Pr(>F)**
Site	1	0.28	8.89	<0.01	1	0.28	16.18	<0.01
Depth	1	0.10	3.24	<0.01	1	0.10	5.78	<0.01
MC	1	0.05	1.76	0.10	1	0.55	2.45	0.04
pH	1	0.10	3.06	0.01	1	0.10	3.51	<0.01
C-N	1	0.19	6.25	0.02	1	0.19	2.93	0.02
MC:pH						0.057	3.42	<0.01
Residual	55	1.74			55	1.69		

Table 5: Table showing the phylogenetic assignations of the MOB OTU´s from the bioinformatic pipeline based on the *pmoA* gene, and the respective read counts along the gradient at Knudsenheia and Ossian Sarsfjellet

			Number of reads										
			Knudsenheia					Ossian Sarsfjellet					
			Dry		Int.		Wet	Dry		Int.		Wet	
OTU	**Genus**	**Species**	**Top**	**Deep**	**Top**	**Deep**	**Top**	**Top**	**Deep**	**Top**	**Deep**	**Top**	**Deep**
X_1	typeId	USCγ	29295	18207	4647	11118	3962	30884	63921	36050	43401	3702	704
X_2	NA	NA	1333	2424	189	338	64	54	351	90	315	8	9
X_3	NA	NA	5	14	0	0	13	125	1384	33	956	0	0
X_4	NA	NA	1	422	1	0	68	46	230	3	18	0	0
X_5	typeId	USCγ	93	478	0	280	26	612	1263	196	334	0	0
X_6	*Methylobacter*	M. sp	0	0	0	534	0	47	0	18	0	0	0
X_7	typeId	USCγ related	6	40	0	0	0	419	1897	0	7	0	0
X_8	typeIIb	USCα	23	8	6	49	3	0	0	0	1	0	7
X_9	typeIIb	USCα	450	55	144	145	3	0	2	13	12	4	6
X_10	typeIIb	USCα	6	1	31	5	0	2	6	0	7	0	5
X_11	*Methylobacter*	*M. tundripaludum*	0	0	0	1482	1	272	17	97	14	0	4
X_12	*Methylocystis*	M. sp._51	0	0	0	10	0	1	0	0	0	0	0
X_13	typeId	USCγ	1	2	0	1	0	1	4	4	2	1	0
X_14	Mmic	*M.japanense*-related	0	0	0	0	0	17	0	15	0	0	0
X_15	NA	NA	0	0	0	0	0	0	1	0	0	0	0
X_16	NA	NA	0	0	0	0	0	0	0	0	1	0	0
X_17	"typeIIb"	USCα	0	0	0	0	0	2	0	1	0	0	0
X_18	"typeIIb"	USCα	0	0	0	0	0	1	0	0	0	0	0
X_19	NA	NA	7	114	1	72	6	39	296	39	98	0	0
X_20	NA	NA	0	0	0	1	0	0	0	0	0	0	0
	Total number of reads		31220	21765	5019	14035	4146	32522	69372	36559	45166	3715	732

All OTU were assigned to the *Proteobacteria* phylum and either the *Alphaproteobacteria* or the *Gammaproteobacteria*. Mmic = Methylomicrobium and NA = Not Assigned by the RDP Classifier.

3.3.2 Redundancy Analysis (RDA) pmoA

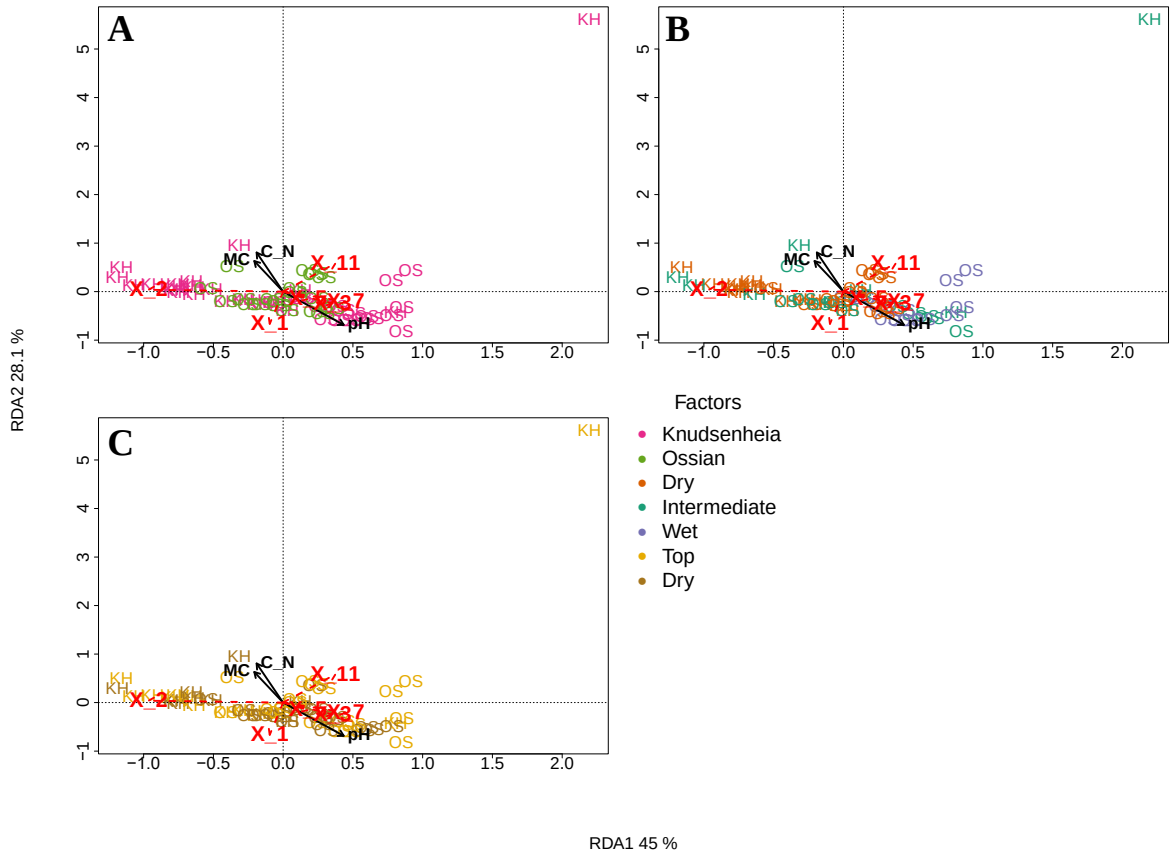

Figure 13: Plot of a distance based redundancy analysis (dbRDA) performed on the MOB communities. A Hellinger transformed OTU-matrix was used to calculate a Bray-Curtis dissimilarity matrix which was used as response variable, with site, depth, moisture, pH and C-N ratio as explanatory variables. In **A;** the sites KH and OS, **B;** moisture gradient, **C;** the depth. Arrows display the variables implemented in the model. The red arrow shows the moisture content (MC). C_N shows the carbon nitrogen ratio. The 6 most abundant MOB OTU's are plotted and shown in red

The RDA from the MOB community including the high C:N ratio samples show that the site and carbon nitrogen ratio is the most influential factors in explaining the MOB community composition (Figure 13). Moisture (MC) does not have a significant effect on the MOB composition according to this model shown in (Figure 13). The X_2 and X_9 OTU's show a negative correlation with pH or a positive correlation with moisture (MC), while the X_11 demonstrate a positive trend with the carbon nitrogen ratio. The KH intermediate top sample plot 1, is a substantial outlier which could owe to a significantly higher abundance of the X_11 OTU,

which clusters to *M. tundripaludum* (Figure 11), and/or the high carbon nitrogen ratio of the samples (Table 2).

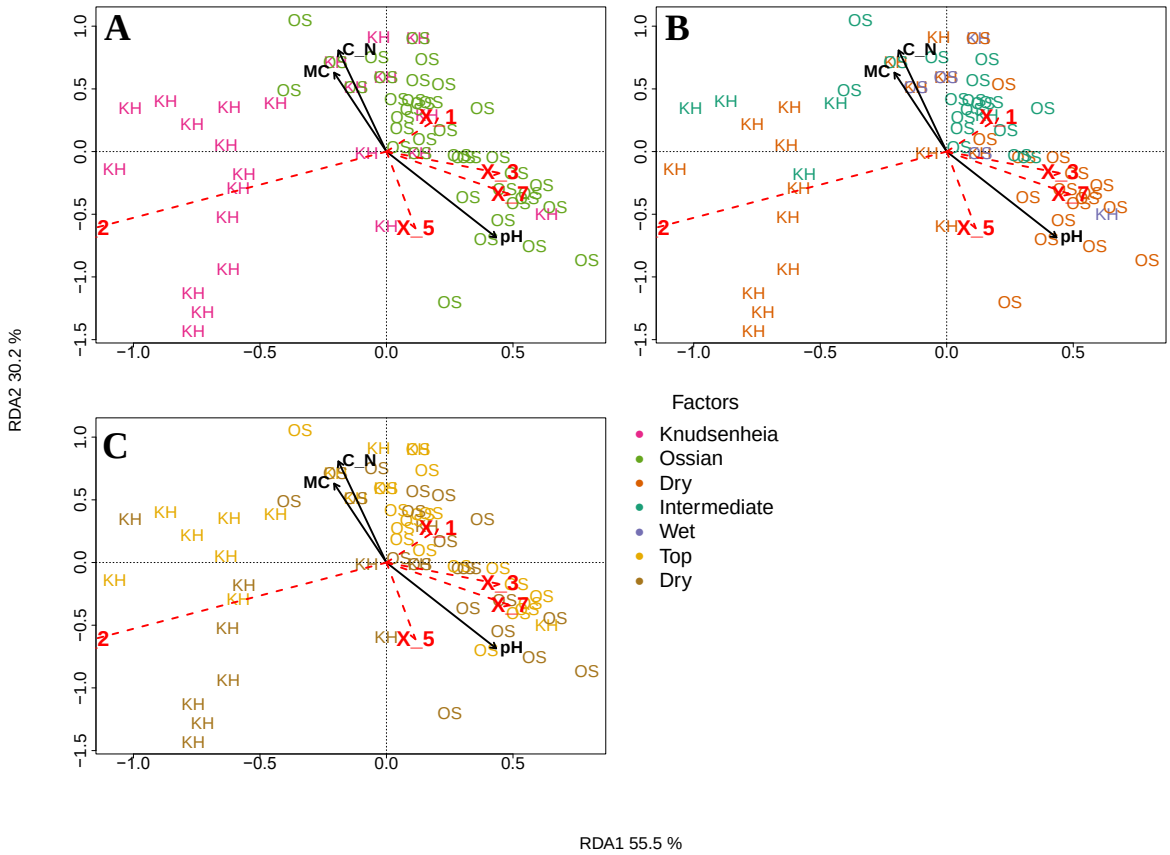

Figure 14: Plot of a distance based redundancy analysis (dbRDA) performed on the MOB communities without samples containing high C_N values and OTU X_11. A Hellinger transformed OTU-matrix was used to calculate a Bray-Curtis dissimilarity matrix which was used as response variable, with site, depth, moisture, pH and C-N ratio as explanatory variables. In **A;** the sites KH and OS, **B;** moisture gradient, **C;** show the depth. Arrows display the variables implemented in the model. The red arrow shows the moisture content. C_N shows the carbon nitrogen ratio. The 5 most abundant MOB OTU's are plotted and shown in red.

Therefore, a second plot was made without this outlier (Figure 14). As for the initial RDA this showed that the MOB community mostly was determined by site. Depth was considered second most influential in the second model, differing from the initial RDA (Table 4). In contrast to the initial model, moisture had a significant effect on the community and there was a significant effect of the interaction between moisture and pH (Table 4).

4 Discussion

4.1 Soil properties – moisture gradient

The two sites (KH and OS) are exposed to different climactic conditions, mainly due to their topology. In OS, the mesic slope and the wet snow-bed area are sheltered to winds by surrounding mountains and ridges, which could result in a warmer environment (Kern et al., 2019). KH is an open plain which is suggested to be more exposed to katabatic winds from adjacent glaciers having a cooling effect on this site (Kern et al., 2019). This is supported also by the differences in vegetation cover between OS and KH (Kern et al., 2019). The variation in water content is in Kern et al. (2019) suggested to be a result of variations in proportion of clay (Figure 4). Yet, the mean differences in clay content between sites (8.3 ± 4.1 for KH and 10.8 ± 2.6 at OS) is quite similar. However, there was a major difference in mean silt content between sites (13.5 ± 9 for KH and 29 ± 6.4 for OS), which also showed a slight negative correlation to water content. Silt could have a role in water drainage and is considered the main soil component determining water content in these soils. Moreover, local depressions could cause accumulation of either snow or rain, resulting in both between- plot- and even in-plot variations in water content. The organic matter content at both OS and KH is lower than in peat soil (Tveit et al., 2013), especially in the deeper layers where the organic matter content is more similar to that of mineral cryosols (Lau et al., 2015). Weathering of carbonates and mica schists are suggested to be causing the high observed pH levels in these soils (Gray et al., 2014; Mann et al., 1986). In addition to silt, high sand content at both sites could allow for good water drainage and could make the soil more permeable to air which in turn, could result in a deeper aerobic layer.

4.3 Bacterial community structure

4.3.1 Primers

The hypervariable regions of the 16S rRNA gene are evolving at different rates (Woese, 1987) and which region(s) that is most favourable to use in studies of microbial biodiversity is highly debated. More conserved regions are considered to be better in determining higher ranking taxa while more variable regions are better in identifying genus and species (Bukin et al., 2019; Kim et al., 2011). In this thesis, primers used to cover the bacterial community amplified the hypervariable V1-V3 region of the 16S rRNA gene (Table 1). This primer pair have recently

proven to be successful in assessing the bacterial diversity in both terrestrial and aquatic environments in Antarctica (Obbels et al., 2016; Tytgat et al., 2016). The V1-V3 fragment delineated from the primer pair used in this thesis, result in ~550 bp paired end reads, which is longer than the ~400 bp fragment produced by the V4 region. In addition, the V1-V3 region is considered to be among the most variable regions of the 16S rRNA gene (Yu & Morrison, 2004), and is therefore considered to be a suitable fragment to obtain higher phylogenetic resolution and highlight finer taxonomic differences between communities (Kim et al., 2011). Secondarily, a recent study demonstrated that fragments including the V2 and V3 regions supports a 'more precise distance-based clustering of reads into species-level OTUs' (Bukin et al., 2019). However, for Illumina, increasing read length makes it more prone to sequencing errors (Allen et al., 2016). Considering Ilumina MiSeq platforms, Allen et al. (2016) reports a 1.4 % error rate for the V1-V3 region after removal of singletons (3.6 % before removal), which is considerably higher than the 0.1 % reported for the V4 region (Kozich et al., 2013). Therefore, a trade-off between taxonomic resolution and sequencing errors must be considered in primer selection. Here we opted for higher taxonomic resolution. Furthermore, Kim et al. (2011) suggest using a phylogenetic distance of 0.04 instead of 0.03 to cluster reads into species-level OTUs' when using the V1-V3 region, as it will result in a more precise number of OTUs'. However, a higher number of OTUs' does not decrease analysis quality, but rather allows a finer separation of OTUs' and their respective functional niches (Bukin et al., 2019). It might, however, inflate estimations of species richness, and must be taken into account when calculating species richness and evenness.

4.3.1 Species richness

Richness estimates take into account the relative abundance of singletons and doubletons and therefore put weight to rare OTU´s. Removal of singletons would therefore lower the estimates, it could be said that it is inflated as is. There are no apparent differences in species richness between sites. However, here we used differences in proportions of OTU's to infer diversity values, which does not take into account the heteroscedasticity, i.e. the differences in variance of the values caused by uneven number of reads per sample. Yet, strictly as a comparison between sites and moisture levels, it is deemed sufficient.

4.3.2 Bacterial communities

Overall, the presence of aerobic- and semiaerobic bacteria in all sites and depths indicate that the aerobic and the aerob/anaerob interface of the active layer are sampled. As reported in several studies from arctic soil environments, the most abundant phyla are *Proteobacteria*, *Actinobacteria*, and *Acidobacteria* (Chu et al., 2010; McCann et al., 2016; Tveit et al., 2013). In addition, *Chloroflexi*, *Gemmatimonadetes*, *Bacteriodetes* and *Plantcomycetes* have been found in various abundances (Hultman et al., 2015; Schostag et al., 2015; Tveit et al., 2013). Moreover, *Cyanobacteria* are found to vary with the season, being most abundant during their growth season in June and July (Schostag et al., 2015), which concur with the period samples used in this study were collected. The overall observed relative abundances of the most abundant phyla that were found in this study (Figure 7 and Figure 8), coincide with these previous findings. However, the observed dominance of *Proteobacteria* and in particular the class *Alphaproteobacteria* (Figure 7 and Figure 8) are higher compared to what was observed in the abovementioned studies. Yet, a study by Chu et al. (2010) showed that pH had a strong effect on the bacterial community structure in arctic cryosols and that *Alphaproteobacteria* demonstrated a strong positive correlation to pH. Soil pH in Chu et al. (2010) varied from 4-6, which is considerably lower than measured at KH and OS (except for KH top dry site, pH 5.4), which might partly explain the higher abundances of *Alphaproteobacteria*. Supportive of this, McCann et al. (2016) reported high abundances of *Alphaproteobacteria* in seven different soil microbiomes around the Ny-Ålesund area. Contrastingly, *Acidobacteria* are shown to negatively correlate with pH (Chu et al., 2010; Lauber et al., 2009), which might explain their relatively low abundance in the communities along the high pH soils. *Acidobacteria* are also considered to be slow growing oligotrophs and found to be more abundant in nutrient poor soil, compared to more nutritious soil (Nemergut et al., 2007; Tarlera et al., 2008), suggesting that they in addition to high pH levels, might be outcompeted by copiotrophic bacteria such as *Alphaproteobacteria*. We found that there was a slight log linear correlation between the *Alphaproteobacteria*:*Acidobacteria* ratio and the C:N ratio (Figure S1). More weight is added to this by Nemergut et al. (2010) which showed a similar relationship in a lowland tropical rainforest. In further support, Fierer et al. (2007) found that there was a negative correlation between abundance of *Acidobacteria* and C mineralization rates, and proposed a classification into r- and K selected species, attributes known from plant and animal ecology.

Cyanobacteria were found in high abundances in the top layer of the wet sites in both KH and OS. *Cyanobacteria* are known to be oxygenic phototrophs and many species have the ability to fix atmospheric N_2. In addition to being light dependent, *Cyanobacteria* use water as an electron donor in the electron transport chain, thus the distribution of *Cyanobacteria* is also influenced by water availability. This could explain the higher abundances of *Cyanobacteria* in the wet top sites. Comparison of the vegetation cover along the moisture gradient at both sites by Kern et al. (2019), showed that overall, cryptogamic soil crusts were the most abundant vegetation type. In accordance with this, *Cyanobacteria* are important colonizers of biological soil crusts mainly due to their role as primary producers and nitrogen fixers but also as producers of extracellular polysaccharides (EPS) which works as a protective sheath against desiccation and fluctuations in water availability (Belnap & Lange, 2013). Interestingly, the highest abundance of biocrusts was observed in the wet sites, comprising up to 40 % of the vegetation type (Kern et al., 2019), which is in support of the high abundance of *Cyanobacteria* at these sites. Moreover, the non-heterocyst forming filamentous cyanobacteria *Leptolyngbya* was found to be the most abundant cyanobacterial genus (Figure 7 and Figure 8), which previously is shown to be essential inhabitants of arctic soil crusts (Pushkareva et al., 2015).

Depth was considered to have the largest effect on the bacterial community structure (Figure 9, Table 3) and the visually most evident change with depth was the shift from *Cyanobacteria* to *Chloroflexi* (Figure 7 and Figure 8). *Chloroflexi* is a metabolically versatile phylum, harbouring phototrophs, heterotrophs and litotrophs (Woese, 1987) and it is tempting to assume that semiaerobic photoheterotrophic *Chloroflexi* occupy the role of *Cyanobacteria* with depth.

Gemmatimonadetes, constitutes on average 2 % of soil communities on a global scale (Janssen, 2006). The phylum is known to harbour both aerobic and anaerobic heterotrophs but were recently discovered also to possess a functional proteobacterial type 2 photosynthetic reaction center (Zeng et al., 2014). A study of soil microaggregates, found that *Gemmatimonadetes* were much more abundant in the inner aggregates rather than in the whole aggregates, suggesting they prefer environments with low oxygen availability (Mummey et al., 2006). And, a study by DeBruyn et al. (2011) showed that *Gemmatimonadetes* negatively correlated with moisture, and

argued that *Gemmatimondetes* either are adapted to drier soils or are outcompeted in more moist soils. This observation is congruent what we observed in this thesis.

Actinobacteria are ubiquitous in soil ecosystems, and are shown to occupy several key steps in degradation of organic matter in arctic ecosystems (Tveit et al., 2013). Except for in the upper layers of the wet sites in both KH and OS, the relative abundances of *Actinobacteria* are close to the reported global average of 13 % (Janssen, 2006). Low relative abundance of *Actinobacteria* in the upper layer of the wet sites could owe to competitive bacteria, as it seemingly corresponds to high abundances of *Cyanobacteria* (Figure 7 and Figure 8), alternatively, soil parameters in these soils inhibits growth of *Actinobacteria*.

High abundance of *Rhizobiales* implies a key role of this taxa in biogeochemical cycles of this system. Several members of *Rhizobiales* possess, like *Cyanobacteria*, the ability to fix N_2. The relative abundance of *Rhizobiales* is lowest in the upper layers of the wet sites (Figure 7 and Figure 8) where Cyanobacteria are highly abundant. Therefore, it is intriguing to assume that for the dry sites, diazotrophic *Rhizobiales* occupy the role as main nitrogen fixers in the absence of *Cyanobacteria*. Nevertheless, the overall high abundance of diazotrophic taxa in all sites and layers highlights the importance of nitrogen fixation to this system.

The family of *Hyphomicrobiacea* harbour some genera known as purple nonsulfur bacteria (*Rhodomicrobium, Rhodoplanes*), which is a nutritionally versatile group. They can utilize amino acids, fatty acids, organic acids, sugars, alcohols and aromatic compounds as carbon sources. In addition, several species can utilize CO_2 and either H_2 or H_2S as electron donors to grow photoautotrophically (Madigan et al., 2012). However, this group is most known for its capability for photoheterotrophy, which is suggested to be part of the reason for the competitive success of this group (Madigan et al., 2012). Conversely, the nutritionally versatile nature of these bacteria could explain why they are abundant at all levels of moisture and at both depths (Figure 7 and Figure 8).

Acetobacteraceae, are obligate aerobic bacteria that are commonly known to perform incomplete oxidation of certain higher alcohols and sugars into organic acids such as acetic acid (Kersters et al., 2006; Madigan et al., 2012). Notably, some genera, such as the type genus *Acetobacter* have the ability to further oxidize acetic acid into CO_2. Interestingly, several genera have the capacity to synthesise cellulose causing cells to become embedded in a network of cellulose microfibrils (Madigan et al., 2012). This mechanism is proposed to function as a floatation device to make cells remain at the surface level in aquatic environments, but could also imply a role in soil crust formation (Madigan et al., 2012).

4.3.3 Redundancy analysis

The dbRDA show that depth is a major factor in determining the bacterial community composition (Figure 9). Although, the community composition implies aerobic conditions both in the top and deep layers, the deeper layer might well be semiaerobic, and consequently inhabit taxa that are either facultative anaerobic or aerotolerant anaerobs. There are also great changes in soil parameters with depth, in terms of both MC, and C:N (Table 2), which in turn are shown to have substantial influence on the diversity and abundance of taxa and ultimately the bacterial community composition (Figure 7 and Figure 8). This change in community composition with depth is also in accordance with previous findings in the arctic (Lipson et al., 2015). The measured soil variable that has the highest impact on community structure was moisture (Table 2). We show that there are distinct changes in community composition with moisture. Largely explained by *Cyanobacteria* which are known to experience a growth peak during summer, have a large impact on the community structure with moisture. Previously, moisture have demonstrated to have an effect on the activity of the microbial community (Huxman et al., 2004), but the effect on composition is not as clear. However, soil moisture may have an indirect effect on other variables, such as the redox status of an ecosystem, which have shown to be a significant predictor of community composition (Lipson et al., 2015). In addition to moisture, pH and the C:N ratio were also significant predictors of the microbial community. Especially pH have in previous studies shown have a major effect on bacterial community composition (Chu et al., 2010; Männistö et al., 2007), but also the C:N ratio (Wan et al., 2015).

4.4 Methane community

A small proportion of MOB sequences was detected in the 16S rRNA gene amplicon. Notably, these were only assigned to the alphaproteobacterial MOB families *Beijerickiaceae* and *Methylocystaceae*. On genus level, the only recognized were members of the *Methylocella, Methylovirgula* and *Methylorosula* genera. Interestingly, all of these have eluded efforts to amplify the *pmoA* gene, indicating that they do not possess the pMMO and would therefore not be detected in amplicon sequencing of the *pmoA* gene (Berestovskaya et al., 2012; Dedysh et al., 2000; Dunfield & Dedysh, 2014; Vorobev et al., 2009). Moreover, there is only one partial sequence of the 16S rRNA gene from a draft genome related to USCγ in the SILVA database (C. R. Edwards et al., 2017). This fragment is 488 nucleotides long and share a 94 % similarity to the 16S rRNA gene sequence of *Thioalkalivibrio* of the *Chromatiales* order (C. R. Edwards et al., 2017). This means that it would not be recognized as a MOB in the 16S rRNA gene sequence data. Yet, the *pmoA* sequence retrieved from this draft genome is closely related to the X_5 phylotype identified in this thesis (Figure 11).

4.4.1 Primers and PCR

Most frequently, the combination of the forward primer A189f and either the reverse primers mb661r (Costello & Lidstrom, 1999) or A682r (Holmes et al., 1995) have been used to amplify the gene encoding the beta subunit of the particulate methane monooxygenase enzyme (*pmoA*) (Esson et al., 2016; Knief, 2015; Martineau et al., 2014; Oshkin et al., 2014; Serrano-Silva et al., 2014). Often, the reverse primers mb661r and A682r are also used in combination to get a sufficient coverage of the MOB community (Esson et al., 2016; Oshkin et al., 2014). Bourne et al. (2001) suggested additional use of the A650r primer to get the broadest possible representation of the MOB community, as done in Serrano-Silva et al. (2014). In this thesis, solely sequence data generated by the reverse primer mb661r are presented, even though amplification and sequencing were done of amplicons generated by the A682r primer. The mb661r primer does not amplify the *amoA* gene from ammonia oxidizing bacteria but neither detect phylotypes that has a phylogenetic position between *pmoA* and *amoA* (Costello & Lidstrom, 1999). Moreover, the mb661r primer, is generally less proficient in amplifying type IIb (*Beijerinckiaceae*) MOB and is interestingly, reported to largely discriminate USCα sequences (Bourne et al., 2001; Deng et al., 2013; Knief, 2015). We used a species level cut-off value of 86 % for the *pmoA* gene sequence as suggested (Wen et al., 2016). Notably, there are also designed PCR primers targeting MOB

subgroups such as the MethT2R- and MethT1bR primers targeting the 16S rRNA gene of type II and type I MOB respectively (Gray et al., 2014; He et al., 2012; Martineau et al., 2010).

The PCR program used to amplify the *pmoA* gene were optimized to obtain the highest possible yield. In the initial PCR amplification, PCR duplicates were pooled before the clean-up step. This was done not only to obtain sufficient template for sequencing, but also to prevent PCR bias. PCR products were run on an agarose-gel to confirm amplicon size and quality (see appendix). An agar concentration of 0.8 % instead of the ordinary 1 % was chosen to let the fragment run easier through the gel which was suggested as a way to identify low yield samples. Only samples that gave a visual band were consider for sequencing.

4.4.2 Methanogens – PCR protocol

The preferred PCR protocol was the combination of primers from Luton et al. (2002) (Table S2) and the PCR program used in Frey et al. (2011). The standard FastStart High Fidelity PCR system (Roche) reaction mix was used according to the manufacturer's recommendation, except using a slightly higher primer concentration. Our results imply that the primer selection and PCR program is vital for amplification of the *mcrA* gene, and hence the detection of methanogens. Moreover, the result show that there is in fact methanogens present in the wet sites. Even though the community composition imply that the samples mostly were collected in the brackets of the oxic, anoxic interface, some samples from the wet sites might have leaned towards anoxic conditions. Studies from the anoxic horizons of the active layer in nearby locations indicate a substantial presence of methanogens (Tveit et al., 2013). It is likely that investigations into the anoxic layers would have resulted in detection of methanogens.

4.4.3 Methanotrophic community

High abundance of the recognized MOB at both depths at the dry and intermediate sites further support the notion that the samples are collected in the oxic portion of the active layer (Table 5). Surprisingly, at both sites, the dominating phylotype X_1 (79.2 – 99.7 %) was related to environmental sequences from the USCγ clade (Figure 11). Closest relative to X_1 was an USCγ phylotype found in an alpine meadow in the Tibetan Plateau (Zheng et al., 2012). These sites are located at an high altitude (3200 m.a.s.l) with an annual mean temperature of -2°C and soils

affected by spatially occurring permafrost, with pH measured around 7.5, which is comparable to the conditions at KH and OS (Zheng et al., 2012). In addition to the OTU X_1, OTU's X_2, 3, 4, 5, 7, 13 and 19 clusters within the USCγ/USCγ like clade, which means that there is a substantial diversity of these atmMOB in the system. Further, OTU's X_13, X_19 and X_2 constitutes separate branches, suggesting that either the dataset did not contain sufficient coverage of the USCγ related sequences, or they represent undescribed USCγ species. The X_5 OTU clusters closely to the *pmoA* sequence of the recently assembled USCγ draft genome from Antarctica (C. R. Edwards et al., 2017), suggesting that they are well adapted to extreme environments. Although USCγ previously have been identified and found in slightly alkaline soils in the Canadian arctic (Martineau et al., 2014), they have to our knowledge previously not been identified in the Svalbard tundra. However, based on real-time PCR of Type I specific primers (Martineau et al., 2010), Gray et al. (2014) reported high abundance of Type I MOB in soils in the Kongsfjorden region. Further, Gray et al. (2014) assumed an affiliation of these Type I MOB to *Methylobacter*, based on the findings of Tveit et al. (2013), but our results suggest that they could in fact be USCγ related. Supportive of this, Gray et al. (2014) found no correlation with CH_4 flux measurements and the observed abundances of Type I MOB, which could owe to the presence of USCγ as they would not necessarily oxidise CH_4 in a rate detectable in gas flux measurements.

Phylotypes clustering to the USCα clade was also found (Figure 12), albeit in lower abundances (Table 5). These have been found to be globally widely distributed in soils (Tveit et al., 2019), including arctic (Lau et al., 2015; Martineau et al., 2014) and subarctic (Mateos-Rivera et al., 2018) soils. The highest abundance of USCα was found in the top layer at the KH dry site, which coincide with where the lowest pH was measured (Table 2). Compatibly, the distribution of USCα and USCγ is considered to be largely determined by soil pH, where the USCα prefers more acidic soils while USCγ contrastingly prefers alkaline soils (Knief, 2015; Martineau et al., 2014). None of the USCα phylotypes clusters with the recently described *M.gorgona* MG08, which is expected, as *Methylocapsa gorgona* MG08 was isolated from a retired subarctic landfill site and clusters closely to phylotypes from more temperate soils (Serrano-Silva et al., 2014; Shrestha et al., 2012; Tveit et al., 2019). Notably, *M.gorgona* MG08 clusters closely to the same

environmental sequences as in Tveit et al. (2019), giving support to the phylogenetic result in this thesis (Figure 12).

The increase in detection of atmMOB in arctic environments could mean that arctic upland tundra soil represents a significant sink of atmCH_4 that not previously have been considered in model predictions of future climate change. Our result suggests a considerable diversity of USCγ and USCγ-like bacteria in the system, with several OTU's forming separate branches, indicative of unique and uncharacterized species. This highlights the need to further investigate atmMOB occurrences in the arctic and make efforts to isolate representatives to obtain information of the biology of these microbes.

Previous studies have reported gammaproteobacterial *Methylococcaceae* and phylotypes closely related to *Methylobacter* and in particular *M. tundripaludum* to be key players in these systems (Graef et al., 2011; Tveit et al., 2013; Wartiainen et al., 2006). Only two phylotypes retrieved in this thesis, X_11 and X_8, are related to *Methylobacter,* whereof X_11 is closely related to the *M. tundripaludum* SV96 type strain (Figure 11). These OTU's are found to be abundant in the KH intermediate deep layer (Table 5), where they comprise ~14 % of the reads. Interestingly the abundance of these OTU's coincide with the high C:N ratio reported for the plot 1 of the intermediate deep site (Table 2). This peak in both abundance of *Methylobacter* related sequences and the C:N ratio could mean that there is an association between the abundance of *Methylobacter* and the C:N ratio but this observation needs further investigations. A high C:N stoichiometry indicates a N-limitation (Cleveland & Liptzin, 2007). Globally the C:N ratio for microbial biomass is ~ 8.5 (Cleveland & Liptzin, 2007), which means that the C:N ratio of the KH intermediate deep layer of 26.9 ± 18.5 indicates a particular limitation in N. The high abundance of the X_11 OTU and/or the high C:N ratio made the sample a considerable outlier in the RDA plot (Figure 13) and consequently supressed the information gained from the analysis. Therefore, a second RDA was made without the high C:N ratio samples from the KH intermediate deep plot 1 and the X_11 OTU (Figure 14).

Considering the effect of the different layers on the whole bacterial community (Figure 9), the effect of depth is surprisingly not so strong on the MOB-community composition (Figure 14). However, there seems to be a more clear separation by site, especially for the dry samples, where the majority of KH samples are found on the negative side of the x-axis in the ordination plot while the OS samples are found on the positive side of the x-axis (Figure 14). This might be caused by the low pH of the upper layer at the KH dry site (Table 2). A study by Gray et al. (2014) showed that the abundance of gammaproteobacterial MOB positively correlated with soil phosphorous (P), which in turn negatively correlated with local pH values. Further, Gray et al. (2014) identified increased CH_4 oxidation rates in soils provided with P supplements in a microcosm with excess CH_4, suggesting that pH indirectly influences their abundances. Correspondingly, the RDA (Figure 14) show that pH has a significant effect on MOB community composition (Table 4). Interestingly, both moisture and the C:N ratio is also demonstrated to have a significant effect on MOB community composition (Table 4). Supporting, a limited number of successful PCR's from the wet sites (Table S1) indicate that MOB are not present due to lack of oxygen, or that PCR inhibitors, such as phenolic compounds, combined with low presence of MOB in the wet sites makes it difficult to obtain PCR product.

Differences in the MOB community composition in nearby locations suggest that there is a spatial variation in MOB composition. This distribution could be determined by local variations in soil parameters, such as the MC and pH. The absence of methanogens could mean that there is a lack of substrate availability for MOB that oxidises CH_4 at high concentrations, and that this allows colonization of atmMOB. Furthermore, USCγ could be widely distributed in arctic tundra soils, and based on our findings, hydrological patterns could be a predictor of the abundance of atmMOB, with a preference to slightly alkaline drier soils.

4.5 Future implications

The bacterial community structure is composed of the same phyla and show similar trends as previously shown in Arctic tundra and in bacterial communities in general. Several taxa are abundant in all moisture levels and at both depths, emphasizing their adaptation to cold environments and suggests an intrinsic genetic repertoire capable of adjusting to different environments. The high abundance of diazotrophic taxa highlights the N limitation in the system.

However, high abundance of *Cyanobacteria* with moisture, could suggest that with more precipitation, the area with high cyanobacterial abundance increases and both N and C will be fixed in higher levels. Thus, providing the system with more nutrients enables increased growth of vascular plants which will further contribute to the greening of Arctic. Adding the effect of increased temperatures in the Arctic, the potential for more rapid nutrient turnover could accelerate this process. The shift from oligotrophic *Acidobacteria* to more copiotrophic *Alphaproteobacteria* supports this notion of a more nutritious soil.

In contrast to previous findings in Svalbard, the MOB community was dominated by USCγ and α. However, they have formerly been found in similar environments and is suggested to be widely distributed. The area of soil similar to that sampled in this thesis, is considered to comprise the majority of the Svalbard tundra. Therefore, the potential importance of USCγ and -α as biological catalysts of atmCH_4 is immense. They appear to prefer drier soils and the distribution of the two groups seems to be highly determined by pH. Lau et al. (2015) found that USCα members oxidized CH_4 a fourfold faster in drier soils (33% saturation) compared to more moist soils (66% and 100%) and that in drier soils, atmMOB were more responsive to temperature changes. In addition, they found that USCα atmMOB oxidized CH_4 a twofold faster at 10°C, than 4°C (Lau et al., 2015). Consequently, although somewhat compensated by higher temperatures, precipitation and moisture in future scenarios could decrease the CH_4 sink capacity of arctic tundra soils as a consequence of reduced activity of atmMOB.

5 Conclusions

We found that the bacterial community changes along the moisture gradient, and that depth is the most influential factor in determining the bacterial community composition. High *Alphaproteobacteria*:*Acidobacteria* ratio with C:N is suggestive of a copiotrophic, oligotrophic competitive relationship. High abundance of diazotrophs emphasizes importance of N_2 fixation in this system. High abundance of *Cyanobacteria* in wet site during summer, a potential player in greening of arctic with increased moisture.

MOB community dominated by USCγ, revealing that drier arctic tundra could constitute a highly significant CH_4 sink in the Arctic. However, future increases in moisture could decrease the sink capacity of these soils, allowing potent CH_4 to trap heat in the atmosphere.

References

Abell, G. C. J., Stralis-Pavese, N., Sessitsch, A., & Bodrossy, L. (2009). Grazing affects methanotroph activity and diversity in an alpine meadow soil. *Environmental Microbiology Reports, 1*(5), 457-465.

Adam, P. S., Borrel, G., Brochier-Armanet, C., & Gribaldo, S. (2017). The growing tree of Archaea: new perspectives on their diversity, evolution and ecology. *Isme Journal, 11*(11), 2407-2425.

Allen, H. K., Bayles, D. O., Looft, T., Trachsel, J., Bass, B. E., Alt, D. P., . . . Casey, T. A. (2016). Pipeline for amplifying and analyzing amplicons of the V1–V3 region of the 16S rRNA gene. *BMC research notes, 9*(1), 380.

Amplicon PCR, P. C.-U., and Index PCR. (2013). 16S metagenomic sequencing library preparation. Retrieved from https://www.illumina.com/content/dam/illumina-support/documents/documentation/chemistry_documentation/16s/16s-metagenomic-library-prep-guide-15044223-b.pdf

Angel, R., & Conrad, R. (2009). In situ measurement of methane fluxes and analysis of transcribed particulate methane monooxygenase in desert soils. *Environmental Microbiology, 11*(10), 2598-2610.

Bach, E. M., Williams, R. J., Hargreaves, S. K., Yang, F., & Hofmockel, K. S. (2018). Greatest soil microbial diversity found in micro-habitats. *Soil Biology & Biochemistry, 118*, 217-226.

Beal, E. J., House, C. H., & Orphan, V. J. (2009). Manganese- and Iron-Dependent Marine Methane Oxidation. *Science, 325*(5937), 184-187.

Belnap, J., & Lange, O. L. (2013). *Biological soil crusts: structure, function, and management* (Vol. 150): Springer Science & Business Media.

Berestovskaya, J. J., Kotsyurbenko, O. R., Tourova, T. P., Kolganova, T. V., Doronina, N. V., Golyshin, P. N., & Vasilyeva, L. V. (2012). Methylorosula polaris gen. nov., sp nov., an aerobic, facultatively methylotrophic psychrotolerant bacterium from tundra wetland soil. *International Journal of Systematic and Evolutionary Microbiology, 62*, 638-646.

Bockheim, J. G., & Tarnocai, C. (1998). Recognition of cryoturbation for classifying permafrost-affected soils. *Geoderma, 81*(3-4), 281-293.

Bodrossy, L., Stralis-Pavese, N., Murrell, J. C., Radajewski, S., Weilharter, A., & Sessitsch, A. (2003). Development and validation of a diagnostic microbial microarray for methanotrophs. *Environmental Microbiology, 5*(7), 566-582.

Boetius, A., Ravenschlag, K., Schubert, C. J., Rickert, D., Widdel, F., Gieseke, A., . . . Pfannkuche, O. (2000). A marine microbial consortium apparently mediating anaerobic oxidation of methane. *Nature, 407*(6804), 623-626.

Borsetto, C., Amos, G. C. A., da Rocha, U. N., Mitchell, A. L., Finn, R. D., Laidi, R. F., . . . Wellington, E. M. H. (2019). Microbial community drivers of PK/NRP gene diversity in selected global soils. *Microbiome, 7*.

Bourne, D. G., McDonald, I. R., & Murrell, J. C. (2001). Comparison of pmoA PCR primer sets as tools for investigating methanotroph diversity in three Danish soils. *Applied and Environmental Microbiology, 67*(9), 3802-3809.

Braker, G., Fesefeldt, A., & Witzel, K.-P. (1998). Development of PCR primer systems for amplification of nitrite reductase genes (nirK and nirS) to detect denitrifying bacteria in environmental samples. *Appl. Environ. Microbiol., 64*(10), 3769-3775.

Bray, J. R., & Curtis, J. T. (1957). An Ordination of the Upland Forest Communities of Southern Wisconsin. *Ecological Monographs, 27*(4), 326-349.

Buan, N. R. (2018). Methanogens: pushing the boundaries of biology. *Emerging Topics in Life Sciences, 2*(4), 629-646.

Bukin, Y. S., Galachyants, Y. P., Morozov, I. V., Bukin, S. V., Zakharenko, A. S., & Zemskaya, T. I. (2019). The effect of 16S rRNA region choice on bacterial community metabarcoding results. *Scientific Data, 6*.

Baani, M., & Liesack, W. (2008). Two isozymes of particulate methane monooxygenase with different methane oxidation kinetics are found in Methylocystis sp strain SCZ. *Proceedings of the National Academy of Sciences of the United States of America, 105*(29), 10203-10208.

Cai, Y. F., Zheng, Y., Bodelier, P. L. E., Conrad, R., & Jia, Z. J. (2016). Conventional methanotrophs are responsible for atmospheric methane oxidation in paddy soils. *Nature Communications, 7*.

Chan, Y. K., Van Nostrand, J. D., Zhou, J. Z., Pointing, S. B., & Farrell, R. L. (2013). Functional ecology of an Antarctic Dry Valley. *Proceedings of the National Academy of Sciences of the United States of America, 110*(22), 8990-8995.

Chapin, D. M., Bliss, L. C., & Bledsoe, L. J. (1991). Environmental-Regulation of Nitrogen-Fixation in a High Arctic Lowland Ecosystem. *Canadian Journal of Botany-Revue Canadienne De Botanique, 69*(12), 2744-2755.

Chauhan, A., Layton, A. C., Vishnivetskaya, T. A., Williams, D., Pfiffner, S. M., Rekepalli, B., . . . Mykytczuk, N. (2014). Metagenomes from thawing low-soil-organic-carbon mineral cryosols and permafrost of the Canadian high Arctic. *Genome Announc., 2*(6), e01217-01214.

Chiri, E., Nauer, P. A., Rainer, E. M., Zeyer, J., & Schroth, M. H. (2017). High Temporal and Spatial Variability of Atmospheric-Methane Oxidation in Alpine Glacier Forefield Soils. *Applied and Environmental Microbiology, 83*(18).

Chu, H. Y., Fierer, N., Lauber, C. L., Caporaso, J. G., Knight, R., & Grogan, P. (2010). Soil bacterial diversity in the Arctic is not fundamentally different from that found in other biomes. *Environmental Microbiology, 12*(11), 2998-3006.

Cleveland, C. C., & Liptzin, D. (2007). C:N:P stoichiometry in soil: is there a “Redfield ratio” for the microbial biomass? *Biogeochemistry, 85*(3), 235-252.

Cooper, E. J. (2014). Warmer shorter winters disrupt Arctic terrestrial ecosystems. *Annual Review of Ecology, Evolution, and Systematics, 45*, 271-295.

Costello, A. M., & Lidstrom, M. E. (1999). Molecular characterization of functional and phylogenetic genes from natural populations of methanotrophs in lake sediments. *Applied and Environmental Microbiology, 65*(11), 5066-5074.

Dam, B., Dam, S., Kube, M., Reinhardt, R., & Liesack, W. (2012). Complete Genome Sequence of Methylocystis sp Strain SC2, an Aerobic Methanotroph with High-Affinity Methane Oxidation Potential. *Journal of Bacteriology, 194*(21), 6008-6009.

Davidson, E. A., & Janssens, I. A. (2006). Temperature sensitivity of soil carbon decomposition and feedbacks to climate change. *Nature, 440*(7081), 165.

DeBruyn, J. M., Nixon, L. T., Fawaz, M. N., Johnson, A. M., & Radosevich, M. (2011). Global biogeography and quantitative seasonal dynamics of Gemmatimonadetes in soil. *Appl. Environ. Microbiol., 77*(17), 6295-6300.

Dedysh, S. N., Liesack, W., Khmelenina, V. N., Suzina, N. E., Trotsenko, Y. A., Semrau, J. D., . . . Tiedje, J. M. (2000). Methylocella palustris gen. nov., sp nov., a new methane-oxidizing acidophilic bacterium from peat bags, representing a novel subtype of serine-pathway methanotrophs. *International Journal of Systematic and Evolutionary Microbiology, 50*, 955-969.

Degelmann, D. M., Borken, W., Drake, H. L., & Kolb, S. (2010). Different Atmospheric Methane-Oxidizing Communities in European Beech and Norway Spruce Soils. *Applied and Environmental Microbiology, 76*(10), 3228-3235.

Deng, Y., Cui, X., Lüke, C., & Dumont, M. G. (2013). Aerobic methanotroph diversity in R iganqiao peatlands on the Q inghai–T ibetan P lateau. *Environmental Microbiology Reports, 5*(4), 566-574.

Dickson, L. G. (2000). Constraints to nitrogen fixation by cryptogamic crusts in a polar desert ecosystem, Devon Island, NWT, Canada. *Arctic Antarctic and Alpine Research, 32*(1), 40-45.

Dlugokencky, E. J., Nisbet, E. G., Fisher, R., & Lowry, D. (2011). Global atmospheric methane: budget, changes and dangers. *Philosophical Transactions of the Royal Society a-Mathematical Physical and Engineering Sciences, 369*(1943), 2058-2072.

Dorr, N., Glaser, B., & Kolb, S. (2010). Methanotrophic Communities in Brazilian Ferralsols from Naturally Forested, Afforested, and Agricultural Sites. *Applied and Environmental Microbiology, 76*(4), 1307-1310.

Dumont, M. G., & Murrell, J. C. (2005). Stable isotope probing - linking microbial identity to function. *Nature Reviews Microbiology, 3*(6), 499-504.

Dunfield, P. F., & Dedysh, S. N. (2014). Methylocella: a gourmand among methanotrophs. *Trends in Microbiology, 22*(7), 368-369.

Edwards, C. R., Onstott, T. C., Miller, J. M., Wiggins, J. B., Wang, W., Lee, C. K., . . . Lau, M. C. Y. (2017). Draft Genome Sequence of Uncultured Upland Soil Cluster Gammaproteobacteria Gives Molecular Insights into High-Affinity Methanotrophy (vol 5, e00047-17, 2017). *Microbiology Resource Announcements, 5*(36).

Edwards, U., Rogall, T., Blocker, H., Emde, M., & Bottger, E. C. (1989). Isolation and Direct Complete Nucleotide Determination of Entire Genes - Characterization of a Gene Coding for 16s-Ribosomal Rna. *Nucleic Acids Research, 17*(19), 7843-7853.

Esson, K. C., Lin, X., Kumaresan, D., Chanton, J. P., Murrell, J. C., & Kostka, J. E. (2016). Alpha-and gammaproteobacterial methanotrophs codominate the active methane-oxidizing communities in an acidic boreal peat bog. *Appl. Environ. Microbiol., 82*(8), 2363-2371.

Etheridge, D. M., Steele, L. P., Francey, R., & Langenfelds, R. (1998). Atmospheric methane between 1000 AD and present: Evidence of anthropogenic emissions and climatic variability. *Journal of Geophysical Research: Atmospheres, 103*(D13), 15979-15993.

Etiope, G., & Lollar, B. S. (2013). Abiotic Methane on Earth. *Reviews of Geophysics, 51*(2), 276-299.

Ettwig, K. F., Butler, M. K., Le Paslier, D., Pelletier, E., Mangenot, S., Kuypers, M. M. M., . . . Strous, M. (2010). Nitrite-driven anaerobic methane oxidation by oxygenic bacteria. *Nature, 464*(7288), 543-+.

Everdingen, R., O. van. (Ed.) (1998, revised in 2005). International Permafrost Association.

Fenner, N., & Freeman, C. (2011). Drought-induced carbon loss in peatlands. *Nature Geoscience, 4*(12), 895.

Fierer, N., Bradford, M. A., & Jackson, R. B. (2007). Toward an ecological classification of soil bacteria. *Ecology, 88*(6), 1354-1364.

Flessa, H., Rodionov, A., Guggenberger, G., Fuchs, H., Magdon, P., Shibistova, O., . . . Blodau, C. (2008). Landscape controls of CH4 fluxes in a catchment of the forest tundra ecotone in northern Siberia. *Global Change Biology, 14*(9), 2040-2056.

Francis, C. A., Roberts, K. J., Beman, J. M., Santoro, A. E., & Oakley, B. B. (2005). Ubiquity and diversity of ammonia-oxidizing archaea in water columns and sediments of the ocean. *Proceedings of the National Academy of Sciences, 102*(41), 14683-14688.

Freeman, C., Evans, C., Monteith, D., Reynolds, B., & Fenner, N. (2001). Export of organic carbon from peat soils. *Nature, 412*(6849), 785.

Frey, B., Niklaus, P. A., Kremer, J., Luscher, P., & Zimmermann, S. (2011). Heavy-Machinery Traffic Impacts Methane Emissions as Well as Methanogen Abundance and Community Structure in Oxic Forest Soils. *Applied and Environmental Microbiology, 77*(17), 6060-6068.

Graef, C., Hestnes, A. G., Svenning, M. M., & Frenzel, P. (2011). The active methanotrophic community in a wetland from the High Arctic. *Environmental Microbiology Reports, 3*(4), 466-472.

Gray, N. D., McCann, C. M., Christgen, B., Ahammad, S. Z., Roberts, J. A., & Graham, D. W. (2014). Soil geochemistry confines microbial abundances across an arctic landscape; implications for net carbon exchange with the atmosphere. *Biogeochemistry, 120*(1-3), 307-317.

Hall, B. G. (2013). Building Phylogenetic Trees from Molecular Data with MEGA. *Molecular Biology and Evolution, 30*(5), 1229-1235.

Hanson, R. S., & Hanson, T. E. (1996). Methanotrophic bacteria. *Microbiological Reviews, 60*(2), 439-+.

Haroon, M. F., Hu, S. H., Shi, Y., Imelfort, M., Keller, J., Hugenholtz, P., . . . Tyson, G. W. (2013). Anaerobic oxidation of methane coupled to nitrate reduction in a novel archaeal lineage (vol 500, pg 567, 2013). *Nature, 501*(7468).

He, R., Wooller, M. J., Pohlman, J. W., Quensen, J., Tiedje, J. M., & Leigh, M. B. (2012). Shifts in Identity and Activity of Methanotrophs in Arctic Lake Sediments in Response to Temperature Changes. *Applied and Environmental Microbiology, 78*(13), 4715-4723.

Henry, S., Bru, D., Stres, B., Hallet, S., & Philippot, L. (2006). Quantitative detection of the nosZ gene, encoding nitrous oxide reductase, and comparison of the abundances of 16S rRNA, narG, nirK, and nosZ genes in soils. *Appl. Environ. Microbiol., 72*(8), 5181-5189.

Holmes, A. J., Costello, A., Lidstrom, M. E., & Murrell, J. C. (1995). Evidence That Particulate Methane Monooxygenase and Ammonia Monooxygenase May Be Evolutionarily Related. *Fems Microbiology Letters, 132*(3), 203-208.

Holmes, A. J., Roslev, P., McDonald, I. R., Iversen, N., Henriksen, K., & Murrell, J. C. (1999). Characterization of methanotrophic bacterial populations in soils showing atmospheric methane uptake. *Applied and Environmental Microbiology, 65*(8), 3312-3318.

Hug, L. A., Baker, B. J., Anantharaman, K., Brown, C. T., Probst, A. J., Castelle, C. J., . . . Banfield, J. F. (2016). A new view of the tree of life. *Nature Microbiology, 1*(5).

Hugelius, G., Strauss, J., Zubrzycki, S., Harden, J. W., Schuur, E. A. G., Ping, C. L., . . . Kuhry, P. (2014). Estimated stocks of circumpolar permafrost carbon with quantified uncertainty ranges and identified data gaps. *Biogeosciences, 11*(23), 6573-6593.

Hultman, J., Waldrop, M. P., Mackelprang, R., David, M. M., McFarland, J., Blazewicz, S. J., . . . Jansson, J. K. (2015). Multi-omics of permafrost, active layer and thermokarst bog soil microbiomes. *Nature, 521*(7551), 208-+.

Huxman, T. E., Snyder, K. A., Tissue, D., Leffler, A. J., Ogle, K., Pockman, W. T., . . . Schwinning, S. (2004). Precipitation pulses and carbon fluxes in semiarid and arid ecosystems. *Oecologia, 141*(2), 254-268.

IPCC. (2013). *Climate Change 2013: The Physical Science Basis. Contribution of Working Group I to the Fifth Assessment Report of the Intergovernmental Panel on Climate Change* (T. F. Stocker, D. Qin, G.-K. Plattner, M. Tignor, S. K. Allen, J. Boschung, A.

Nauels, Y. Xia, V. Bex, & P. M. Midgley Eds.). Cambridge, United Kingdom and New York, NY, USA: Cambridge University Press.

Janssen, P. H. (2006). Identifying the dominant soil bacterial taxa in libraries of 16S rRNA and 16S rRNA genes. *Appl. Environ. Microbiol., 72*(3), 1719-1728.

Johnson, S. S., Hebsgaard, M. B., Christensen, T. R., Mastepanov, M., Nielsen, R., Munch, K., . . . Willerslev, E. (2008). Ancient bacteria show evidence of DNA repair (vol 104, pg 14401, 2007). *Proceedings of the National Academy of Sciences of the United States of America, 105*(30), 10631-10631.

Jones, D. T., Taylor, W. R., & Thornton, J. M. (1992). The Rapid Generation of Mutation Data Matrices from Protein Sequences. *Computer Applications in the Biosciences, 8*(3), 275-282.

Kern, R., Hotter, V., Frossard, A., Albrecht, M., Baum, C., Tytgat, B., . . . Karsten, U. (2019). Comparative vegetation survey with focus on cryptogamic covers in the high Arctic along two differing catenas. *Polar Biology, 42*(11), 2131-2145.

Kersters, K., Lisdiyanti, P., Komagata, K., & Swings, J. (2006). The family acetobacteraceae: the genera acetobacter, acidomonas, asaia, gluconacetobacter, gluconobacter, and kozakia. *The Prokaryotes: Volume 5: Proteobacteria: Alpha and Beta Subclasses*, 163-200.

Kim, M., Morrison, M., & Yu, Z. T. (2011). Evaluation of different partial 16S rRNA gene sequence regions for phylogenetic analysis of microbiomes. *Journal of Microbiological Methods, 84*(1), 81-87.

Kirk, J. L., Beaudette, L. A., Hart, M., Moutoglis, P., Klironomos, J. N., Lee, H., & Trevors, J. T. (2004). Methods of studying soil microbial diversity. *Journal of Microbiological Methods, 58*(2), 169-188.

Kirschke, S., Bousquet, P., Ciais, P., Saunois, M., Canadell, J. G., Dlugokencky, E. J., . . . Zeng, G. (2013). Three decades of global methane sources and sinks. *Nature Geoscience, 6*(10), 813-823.

Knief, C. (2015). Diversity and Habitat Preferences of Cultivated and Uncultivated Aerobic Methanotrophic Bacteria Evaluated Based on pmoA as Molecular Marker. *Frontiers in Microbiology, 6*.

Knief, C., Kolb, S., Bodelier, P. L. E., Lipski, A., & Dunfield, P. F. (2006). The active methanotrophic community in hydromorphic soils changes in response to changing methane concentration. *Environmental Microbiology, 8*(2), 321-333.

Knief, C., Lipski, A., & Dunfield, P. F. (2003). Diversity and activity of methanotrophic bacteria in different upland soils. *Applied and Environmental Microbiology, 69*(11), 6703-6714.

Kolb, S., Knief, C., Dunfield, P. F., & Conrad, R. (2005). Abundance and activity of uncultured methanotrophic bacteria involved in the consumption of atmospheric methane in two forest soils. *Environmental Microbiology, 7*(8), 1150-1161.

Kolbert, C. P., & Persing, D. H. (1999). Ribosomal DNA sequencing as a tool for identification of bacterial pathogens (vol 2, pg 299, 1999). *Current Opinion in Microbiology, 2*(4), 452-452.

Kotsyurbenko, O. (2005). Trophic interactions in the methanogenic microbial community of low-temperature terrestrial ecosystems. *Fems Microbiology Ecology, 53*(1), 3-13.

Koven, C. D., Riley, W. J., & Stern, A. (2013). Analysis of Permafrost Thermal Dynamics and Response to Climate Change in the CMIP5 Earth System Models. *Journal of Climate, 26*(6), 1877-1900.

Koyama, A., Wallenstein, M. D., Simpson, R. T., & Moore, J. C. (2014). Soil bacterial community composition altered by increased nutrient availability in Arctic tundra soils. *Frontiers in Microbiology, 5*.

Kozich, J. J., Westcott, S. L., Baxter, N. T., Highlander, S. K., & Schloss, P. D. (2013). Development of a Dual-Index Sequencing Strategy and Curation Pipeline for Analyzing Amplicon Sequence Data on the MiSeq Illumina Sequencing Platform. *Applied and Environmental Microbiology, 79*(17), 5112-5120.

Kumar, S., Stecher, G., Li, M., Knyaz, C., & Tamura, K. (2018). MEGA X: Molecular Evolutionary Genetics Analysis across Computing Platforms. *Molecular Biology and Evolution, 35*(6), 1547-1549.

Kviderova, J., Elster, J., & Simek, M. (2011). In situ response of Nostoc commune s.l. colonies to desiccation in Central Svalbard, Norwegian High Arctic. *Fottea, 11*(1), 87-97.

Lau, M. C. Y., Stackhouse, B. T., Layton, A. C., Chauhan, A., Vishnivetskaya, T. A., Chourey, K., . . . Onstott, T. C. (2015). An active atmospheric methane sink in high Arctic mineral cryosols. *Isme Journal, 9*(8), 1880-1891.

Lauber, C. L., Hamady, M., Knight, R., & Fierer, N. (2009). Pyrosequencing-Based Assessment of Soil pH as a Predictor of Soil Bacterial Community Structure at the Continental Scale. *Applied and Environmental Microbiology, 75*(15), 5111-5120.

Le, S. Q., & Gascuel, O. (2008). An improved general amino acid replacement matrix. *Molecular Biology and Evolution, 25*(7), 1307-1320.

Leake, J. R., Ostle, N. J., Rangel-Castro, J. I., & Johnson, D. (2006). Carbon fluxes from plants through soil organisms determined by field (CO2)-C-13 pulse-labelling in an upland grassland. *Applied Soil Ecology, 33*(2), 152-175.

Legendre, P., & Legendre, L. F. (2012). *Numerical ecology* (Vol. 24): Elsevier.

Liebner, S., Ganzert, L., Kiss, A., Yang, S., Wagner, D., & Svenning, M. M. (2015). Shifts in methanogenic community composition and methane fluxes along the degradation of discontinuous permafrost. *Frontiers in Microbiology, 6*, 356.

Liebner, S., Rublack, K., Stuehrmann, T., & Wagner, D. (2009). Diversity of Aerobic Methanotrophic Bacteria in a Permafrost Active Layer Soil of the Lena Delta, Siberia. *Microbial Ecology, 57*(1), 25-35.

Liengen, T. (1999). Environmental factors influencing the nitrogen fixation activity of free-living terrestrial cyanobacteria from a high arctic area, Spitsbergen. *Canadian Journal of Microbiology, 45*(7), 573-581.

Liengen, T., & Olsen, R. A. (1997). Nitrogen fixation by free-living cyanobacteria from different coastal sites in a high arctic tundra, Spitsbergen. *Arctic and Alpine Research, 29*(4), 470-477.

Lipson, D. A., Raab, T. K., Parker, M., Kelley, S. T., Brislawn, C. J., & Jansson, J. (2015). Changes in microbial communities along redox gradients in polygonized A rctic wet tundra soils. *Environmental Microbiology Reports, 7*(4), 649-657.

López-Gutiérrez, J. C., Henry, S., Hallet, S., Martin-Laurent, F., Catroux, G., & Philippot, L. (2004). Quantification of a novel group of nitrate-reducing bacteria in the environment by real-time PCR. *Journal of Microbiological Methods, 57*(3), 399-407.

Lovley, D. R., & Phillips, E. J. P. (1987). Competitive Mechanisms for Inhibition of Sulfate Reduction and Methane Production in the Zone of Ferric Iron Reduction in Sediments. *Applied and Environmental Microbiology*, *53*(11), 2636-2641.

Luton, P. E., Wayne, J. M., Sharp, R. J., & Riley, P. W. (2002). The mcrA gene as an alternative to 16S rRNA in the phylogenetic analysis of methanogen populations in landfill. *Microbiology-Sgm, 148*, 3521-3530.

Madigan, M. T., Martinko, J., Stahl, D., & Clark, D. (2012). Biology of Microorganisms 13. In: Pearson.

Makhalanyane, T. P., Van Goethem, M. W., & Cowan, D. A. (2016). Microbial diversity and functional capacity in polar soils. *Current Opinion in Biotechnology, 38*, 159-166.

Mann, D., Sletten, R., & Ugolini, F. (1986). Soil development at Kongsfjorden, Spitsbergen. *Polar Research, 4*(1), 1-16.

Martineau, C., Pan, Y., Bodrossy, L., Yergeau, E., Whyte, L. G., & Greer, C. W. (2014). Atmospheric methane oxidizers are present and active in Canadian high Arctic soils. *Fems Microbiology Ecology, 89*(2), 257-269.

Martineau, C., Whyte, L. G., & Greer, C. W. (2010). Stable Isotope Probing Analysis of the Diversity and Activity of Methanotrophic Bacteria in Soils from the Canadian High Arctic. *Applied and Environmental Microbiology, 76*(17), 5773-5784.

Martinez-Cruz, K., Leewis, M. C., Herriott, I. C., Sepulveda-Jauregui, A., Anthony, K. W., Thalasso, F., & Leigh, M. B. (2017). Anaerobic oxidation of methane by aerobic methanotrophs in sub-Arctic lake sediments. *Science of the Total Environment, 607*, 23-31.

Mateos-Rivera, A., Øvreås, L., Wilson, B., Yde, J. C., & Finster, K. W. (2018). Activity and diversity of methane-oxidizing bacteria along a Norwegian sub-Arctic glacier forefield. *Fems Microbiology Ecology, 94*(5), fiy059.

McCann, C. M., Wade, M. J., Gray, N. D., Roberts, J. A., Hubert, C. R. J., & Graham, D. W. (2016). Microbial Communities in a High Arctic Polar Desert Landscape. *Frontiers in Microbiology, 7*.

McDonald, I. R., & Murrell, J. C. (1997). The particulate methane monooxygenase gene pmoA and its use as a functional gene probe for methanotrophs. *Fems Microbiology Letters, 156*(2), 205-210.

Mummey, D., Holben, W., Six, J., & Stahl, P. (2006). Spatial stratification of soil bacterial populations in aggregates of diverse soils. *Microbial Ecology, 51*(3), 404-411.

Männistö, M. K., Tiirola, M., & Häggblom, M. M. (2007). Bacterial communities in Arctic fjelds of Finnish Lapland are stable but highly pH-dependent. *Fems Microbiology Ecology, 59*(2), 452-465.

Nauer, P. A., Dam, B., Liesack, W., Zeyer, J., & Schroth, M. H. (2012). Activity and diversity of methane-oxidizing bacteria in glacier forefields on siliceous and calcareous bedrock. *Biogeosciences, 9*(6), 2259-2274.

Nemergut, D. R., Anderson, S. P., Cleveland, C. C., Martin, A. P., Miller, A. E., Seimon, A., & Schmidt, S. K. (2007). Microbial community succession in an unvegetated, recently deglaciated soil. *Microbial Ecology, 53*(1), 110-122.

Nemergut, D. R., Cleveland, C. C., Wieder, W. R., Washenberger, C. L., & Townsend, A. R. (2010). Plot-scale manipulations of organic matter inputs to soils correlate with shifts in microbial community composition in a lowland tropical rain forest. *Soil Biology and Biochemistry, 42*(12), 2153-2160.

Obbels, D., Verleyen, E., Mano, M. J., Namsaraev, Z., Sweetlove, M., Tytgat, B., . . . Vyverman, W. (2016). Bacterial and eukaryotic biodiversity patterns in terrestrial and aquatic habitats in the Sor Rondane Mountains, Dronning Maud Land, East Antarctica. *Fems Microbiology Ecology, 92*(6).

Okano, Y., Hristova, K. R., Leutenegger, C. M., Jackson, L. E., Denison, R. F., Gebreyesus, B., . . . Scow, K. M. (2004). Application of real-time PCR to study effects of ammonium on population size of ammonia-oxidizing bacteria in soil. *Appl. Environ. Microbiol., 70*(2), 1008-1016.

Oksanen, J., Kindt, R., Legendre, P., O'Hara, B., Stevens, M. H. H., Oksanen, M. J., & Suggests, M. (2007). The vegan package. *Community ecology package, 10*, 631-637.

Op den Camp, H. J. M., Islam, T., Stott, M. B., Harhangi, H. R., Hynes, A., Schouten, S., . . . Dunfield, P. F. (2009). Environmental, genomic and taxonomic perspectives on methanotrophic Verrucomicrobia. *Environmental Microbiology Reports, 1*(5), 293-306.

Oshkin, I. Y., Belova, S. E., Danilova, O. V., Miroshnikov, K. K., Rijpstra, W. I. C., Damste, J. S. S., . . . Dedysh, S. N. (2016). Methylovulum psychrotolerans sp nov:, a cold-adapted methanotroph from low-temperature terrestrial environments, and emended description of the genus Methylovulum. *International Journal of Systematic and Evolutionary Microbiology, 66*, 2417-2423.

Oshkin, I. Y., Wegner, C.-E., Lüke, C., Glagolev, M. V., Filippov, I. V., Pimenov, N. V., . . . Dedysh, S. N. (2014). Gammaproteobacterial methanotrophs dominate cold methane seeps in floodplains of West Siberian rivers. *Appl. Environ. Microbiol., 80*(19), 5944-5954.

Pearson, E. S. (1931). The test of significance for the correlation coefficient. *Journal of the American Statistical Association, 26*(174), 128-134.

Pereira, F., Carneiro, J., Matthiesen, R., van Asch, B., Pinto, N., Gusmao, L., & Amorim, A. (2010). Identification of species by multiplex analysis of variable-length sequences. *Nucleic Acids Research, 38*(22).

Pushkareva, E., Pessi, I. S., Wilmotte, A., & Elster, J. (2015). Cyanobacterial community composition in Arctic soil crusts at different stages of development. *Fems Microbiology Ecology, 91*(12).

R Core, T. (2019). R: A language and environment for statistical computing. *R Foundation for Statistical Computing*.

Rai, A. N., Soderback, E., & Bergman, B. (2000). Cyanobacterium-plant symbioses. *New Phytologist, 147*(3), 449-481.

Rognes, T., Flouri, T., Nichols, B., Quince, C., & Mahe, F. (2016). VSEARCH: a versatile open source tool for metagenomics. *Peerj, 4*.

Roslev, P., & Iversen, N. (1999). Radioactive fingerprinting of microorganisms that oxidize atmospheric methane in different soils. *Applied and Environmental Microbiology, 65*(9), 4064-4070.

Rösch, C., & Bothe, H. (2005). Improved assessment of denitrifying, N2-fixing, and total-community bacteria by terminal restriction fragment length polymorphism analysis using multiple restriction enzymes. *Appl. Environ. Microbiol., 71*(4), 2026-2035.

Saunois, M., Bousquet, P., Poulter, B., Peregon, A., Ciais, P., Canadell, J. G., . . . Zhu, Q. (2016). The global methane budget 2000-2012. *Earth System Science Data, 8*(2), 697-751.

Sayers, E. W., Agarwala, R., Bolton, E. E., Brister, J. R., Canese, K., Clark, K., . . . Hefferon, T. (2019). Database resources of the national center for biotechnology information. *Nucleic Acids Research, 47*(Database issue), D23.

Schoell, M. (1988). Multiple Origins of Methane in the Earth. *Chemical Geology, 71*(1-3), 1-10.

Schostag, M., Stibal, M., Jacobsen, C. S., Baelum, J., Tas, N., Elberling, B., . . . Prieme, A. (2015). Distinct summer and winter bacterial communities in the active layer of Svalbard permafrost revealed by DNA- and RNA-based analyses. *Frontiers in Microbiology, 6*.

Schuur, E. A. G., McGuire, A. D., Schadel, C., Grosse, G., Harden, J. W., Hayes, D. J., . . . Vonk, J. E. (2015). Climate change and the permafrost carbon feedback. *Nature, 520*(7546), 171-179.

Semrau, J. D., Chistoserdov, A., Lebron, J., Costello, A., Davagnino, J., Kenna, E., . . . Lidstrom, M. E. (1995). Particulate Methane Monooxygenase Genes in Methanotrophs. *Journal of Bacteriology, 177*(11), 3071-3079.

Semrau, J. D., DiSpirito, A. A., & Yoon, S. (2010). Methanotrophs and copper. *Fems Microbiology Reviews, 34*(4), 496-531.

Serrano-Silva, N., Valenzuela-Encinas, C., Marsch, R., Dendooven, L., & Alcantara-Hernandez, R. J. (2014). Changes in methane oxidation activity and methanotrophic community composition in saline alkaline soils. *Extremophiles, 18*(3), 561-571.

Shaver, G. R., & Chapin, F. S. (1980). Response to Fertilization by Various Plant-Growth Forms in an Alaskan Tundra - Nutrient Accumulation and Growth. *Ecology, 61*(3), 662-675.

Shindell, D. T., Faluvegi, G., Koch, D. M., Schmidt, G. A., Unger, N., & Bauer, S. E. (2009). Improved attribution of climate forcing to emissions. *Science, 326*(5953), 716-718.

Shrestha, P. M., Kammann, C., Lenhart, K., Dam, B., & Liesack, W. (2012). Linking activity, composition and seasonal dynamics of atmospheric methane oxidizers in a meadow soil. *Isme Journal, 6*(6), 1115-1126.

Smith, V. R. (1984). Effects of Abiotic Factors on Acetylene-Reduction by Cyanobacteria Epiphytic on Moss at a Sub-Antarctic Island. *Applied and Environmental Microbiology, 48*(3), 594-600.

Solheim, B., Zielke, M., Bjerke, J. W., & Rozema, J. (2006). Effects of enhanced UV-B radiation on nitrogen fixation in arctic ecosystems. *Plant Ecology, 182*(1-2), 109-118.

Steinberg, L. M., & Regan, J. M. (2008). Phylogenetic Comparison of the Methanogenic Communities from an Acidic, Oligotrophic Fen and an Anaerobic Digester Treating Municipal Wastewater Sludge. *Applied and Environmental Microbiology, 74*(21), 6663-6671.

Stewart, K. J., Coxson, D., & Grogan, P. (2011). Nitrogen Inputs by Associative Cyanobacteria across a Low Arctic Tundra Landscape. *Arctic Antarctic and Alpine Research, 43*(2), 267-278.

Stralis-Pavese, N., Abell, G. C. J., Sessitsch, A., & Bodrossy, L. (2011). Analysis of methanotroph community composition using a pmoA-based microbial diagnostic microarray. *Nature Protocols, 6*(5), 609-624.

Tarlera, S., Jangid, K., Ivester, A. H., Whitman, W. B., & Williams, M. A. (2008). Microbial community succession and bacterial diversity in soils during 77,000 years of ecosystem development. *Fems Microbiology Ecology, 64*(1), 129-140.

Thauer, R. K. (1998). Biochemistry of methanogenesis: a tribute to Marjory Stephenson. *Microbiology-Uk, 144*, 2377-2406.

Torsvik, V., Daae, F. L., Sandaa, R.-A., & Øvreås, L. (1998). Novel techniques for analysing microbial diversity in natural and perturbed environments. *Journal of biotechnology, 64*(1), 53-62.

Turetsky, M. R. (2003). The role of bryophytes in carbon and nitrogen cycling. *Bryologist, 106*(3), 395-409.

Tveit, A. T., Hestnes, A. G., Robinson, S. L., Schintlmeister, A., Dedysh, S. N., Jehmlich, N., . . . Svenning, M. M. (2019). Widespread soil bacterium that oxidizes atmospheric methane. *Proceedings of the National Academy of Sciences of the United States of America, 116*(17), 8515-8524.

Tveit, A. T., Schwacke, R., Svenning, M. M., & Urich, T. (2013). Organic carbon transformations in high-Arctic peat soils: key functions and microorganisms. *Isme Journal, 7*(2), 299-311.

Tveit, A. T., Urich, T., Frenzel, P., & Svenning, M. M. (2015). Metabolic and trophic interactions modulate methane production by Arctic peat microbiota in response to warming. *Proceedings of the National Academy of Sciences of the United States of America, 112*(19), E2507-E2516.

Tytgat, B., Verleyen, E., Obbels, D., Peeters, K., De Wever, A., D'hondt, S., . . . Willems, A. (2014). Bacterial Diversity Assessment in Antarctic Terrestrial and Aquatic Microbial Mats: A Comparison between Bidirectional Pyrosequencing and Cultivation. *Plos One, 9*(6).

Tytgat, B., Verleyen, E., Sweetlove, M., D'hondt, S., Clercx, P., Van Ranst, E., . . . Willems, A. (2016). Bacterial community composition in relation to bedrock type and macrobiota in soils from the Sor Rondane Mountains, East Antarctica. *Fems Microbiology Ecology, 92*(9).

Vorobev, A. V., Baani, M., Doronina, N. V., Brady, A. L., Liesack, W., Dunfield, P. F., & Dedysh, S. N. (2011). Methyloferula stellata gen. nov., sp nov., an acidophilic, obligately methanotrophic bacterium that possesses only a soluble methane monooxygenase. *International Journal of Systematic and Evolutionary Microbiology, 61*, 2456-2463.

Vorobev, A. V., de Boer, W., Folman, L. B., Bodelier, P. L. E., Doronina, N. V., Suzina, N. E., . . . Dedysh, S. N. (2009). Methylovirgula ligni gen. nov., sp nov., an obligately acidophilic, facultatively methylotrophic bacterium with a highly divergent mxaF gene. *International Journal of Systematic and Evolutionary Microbiology, 59*, 2538-2545.

Wallmann, K., Pinero, E., Burwicz, E., Haeckel, M., Hensen, C., Dale, A., & Ruepke, L. (2012). The Global Inventory of Methane Hydrate in Marine Sediments: A Theoretical Approach. *Energies, 5*(7), 2449-2498.

Wan, X., Huang, Z., He, Z., Yu, Z., Wang, M., Davis, M. R., & Yang, Y. (2015). Soil C: N ratio is the major determinant of soil microbial community structure in subtropical coniferous and broadleaf forest plantations. *Plant and Soil, 387*(1-2), 103-116.

Wang, Q., Garrity, G. M., Tiedje, J. M., & Cole, J. R. (2007). Naive Bayesian classifier for rapid assignment of rRNA sequences into the new bacterial taxonomy. *Applied and Environmental Microbiology, 73*(16), 5261-5267.

Wania, R., Melton, J., Hodson, E., Poulter, B., Ringeval, B., Spahni, R., . . . Eliseev, A. (2013). Present state of global wetland extent and wetland methane modelling: methodology of a model inter-comparison project (WETCHIMP).

Wartiainen, I., Hestnes, A. G., McDonald, I. R., & Svenning, M. M. (2006). Methylobacter tundripaludum sp nov., a methane-oxidizing bacterium from Arctic wetland soil on the Svalbard islands, Norway (78 degrees N). *International Journal of Systematic and Evolutionary Microbiology, 56*, 109-113.

Wen, X., Yang, S. Z., & Liebner, S. (2016). Evaluation and update of cutoff values for methanotrophic pmoA gene sequences. *Archives of Microbiology, 198*(7), 629-636.

Whalen, S. C., Reeburgh, W. S., & Sandbeck, K. A. (1990). Rapid Methane Oxidation in a Landfill Cover Soil. *Applied and Environmental Microbiology, 56*(11), 3405-3411.

Whitman, W. B., Bowen, T. L., & Boone, D. R. (2006). The methanogenic bacteria. *The Prokaryotes: Volume 3: Archaea. Bacteria: Firmicutes, Actinomycetes*, 165-207.

Winfrey, M. R., & Ward, D. M. (1983). Substrates for Sulfate Reduction and Methane Production in Intertidal Sediments. *Applied and Environmental Microbiology, 45*(1), 193-199.

Woese, C. R. (1987). Bacterial evolution. *Microbiological Reviews, 51*(2), 221.

Woese, C. R., & Fox, G. E. (1977). Phylogenetic structure of the prokaryotic domain: the primary kingdoms. *Proceedings of the National Academy of Sciences, 74*(11), 5088-5090.

Wu, L. Y., Thompson, D. K., Li, G. S., Hurt, R. A., Tiedje, J. M., & Zhou, J. Z. (2001). Development and evaluation of functional gene arrays for detection of selected genes in the environment. *Applied and Environmental Microbiology, 67*(12), 5780-5790.

Yu, Z. T., & Morrison, M. (2004). Comparisons of different hypervariable regions of rrs genes for use in fingerprinting of microbial communities by PCR-denaturing gradient gel electrophoresis. *Applied and Environmental Microbiology, 70*(8), 4800-4806.

Zelles, L. (1999). Fatty acid patterns of phospholipids and lipopolysaccharides in the characterisation of microbial communities in soil: a review. *Biology and Fertility of Soils, 29*(2), 111-129.

Zeng, Y. H., Feng, F. Y., Medova, H., Dean, J., & Koblizek, M. (2014). Functional type 2 photosynthetic reaction centers found in the rare bacterial phylum Gemmatimonadetes. *Proceedings of the National Academy of Sciences of the United States of America, 111*(21), 7795-7800.

Zhao, R., Wang, H. M., Cheng, X. Y., Yun, Y., & Qiu, X. (2018). Upland soil cluster. dominates the methanotroph communities in the karst Heshang Cave. *Fems Microbiology Ecology, 94*(12).

Zheng, Y., Yang, W., Sun, X., Wang, S. P., Rui, Y. C., Luo, C. Y., & Guo, L. D. (2012). Methanotrophic community structure and activity under warming and grazing of alpine meadow on the Tibetan Plateau. *Applied Microbiology and Biotechnology, 93*(5), 2193-2203.

Zielke, M., Ekker, A. S., Olsen, R. A., Spjelkavik, S., & Solheim, B. (2003). The influence of abiotic factors on biological nitrogen fixation in different types of vegetation in the High Arctic, Svalbard (vol 34, pg 295, 2002). *Arctic Antarctic and Alpine Research, 35*(4), 538-538.

Øvreås, L. (2000). Population and community level approaches for analysing microbial diversity in natural environments. *Ecology Letters, 3*(3), 236-251.

Appendix

In the appendix we show the PCR (Figure S2-S8) from even number samples (Table S1) and the PCR primers not used to obtain data presented in the thesis (Table S2). And the log linear relationship between the *Alphaproteobacteria:Acidobacteria* ratio (Figure S1)

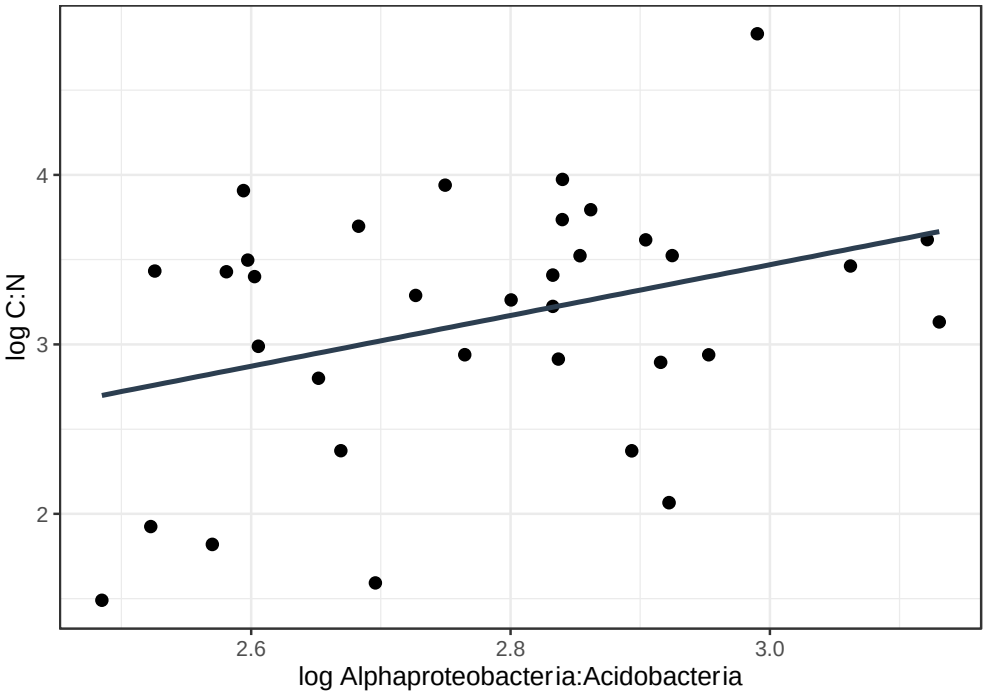

Figure S1: Figure showing the log linear relationship between the plot C:N ratio and the Alphaproteobacteria:Acidobacteria ratio. Plotted are mean values for the combination of site, site, plot and depth.

Table S1: Table of the measures soil parameter for each sample replicate. KH = Knudsenheia, OS = Ossian Sarsfjelletm MC = Moisture, TC = Total carbon, TN = Total nitrogen, C:N = Carbon nitrogen ratio. Positive PCR product is marked with an x

Sample information							PCR				Chemical soil properties						Phys. soil properties		
Sample code	**Number**	**Site**	**Site**	**Plot**	**Layer**	**Rep.**	**16S**	**mb661r**	**A682r**	**mcrA**	**MC (%)**	**OM (%)**	**TC (%)**	**TN (%)**	**C:N**	**pH**	**Sand (%)**	**Silt (%)**	**Clay (%)**
K.1.1.T.17a	**T001**	**KH**	Dry	P1	Top	a	x	x	x		16.53	36.91	7.57	0.41	18.46	5.24	84.3	9.60	6.10
K.1.1.T.17b	**T002**					b	x	x	x		12.30	13.85	7.57	0.41	18.46	5.25	84.3	9.60	6.10
K.1.1.T.17c	**T003**					c	x	x	x		15.35	16.69	7.57	0.41	18.46	5.41	84.3	9.60	6.10
K.1.1.D.17a	**T004**				Down	a	x	x	x		17.31	5.07	1.62	0.13	12.46	7.00	74.05	18.35	7.60
K.1.1.D.17b	**T005**					b	x	x	x		18.77	3.77	1.62	0.13	12.46	7.19	74.05	18.35	7.60
K.1.1.D.17c	**T006**					c	x	x	x		16.59	4.52	1.62	0.13	12.46	7.37	74.05	18.35	7.60
K.1.2.T.17a	**T007**			P2	Top	a	x	x	x		39.15	37.98	17.74	0.83	21.37	5.31	NA	NA	NA
K.1.2.T.17b	**T008**					b	x	x	x		28.74	25.92	17.74	0.83	21.37	5.45	NA	NA	NA
K.1.2.T.17c	**T009**					c	x	x	x		39.38	42.19	17.74	0.83	21.37	5.41	NA	NA	NA
K.1.2.D.17a	**T010**				Down	a	x	x			20.94	4.48	1.80	0.15	12.00	7.16	61.85	30.00	8.15
K.1.2.D.17b	**T011**					b	x	x	x		21.64	4.60	1.80	0.15	12.00	6.92	61.85	30.00	8.15
K.1.2.D.17c	**T012**					c	x	x	x		18.87	4.39	1.80	0.15	12.00	7.04	61.85	30.00	8.15
K.1.3.T.17a	**T013**			P3	Top	a	x	x	x		32.49	25.97	14.37	0.75	19.16	5.77	74.70	16.40	8.90
K.1.3.T.17b	**T014**					b	x	x	x		33.59	34.63	14.37	0.75	19.16	5.74	74.70	16.40	8.90
K.1.3.T.17c	**T015**					c	x	x	x		34.05	30.10	14.37	0.75	19.16	5.58	74.70	16.40	8.90
K.1.3.D.17a	**T016**				Down	a	x	x	x		19.23	4.05	1.96	0.15	13.07	7.36	60.70	28.55	10.75
K.1.3.D.17b	**T017**					b	x		x		19.64	4.23	1.96	0.15	13.07	7.39	60.70	28.55	10.75
K.1.3.D.17c	**T018**					c	x	x			19.73	4.23	1.96	0.15	13.07	7.50	60.70	28.55	10.75
K.2.1.T.17a	**T019**		Int.	P1	Top	a	x		x		66.83	37.86	16.31	0.96	16.99	6.86	65.35	19.25	15.40
K.2.1.T.17b	**T020**					b	x				56.38	23.23	16.31	0.96	16.99	7.06	65.35	19.25	15.40
K.2.1.T.17c	**T021**					c	x		x		54.40	26.33	16.31	0.96	16.99	6.85	65.35	19.25	15.40
K.2.1.D.17a	**T022**				Down	a	x	x	x		14.07	1.83	2.06	0.04	51.50	7.62	58.25	30.60	11.15
K.2.1.D.17b	**T023**					b	x	x	x		15.27	1.95	2.06	0.04	51.50	7.67	58.25	30.60	11.15
K.2.1.D.17c	**T024**					c	x	x	x		13.92	1.48	2.06	0.04	51.50	7.69	58.25	30.60	11.15
K.2.2.T.17a	**T025**			P2	Top	a	x		x		75.29	73.06	37.19	1.64	22.68	6.65	NA	NA	NA
K.2.2.T.17b	**T026**					b	x	x			74.71	77.86	37.19	1.64	22.68	6.76	NA	NA	NA
K.2.2.T.17c	**T027**					c	x		x		76.02	70.57	37.19	1.64	22.68	6.68	NA	NA	NA
K.2.2.D.17a	**T028**				Down	a	x	x	x		17.48	4.02	1.72	0.11	15.64	7.38	88.85	6.85	4.30
K.2.2.D.17b	**T029**					b	x	x	x		7.04	1.33	1.72	0.11	15.64	7.18	88.85	6.85	4.30
K.2.2.D.17c	**T030**					c	x	x	x		17.78	2.50	1.72	0.11	15.64	7.52	88.85	6.85	4.30

K.2.3.T.17a	**T031**			P3	Top	a	x		x	x	59.47	30.41	14.87	0.85	17.49	6.78	86.25	4.95	8.80
K.2.3.T.17b	**T032**					b	x				59.02	36.13	14.87	0.85	17.49	NA	86.25	4.95	8.80
K.2.3.T.17c	**T033**					c		x	x	x	48.41	19.12	14.87	0.85	17.49	NA	86.25	4.95	8.80
K.2.3.D.17a	**T034**				Down	a					16.65	3.68	1.76	0.13	13.54	7.24	88.25	8.35	3.40
K.2.3.D.17b	**T035**					b	x		x		20.14	2.77	1.76	0.13	13.54	7.27	88.25	8.35	3.40
K.2.3.D.17c	**T036**					c	x				13.86	2.82	1.76	0.13	13.54	7.42	88.25	8.35	3.40
K.3.1.T.17a	**T037**		Wet	P1	Top	a	x			x	68.29	43.98	16.31	0.96	16.99	NA	88.1	5.00	6.90
K.3.1.T.17b	**T038**					b	x	x			64.49	40.64	16.31	0.96	16.99	NA	88.1	5.00	6.90
K.3.1.T.17c	**T039**					c					52.64	20.88	16.31	0.96	16.99	NA	88.1	5.00	6.90
K.3.1.D.17a	**T040**				Down	a	x				17.41	1.91	1.07	0.07	15.29	7.37	83.65	12.2	4.15
K.3.1.D.17b	**T041**					b					22.17	2.55	1.07	0.07	15.29	6.92	83.65	12.2	4.15
K.3.1.D.17c	**T042**					c	x				17.95	1.53	1.07	0.07	15.29	7.53	83.65	12.2	4.15
K.3.2.T.17a	**T043**			P2	Top	a	x			x	67.75	33.00	16.83	0.97	17.35	NA	78.30	5.65	16.05
K.3.2.T.17b	**T044**					b	x			x	77.68	48.45	16.83	0.97	17.35	NA	78.30	5.65	16.05
K.3.2.T.17c	**T045**					c	x		x		61.9	22.04	16.83	0.97	17.35	6.77	78.30	5.65	16.05
K.3.2.D.17a	**T046**				Down	a					20.78	1.64	1.08	0.08	13.5	7.18	90.80	5.65	3.55
K.3.2.D.17b	**T047**					b	x				23.77	2.46	1.08	0.08	13.5	7.41	90.80	5.65	3.55
K.3.2.D.17c	**T048**					c	x				23.45	2.28	1.08	0.08	13.5	6.9	90.80	5.65	3.55
K.3.3.T.17a	**T049**			P3	Top	a			x		82.25	54.35	22.39	1.24	18.06	7.06	77.70	8.75	13.55
K.3.3.T.17b	**T050**					b		x	x		83.23	54.57	22.39	1.24	18.06	7.19	77.70	8.75	13.55
K.3.3.T.17c	**T051**					c	x		x		71.94	34.71	22.39	1.24	18.06	7.21	77.70	8.75	13.55
K.3.3.D.17a	**T052**				Down	a					21.22	2.57	1.5	0.12	12.5	7.62	89.85	6.55	3.60
K.3.3.D.17b	**T053**					b	x		x		23.46	2.65	1.5	0.12	12.5	7.46	89.85	6.55	3.60
K.3.3.D.17c	**T054**					c	x				23.02	2.65	1.5	0.12	12.5	7.41	89.85	6.55	3.60
O.1.1.T.17a	**T055**	**OS**	Dry	P1	Top	a	x	x	x		27.24	18.12	7.36	0.37	19.89	NA	75.3	16.55	8.15
O.1.1.T.17b	**T056**					b	x	x	x		21.64	7.88	7.36	0.37	19.89	NA	75.3	16.55	8.15
O.1.1.T.17c	**T057**					c		x	x		29.00	23.68	7.36	0.37	19.89	6.93	75.3	16.55	8.15
O.1.1.D.17a	**T058**				Down	a	x	x	x		18.89	4.43	2.02	0.14	14.43	7.19	57.2	32.05	10.75
O.1.1.D.17b	**T059**					b	x	x	x		16.90	2.77	2.02	0.14	14.43	7.46	57.2	32.05	10.75
O.1.1.D.17c	**T060**					c	x	x	x		19.95	3.78	2.02	0.14	14.43	7.35	57.2	32.05	10.75
O.1.2.T.17a	**T061**			P2	Top	a	x	x	x		17.10	8.43	5.10	0.31	16.45	7.08	71.2	19.20	9.60
O.1.2.T.17b	**T062**					b	x	x	x		21.58	14.15	5.10	0.31	16.45	6.79	71.2	19.20	9.60
O.1.2.T.17c	**T063**					c	x	x	x		21.14	11.18	5.10	0.31	16.45	9.79	71.2	19.20	9.60
O.1.2.D.17a	**T064**				Down	a		x	x		15.20	2.20	1.63	0.11	14.82	7.44	52.8	35.35	11.85
O.1.2.D.17b	**T065**					b	x	x	x		17.97	2.99	1.63	0.11	14.82	7.43	52.8	35.35	11.85
O.1.2.D.17c	**T066**					c	x	x	x		20.41	4.24	1.63	0.11	14.82	7.10	52.8	35.35	11.85
O.1.3.T.17a	**T067**			P3	Top	a	x	x	x		23.35	10.87	5.99	0.35	17.11	6.93	68.55	22.30	9.15

O.1.3.T.17b	**T068**				b	x	x	x	25.03	11.24	5.99	0.35	17.11	6.9	68.55	22.30	9.15
O.1.3.T.17c	**T069**				c	x	x	x	25.30	10.25	5.99	0.35	17.11	6.93	68.55	22.30	9.15
O.1.3.D.17a	**T070**			Down	a		x	x	21.53	4.04	1.74	0.13	13.38	6.97	53.3	36.55	10.15
O.1.3.D.17b	**T071**				b	x	x	x	18.73	4.04	1.74	0.13	13.38	7.15	53.3	36.55	10.15
O.1.3.D.17c	**T072**				c	x	x	x	17.79	3.84	1.74	0.13	13.38	7.04	53.3	36.55	10.15
O.2.1.T.17a	**T073**	Int.	P1	Top	a	x	x	x	35.69	14.75	16.02	0.86	18.63	6.29	61.85	26.85	11.3
O.2.1.T.17b	**T074**				b		x	x	26.93	22.99	16.02	0.86	18.63	6.27	61.85	26.85	11.3
O.2.1.T.17c	**T075**				c	x	x	x	30.44	29.51	16.02	0.86	18.63	6.22	61.85	26.85	11.3
O.2.1.D.17a	**T076**			Down	a	x	x	x	27.05	8.83	4.68	0.33	14.18	6.64	56.55	34.75	8.70
O.2.1.D.17b	**T077**				b	x	x	x	27.12	31.82	4.68	0.33	14.18	6.34	56.55	34.75	8.70
O.2.1.D.17c	**T078**				c	x	x	x	27.00	6.84	4.68	0.33	14.18	6.21	56.55	34.75	8.70
O.2.2.T.17a	**T079**		P2	Top	a	x	x	x	46.02	46.49	22.45	1.23	18.25	6.43	57.95	22.40	19.65
O.2.2.T.17b	**T080**				b	x	x	x	43.49	45.53	22.45	1.23	18.25	6.54	57.95	22.40	19.65
O.2.2.T.17c	**T081**				c	x	x	x	29.52	30.33	22.45	1.23	18.25	6.17	57.95	22.40	19.65
O.2.2.D.17a	**T082**			Down	a	x	x	x	42.61	20.65	7.46	0.51	14.63	6.92	59.05	32.05	8.90
O.2.2.D.17b	**T083**				b	x	x	x	36.54	14.23	7.46	0.51	14.63	6.73	59.05	32.05	8.90
O.2.2.D.17c	**T084**				c	x	x	x	27.52	7.40	7.46	0.51	14.63	6.76	59.05	32.05	8.90
O.2.3.T.17a	**T085**		P3	Top	a	x	x	x	30.35	24.21	14.55	0.85	17.12	6.56	63.50	23.00	13.50
O.2.3.T.17b	**T086**				b	x	x	x	30.24	29.22	14.55	0.85	17.12	6.28	63.50	23.00	13.50
O.2.3.T.17c	**T087**				c	x	x	x	34.69	39.76	14.55	0.85	17.12	6.42	63.50	23.00	13.50
O.2.3.D.17a	**T088**			Down	a	x	x	x	32.80	11.17	NA	NA	NA	7.10	50.90	39.60	9.50
O.2.3.D.17b	**T089**				b	x	x	x	32.55	12.12	NA	NA	NA	6.79	50.90	39.60	9.50
O.2.3.D.17c	**T090**				c	x	x	x	33.40	12.14	NA	NA	NA	7.20	50.90	39.60	9.50
O.3.1.T.17a	**T091**	Wet	P1	Top	a	x			54.52	16.77	8.19	0.48	17.06	7.13	63.45	25.7	10.85
O.3.1.T.17b	**T092**				b				58.34	20.13	8.19	0.48	17.06	7.09	63.45	25.7	10.85
O.3.1.T.17c	**T093**				c				41.36	10.87	8.19	0.48	17.06	7.31	63.45	25.7	10.85
O.3.1.D.17a	**T094**			Down	a	x	x		16.24	1.66	2.06	0.09	22.89	7.50	58.50	30.4	11.10
O.3.1.D.17b	**T095**				b	x		x	20.83	3.01	2.06	0.09	22.89	7.60	58.50	30.4	11.10
O.3.1.D.17c	**T096**				c	x			21.74	3.58	2.06	0.09	22.89	7.56	58.50	30.4	11.10
O.3.2.T.17a	**T097**		P2	Top	a	x			44.13	12.57	7.62	0.48	15.88	7.34	55.85	31.45	12.70
O.3.2.T.17b	**T098**				b	x			49.85	16.10	7.62	0.48	15.88	7.21	55.85	31.45	12.70
O.3.2.T.17c	**T099**				c	x		x	47.93	14.06	7.62	0.48	15.88	7.47	55.85	31.45	12.70
O.3.2.D.17a	**T100**			Down	a	x	x	x	21.43	3.89	2.23	0.12	18.58	7.34	52.45	36.15	11.40
O.3.2.D.17b	**T101**				b	x			21.87	4.12	2.23	0.12	18.58	7.25	52.45	36.15	11.40
O.3.2.D.17c	**T102**				c	x		x	17.25	2.31	2.23	0.12	18.58	7.52	52.45	36.15	11.40
O.3.3.T.17a	**T103**		P3	Top	a	x		x	47.10	19.81	8.19	0.62	13.21	6.63	63.70	27.55	8.75
O.3.3.T.17b	**T104**				b	x	x	x	41.58	13.7	8.19	0.62	13.21	6.19	63.70	27.55	8.75

O.3.3.T.17c	**T105**		c	x		x	49.82	18.21	8.19	0.62	13.21	6.11	63.70	27.55	8.75
O.3.3.D.17a	**T106**	Down	a	x			27.43	4.86	3.76	0.28	13.43	7.11	60.10	30.95	8.95
O.3.3.D.17b	**T107**		b	x		x	34.70	9.16	3.76	0.28	13.43	6.87	60.10	30.95	8.95
O.3.3.D.17c	**T108**		c	x	x	x	23.40	4.46	3.76	0.28	13.43	6.46	60.10	30.95	8.95

PCR

Table S2: Primers used to amplify *mcrA* gene for methanogens

Primers	Primer sequence	Reference
MLf	5′-GGTGGTGTMGGATTCACACARTAYGCWACAGC-3′	(Luton et al., 2002)
MLr	5′-TTCATTGCRTAGTTWGGRTAGTT-3′	
Mlasf	5′-GGTGGTGTMGGDTTCACMCARTA-3′	(Steinberg & Regan, 2008)
mcrArev	5′-CGTTCATBGCGTAGTTVGGRTAGT-3′	
A682r	5´-GAASGCNGAGAAGAASGC-3´	(Holmes et al., 1995)

PCR A189f/mb661r pmoA

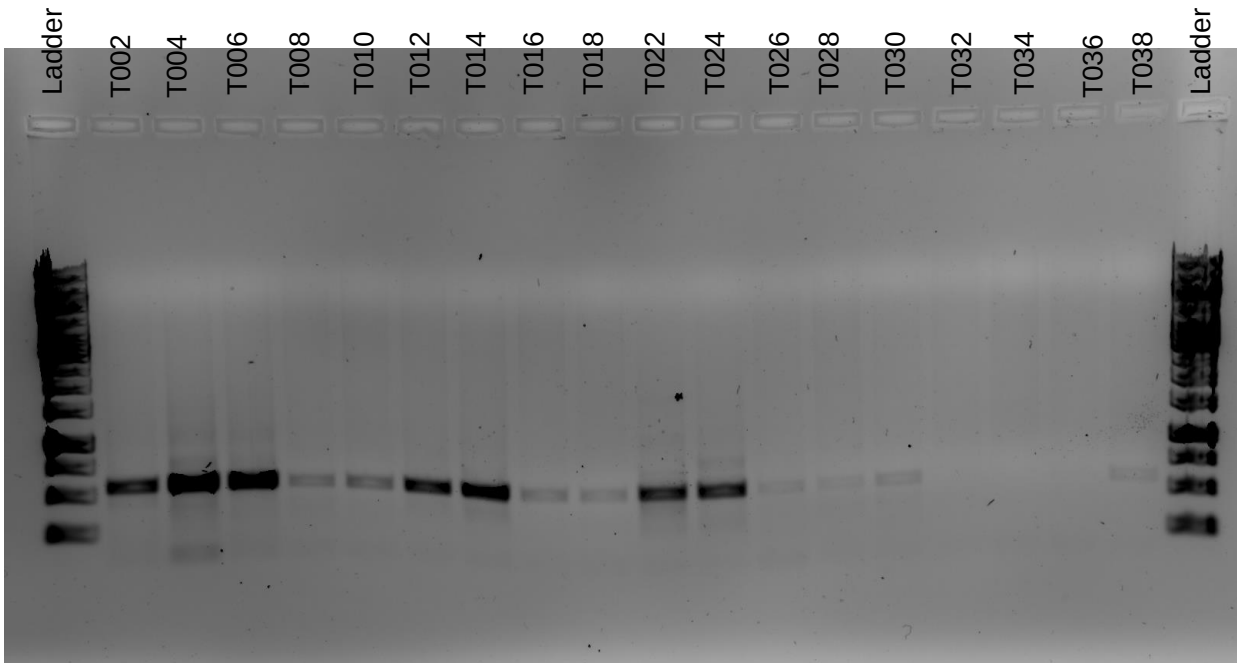

Figure S2: Confirmation of product and quality check for even samples 2 - 38. GeneRuler 1 kb DNA ladder (Thermo Scientific) is used as the ladder

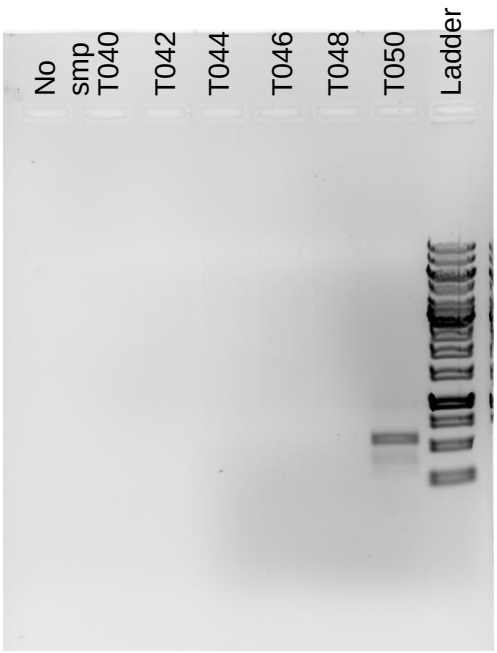

Figure S3: Confirmation of product and quality check for even samples 40-50. GeneRuler 1 kb DNA ladder (Thermo Scientific) is used as the ladder

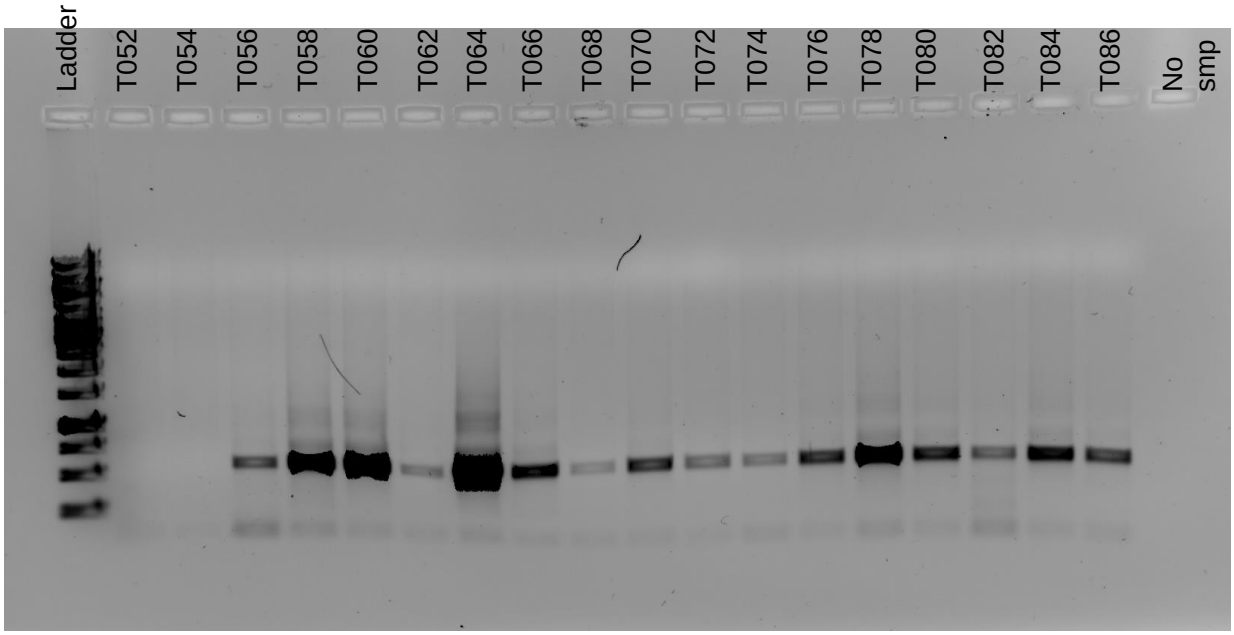

Figure S4: Confirmation of product and quality check for even samples 52-86. GeneRuler 1 kb DNA ladder (Thermo Scientific) is used as the ladder

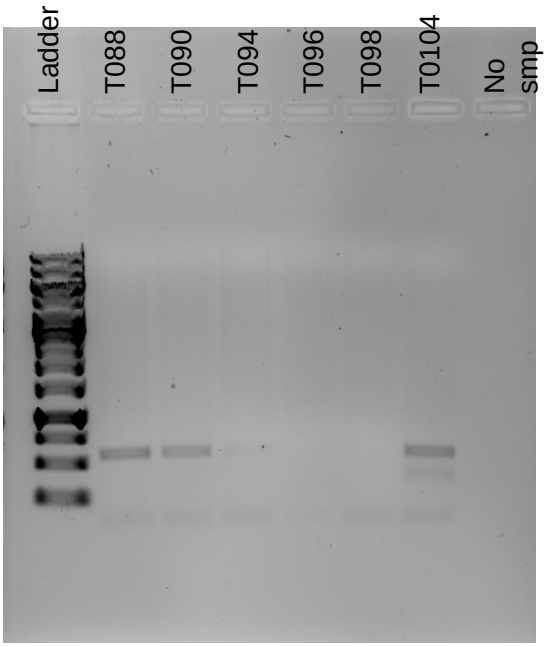

Figure S5: Confirmation of product and quality check for even samples 88-104. GeneRuler 1 kb DNA ladder (Thermo Scientific) is used as the ladder

PCR A189f/A682r pmoA

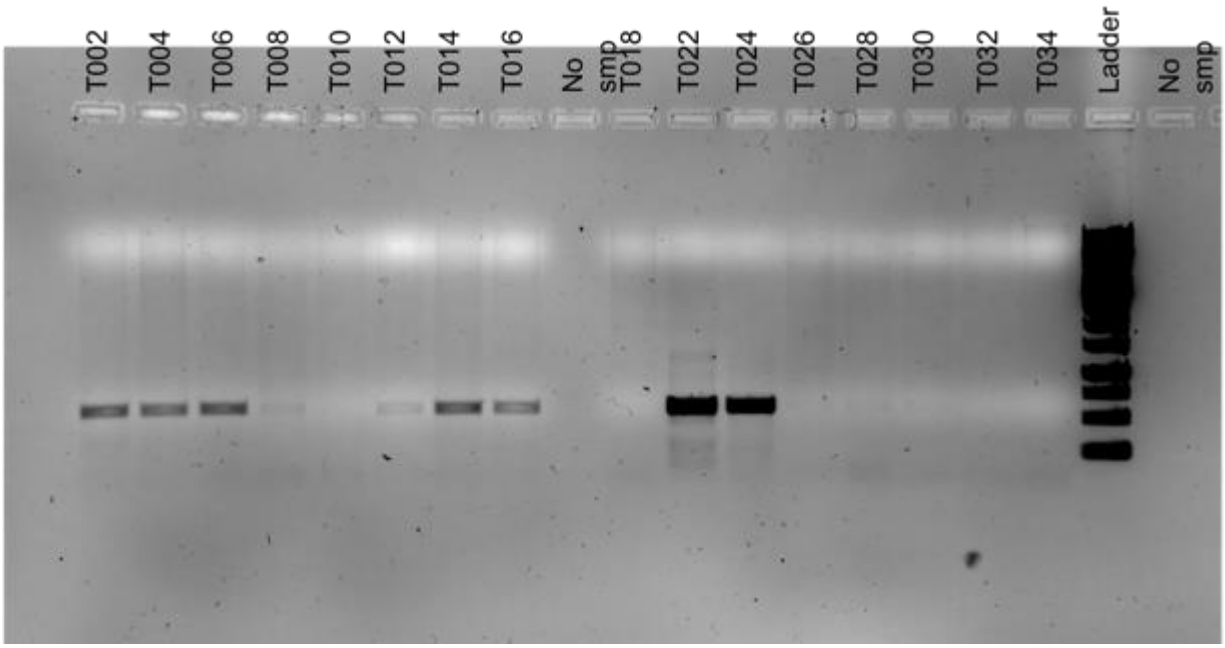

Figure S6: Confirmation of product and quality check for even samples 2-34. GeneRuler 1 kb DNA ladder (Thermo Scientific) is used as the ladder

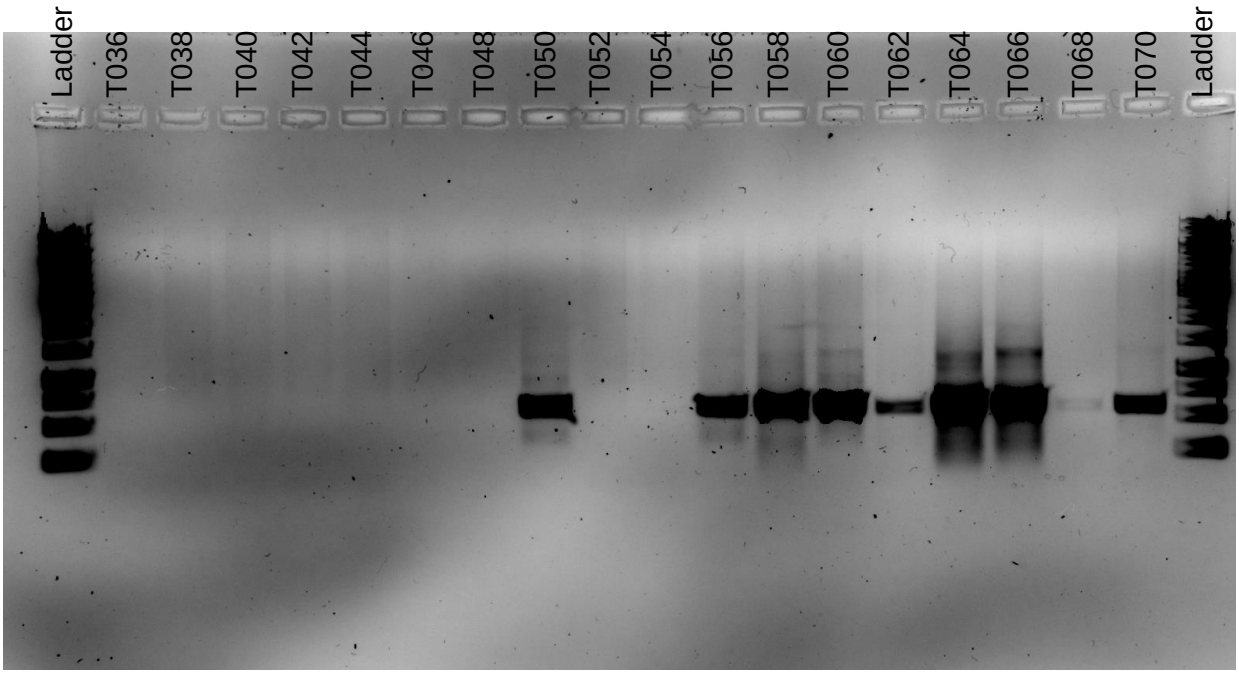

Figure S7: Confirmation of product and quality check for even samples 36-70. GeneRuler 1 kb DNA ladder (Thermo Scientific) is used as the ladder

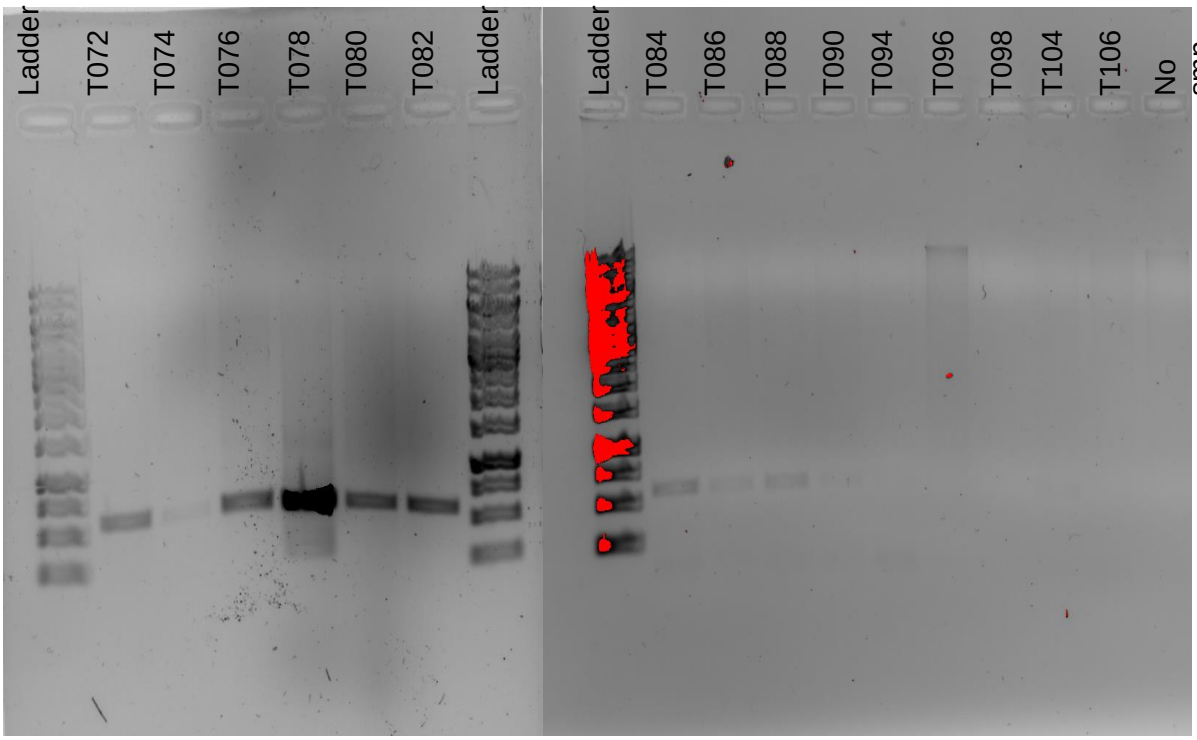

Figure S8: Confirmation of product and quality check for even samples 72-106. GeneRuler 1 kb DNA ladder (Thermo Scientific) is used as the ladder